Mariana Antunes Coutinho

Licenciatura em Bioquímica

Development and Experimentation of New Tools for Bioassays with Red Blood Cells

Dissertação para obtenção do Grau de Mestre em Biotecnologia

Orientador: Dr. Abel Oliva, Doutor, ITQB-UNL
Co-orientador: Dr. Hugo Águas, Doutor, FCT-UNL

Júri:

Presidente: Prof. Doutora Cecília Roque, FCT-UNL

Arguentes: Prof. Doutor Ricardo Franco, FCT-UNL

Vogal: Prof. Doutor Abel Oliva, ITQB-UNL

FACULDADE DE CIÊNCIAS E TECNOLOGIA
UNIVERSIDADE NOVA DE LISBOA

Março 2016

Development and Experimentation of New Tools for Bioassays with Red Blood Cells:

Science never solves a problem without creating ten more.

- George Bernard Shaw

Acknowledgments

This thesis would not have been possible without the guidance, support and help of certain people to whom I wish to express my heartfelt thanks, in particular:

To Professor Abel Oliva, my supervisor, for allowing me to be part of this project, and for all his concern, patience and availability shown in the course of it.

To Professor Hugo Águas, my co-supervisor, for the opportunity, support and kind expression of sympathy.

To the institutions which provided me all the resources required for caring out this work, Instituto de Tecnologia Química e Biológica (ITQB) e CENIMAT.

To the entire Biomolecular Diagnostics group, who received me so well and provided me with an excellent work environment: to Carmo, my "second mother", always so helpful, patient and worried. For all the personal and professional advices and all the transmitted knowledge which made the difference on my work. To Rita, "my partner in crime", for the friendship, permanent availability and help, anytime without exception. To Mariana, for the fellowship and true friendship which has arisen and remained forever. To Catarina, which turned possible to conduct all the microfluidic assays. For all her dedication, commitment and availability to educate me with so much care. To Sofia, for all her attention and concern. To Ana Pepe and Kamila for the good moments of laughs. Finally, to the trainees, Antonio Claudio, Miguel, Nuno, Carolina and Patricia, for their sympathy and good environment provided at the laboratory.

To Mário, from Molecular Thermodynamics Laboratory, for his tireless help, permanent concern and helpful advices. To my "more than colleagues" from 4th floor of ITQB, Isabel, Anabela and Joana for their good willing and for making me smile every day. To Tiago, for his encouragement and support words and for distracting me when I needed.

To my best friends, for being the really best friends of the world: to Sara, Inês, Madalena, for being the other part of myself, not only during this phase, but for the last 11 years of my life. For the support and unconditional friendship. For making me always believe on my own skills and competences. Part of my success I owe to you. To my other but not less important friends, who have accompanied me not only on this but in all journeys throughout my life, Sara Silva, Mafalda, Ana, and to my colleagues and friends from the Faculty during the last six years.

Lastly, and most of all, I would like to gratefully thank the tireless and invaluable support of all my family: to my parents, which with so much sacrifice have made this dream come true, for suffering with my concerns and for rejoicing with my accomplishments.

To my dear sisters, Inês and Rute, for their love and unconditional care, for ALWAYS believing in me and never let me give up. For all the advices and right words on the right moments. For being the best example I could have and for making me what I am today. To my brother-in-law André, for all his care, concern and help and for being a true "older brother" for me. And finally to the most recent family member, my nephew Duarte, which despite being so tiny, became my inexhaustible source of strength, through a single look or smile. Thank you my little prince!

Abstract

The aim of this work was to develop new tools for handling and studying of erythrocytes. In this context, biological nanoprobes were developed, combining Quantum Dots nanoparticles with specific antibodies to detect proteins in erythrocytes. Also, a microfluidic platform was designed and constructed to evaluate the cytotoxic effect in single-cell analysis of used QDs.

To determine the experimental conditions for bioconjugation, preliminary studies were performed to analyse the electrophoretic behaviour of QDs and their pH stability. It was demonstrated that the mobility depends on the surface charge of QDs and it is not affected in pH range between 5 and 8.

To evaluate the cytotoxic effect of non-conjugated nanoparticles, QDs functionalized with three different groups were used: PDDA, PEG and COOH, at concentrations of 10, 50 and 100nM. The results showed that the interaction between QDs and cells induces a general oxidative stress, which increases with the concentration of QDs.

The conjugation reaction between COOH-QDs and monoclonal antibodies against antigenic protein AMA1 and transmembrane Glycophorin A protein was performed by EDC/NHS chemistry. The QDs-Ab complexes were characterized by agarose gel, comparing their molecular weight and electrophoretic mobility with non-conjugated nanoparticles. Using SDS-PAGE and Immunoblotting techniques, the samples were analysed in order to evaluate their ligation properties, as well as their biological activity.

The final bioconjugates were then biological tested, namely in detection of GPA protein in erythrocytes and antigenic AMA1 protein in infected *B.ovis* erythrocytes, through the immunofluorescence assays on slide and in solution. Comparing the results obtained with QDs and the traditional assays with FITC conjugated antibodies, QDs-Ab complexes appear to be more resistant during large periods of excitation.

Keywords: Erythrocytes, Quantum Dots, Oxidative Stress, Microfluidics, *Babesia ovis*

Resumo

O objetivo deste trabalho consistiu no desenvolvimento de novas ferramentas para o estudo e manipulação de eritrócitos. Neste contexto, foram criadas nanosondas biológicas através da conjugação de nanopartículas (Quantum Dots) com anticorpos específicos para a deteção de proteínas presentes nos eritrócitos. Foi também desenhada e construída uma plataforma de microfluídica para poder avaliar o efeito citotóxico dos QDs usados na bioconjugação.

Para determinar as condições experimentais para a conjugação, foram elaborados estudos preliminares para analisar o comportamento electroforético dos QDs e a sua estabilidade em valores de pH diferentes. Foi demonstrado que a mobilidade depende da carga da superfície dos QDs e que não é afetada numa gama de pH entre 5 e 8.

Para avaliar o efeito citotóxico das nanopartículas não conjugadas, foram utilizados QDs com três funcionalizações diferentes: PDDA, PEG e COOH a 10, 50 e 100nM. Os resultados mostram que a interação dos QDs com as células induz um stress oxidativo generalizado, que aumenta com a concentração dos mesmos.

A reação de conjugação entre COOH-QDs e anticorpos monoclonais contra a proteína antigénica AMA1 e contra a proteína transmembranar Glicoforina A foi realizada usando a via química EDC/NHS. Os complexos QDs-Ab foram posteriormente caracterizados através de géis de agarose, comparando o seu peso molecular e a sua mobilidade electroforética com nanopartículas não conjugadas. Através das técnicas *SDS-PAGE* e *Immunoblotting*, as amostras foram analisadas de forma a avaliar as propriedades de ligação, assim como a sua atividade biológica.

Os bioconjugados desenvolvidos foram depois testados a nível biológico, nomeadamente na deteção das proteínas GPA em eritrócitos e AMA1 em eritrócitos ovinos infetados com *B.ovis*, através de ensaios de imunofluorescência em lâmina e em solução. Comparando os resultados obtidos com QDs e os ensaios tradicionais usando anticorpos secundários conjugados com FITC, os complexos QDs-Ab aparentam ser mais resistentes em períodos de excitação maiores.

Palavras-chave: Eritrócitos, Quantum Dots, Stress Oxidativo, Microfluídica, *Babesia ovis*

List of Abbreviations

Ab antibody

AMA-1 apical membrane antigen 1

BSA bovine serum albumin

COOH carboxylic acid

DAPI 4', 6-diamidino-2-phenylindole dihydrochloride

EDC 1-ethyl-3-(3-dimethylaminopropyl)carbodiiamide

Fc fragment crystallisable

GPA glycophorin A

Hgb hemoglobin

H_2DCFDA 2', 7'-dichlorodihydrofluorescein diacetate

IgG Immunoglobulin G

IHC Immunohistochemistry

LEDs light emitting devices

LOC Lab-On-a-Chip

NaP sodium phosphate buffer

NHS *N*-hydroxysuccinimide

PDDA polydiallyldimethylammonium Chloride

PDMS polydimethylsiloxane

PEG polyethyleneglycol

PGMEA propylene glycol methyl ether acetate

PVDF polyvinylidene fluoride

QDs Quantum Dots

RBCs red blood cells

ROS reactive oxygen species

r.t. room temperature

Si silicon

SMCC 4-(N-maleimidomethyl) cyclohexanecarboxylic acid N-hydroxysuccinimide ester

Sulfo-SMCC 4-(N-maleimidomethyl) cyclohexane-1-carboxylic acid 3-sulfo-N-hydroxysuccinimide ester sodium

TBE tris borate EDTA

TBS tris buffered saline

TES N-[tris(hydroxymethyl)methyl]- 2-aminoethanesulfonic acid, 2-[(2-hydroxy-1, 1-bis(hydroxymethyl)ethyl)amino]ethanesulfonic acid

TP Transmembrane Protein

TTBS tris buffered saline with Tween

VyMs Veja y Martinez buffer

WBCs white blood cells

List of Contents

List of Figures

List of Tables

Chapter 1 | Introduction

1.1. Motivation

Blood is an important connective tissue and is vital to body's survival due to its functions: transportation, regulation and protection. When some pathological condition occurs, blood is altered, affecting the entire health of the individual. Thus, monitoring blood can be an important source of clinical information related to the functioning of all tissues and organs of the body.

The tissue below (Figure 1.1) is composed by blood cells suspended in plasma. In particular, 96% of the total population of blood cells is made by red blood cells (RBCs) or erythrocytes (Figure 1.1). Erythrocytes are important for scientific and medical investigation given that some clinical conditions are directly associated with changes in their morphology or physiology (for example, anemia which is characterized by insufficient red cell mass, with values lower than 12.5g/dL). As a result, red blood cells are a convenient subject which should help investigators to know more about the blood disorders that may affect the individual's health.

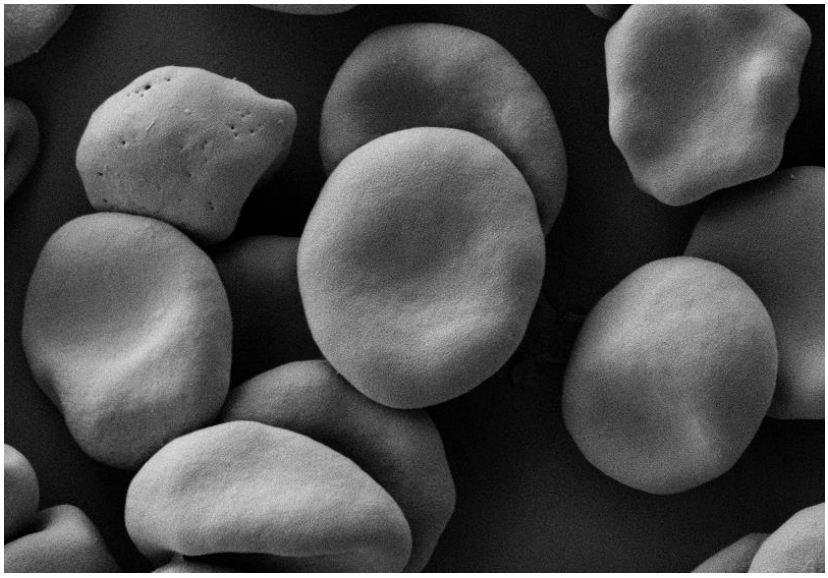

Figure 1.1 | Red blood cells by Scanning Electron Microscope: Red blood cells 1% suspension obtained from whole human blood. The cells were fixed with 0.075M of sodium calcodilate (CaCo), 2.25mM of MgCl2 and 1% of glutaraldehyde.

Thus, it is important to develop strategies and explore new approaches in order to deepen knowledge in this area.

Microfluidic platforms have the potential to better understand the process at a single cell level. Microfluidic represents an innovative technology based on narrow fluid channels (< 100µm) that can be applied in this area. Chips with microchannels for biological experiments requires small samples volumes and reduced consumption of reagents. Furthermore, this approach allows the miniaturization, integration and parallelization of biochemical processes in a controlled environment, decreasing the possibility of cross contamination. The use of microfabricated chips for monitoring and diagnostic of living cells offers a new tool for medical applications in real-time, allowing the fulfilling of experimental

assays that are cumbersome or even not possible with other techniques. Developing chips for analysis of individual cells is a challenge but can provide new options for biological and clinical research.

Also in the context of this work, and regarding the exploration of new approaches for cell studies, a type of nanoparticles has been experimentally tested as an alternative to traditional fluorophores, in particular, for cellular labeling. Quantum dots are fluorescent nanocrystals that have been attracting increased interest in bioresearch given their distinct characteristics. They present advantageous optical properties such as strong light absorbance, bright fluorescence and high photostability which make them ideal to be conjugated with biomolecules for application in life science research, diagnostic and therapeutics.

The aim of this work was focused on the development of new approaches to analyze blood. For this purpose, two tools were developed: the preparation of probes with Quantum Dots and specific antibodies to detect proteins related to pathological disorders and a microfluidic platform to capture and to analyze the oxidative stress produced by the interaction of QDs with cells. Within the aim of this work, the following goals were pursued:

- To bioconjugate specific antibodies with Quantum Dots nanoparticles towards the identification of two transmembrane proteins:
    - Glycophorin A, located on erythrocytes membrane
    - Apical Membrane Antigen 1 which is expressed on the surface of erythrocytes invaded by *Babesia ovis* parasites.
- To design, construct and optimize the setup of experimental microfluidic assays to evaluate the cytotoxic effect of Quantum dots in erythrocytes in oxidative stress, using a microfluidic platform through the single-cell approach.

1.2. Cell analysis

Cells are the essential units of biological processes (Lecault at al., 2012) and they are complex and dynamic entities. Cellular analysis is present in areas like life science, diagnostics and pharmaceutical industry (El-Ali et al., 2006; Dittrich et al., 2006). Part of research from basic cell biology and microbiology to applications in biotechnology is conducted through cell populations with high cell numbers (Schmid et al., 2010). However, interpretation of cell population data frequently implies the hypothesis that each cell in population is similar and sometimes, this is not true and can result in false interpratation (Yin and Marshall, 2012). For example, cell populations can be submitted to fast environmental changes, such as stress or perturbation and during such modifications, it can be observed that some cells deal better with the new conditions compared with other cells within the same population, even cells with identical functions usually respond differently.

Cellular heterogeneity is an intrinsic characteristic of cell populations and it can be seen in cells of the same type. Realize the cellular heterogeneity has been the main challenge of technological development over the past years because knowing why and how these differences appear, it is easier to obtain a better understanding of cell biology. Moreover, this can improve the capacity to detect early disease stages to be able to act more quickly, before significant health consequences (Roman et al., 2007). One way to resolve this problem is to analyze a population at individual cell level. Single cells

correspond to the minimal functional unit of life. Nowadays, one of the main objectives is to comprehend the working mechanisms in this minimal unit (Schmid et al., 2010). These purpose can just be reached using highly sensitive methods with resolutions at the single cell and if possible, at subcellular level. So, to achieve a full single cell analysis, the development of high throughput systems competent of manipulation and analyzing individual cells is indispensable (Yin and Marshall, 2012). The challenge in single cell analysis is to reach this sensitivity precision, throughput and economy desired to detect and study complex subpopulation cells and during the same time (Lecault at al., 2012).

1.2.1. Red Blood Cells

Blood is often mentioned to as “liquid organ” and is a complex mixture of many types of components where each one has diverse properties. It is distributed via the vascular system throughout the entire body, making it indispensable for the existence of the organism. Blood contains innumerable information about the functioning of the body and it can be used to diagnose diseases.

Blood exhibits a wide variety of functions, such as supplying oxygen to tissues and nutrients, removing waste (such as carbon dioxide, urea and lactic acid), immunological functions (including circulation of white blood cells and detection of foreign material by antibodies), coagulation by the platelets (which is one part of the body’s self-repair mechanism), messenger functions (including the transport of hormones and the signaling of tissue damage), regulating body pH and temperature and finally, hydraulic functions (including the regulation of the colloidal osmotic pressure of blood).

Blood is composed by different type of cells (blood cells) suspended in a fluid, called plasma (Figure 1.2). The blood plasma or liquid portion of the blood, represents approximately 55% of the entire blood. This liquid component is constituted mostly by water (91%). It also contains 7% of plasma proteins (including albumins, globulins and fibrinogen) and 2% of other solutes (such as ions, nutrients, hormones, waste products and respiratory gases). The blood cells make up the remaining 45% of blood volume and they are primarily synthesized in the bone marrow. These composition of blood cells can be divided into three types: red blood cells (or erythrocytes), white blood cells (or leukocytes) and platelets (or thrombocytes). Platelets are particles smaller than red and white blood cells and they are present in a fewer number than erythrocytes with a ratio of about 1 platelet to every 20 red blood cells. These cells exhibit a discoid shape and contain no nucleus, helping in clotting process. The white blood cells represents only approximately 3% of all blood cells, with a ratio of about 1 to every 600/700 red blood cells. They are involved in the immune defense. Leukocytes are divided into three main subtypes: Granulocytes, representing 70% of all leukocytes and are constituted by 65% of neutrophils (which are involved in first response to infections and in inflammatory processes), 4% of Eosinophils (reacting first against infections by parasites) and 1% of Basophils (which are mainly responsible for antigenic and allergic response). Granulocytes are nuclear cells. White blood cells are also constituted approximately by 6% of monocytes (or macrophages) which are responsible for the ingestion of foreign cells, dead cells and cell debris by endocytosis. Finally, lymphocytes represent 25% of leukocytes and they are involved in production of antibodies and they are divided into three types: B cells (which produce antibodies and have memory for previously ingested pathogens), T cells (playing an essential role in

cell mediated immunity) and natural killer cells (which are able to kill cells such as undetected virus cells or cells that have cancerous).

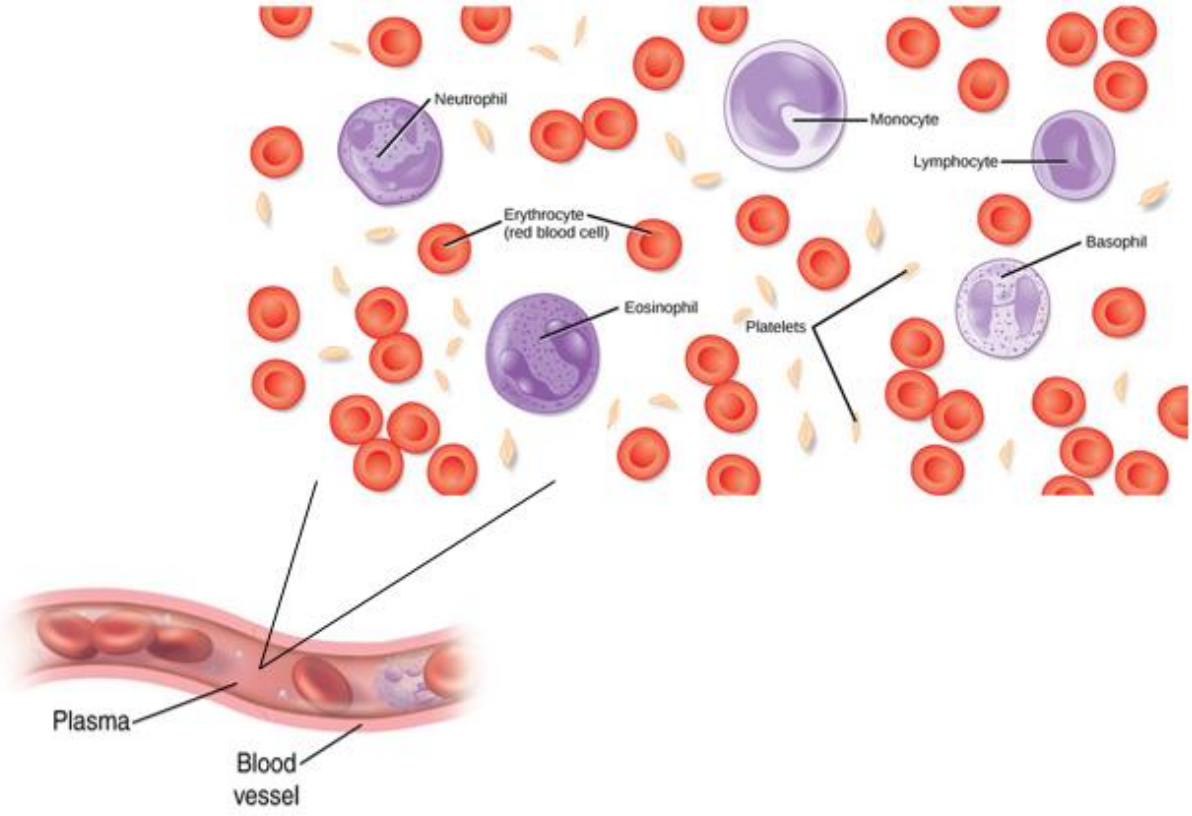

Figure 1.2 | The components of blood: It is composed by: erythrocytes (or red blood cells) that are cells without nucleus and they contain hemogloblin and carry oxygen. Leukocytes (or white blood cells) taht contain a nucleus and are present in lower number when compared with erythrocytes. They help to defend the body against infection and disease. At last, platelets which is the component of blood responsible for initiating blood clotting. Like erythrocytes, they haven't a nucleus (Adapted from: https://www.urmc.rochester.edu).

Current methods for blood testing need large sample volume to be executed (3-5mL). A microfluidic approach is an attractive alternative for blood analysis due to its miniaturization benefits such as reduced reagent consumption, reduced sample requirement and decreased analysis time. Currently, several microfluidic systems are being developed to overtake a diversity of clinical problems for example, the detection of pathogens *in vivo* through the development of integrated microfluidic devices. These microfluidic devices are suitable candidates for point of care diagnostics due to small size and low cost production.

1.3. Quantum Dots

Semiconductor nanocrystals, also known as Quantum Dots (QDs), have been introduced in recent years as a new type of nanoparticles for applications in biology and medicine, in particular, for labeling biomolecules. They have proven useful as an alternative to conventional fluorescent dyes due to their bright fluorescence, narrow emission, broad UV excitation and high photostability (Parak et al., 2005).

Quantum Dots are nanoparticles mainly made of a core composed by a semiconductor metal in a spherical crystalline form and this core is capped with a shell consisting of another semiconductor metal that has a larger spectral band gap (Figure 1.3) (Azzazy et al., 2007; Hermanson, 2008). QDs cores are usually composed by elements from groups II and VI (e.g. CdSe, CdTe, CdS and ZnSe) or groups III and V (e.g. InP and InAs). The commonly used QDs for biological applications are made of CdSe cores coated with a layer of ZnS because their chemistry is suitable for attaching biomolecules. The ZnS protects the core surface from oxidation, avoid leaching of the CdSe into the solution, promoting the minimal interaction with the surrounding environment, helping to their photostability (Bruchez, 2005) and finally, improves the photoluminescence yield (Kortan et al., 1990; Mews et al., 1994). The size of this core/shell structure is about 2-10 nm (usually less than 10 nm) but with functionalized amphiphilic molecules, the size of final nanoparticle can be larger than 10nm which allows an interaction with various type of biomolecules (Azzazy et al., 2007).

1.3.1. Properties

Quantum Dots are inorganic fluorophores that have size-tunable emission (i.e. there is an expected relationship between the size of the QDs and its emission wavelength), strong light absorbance, bright fluorescence, narrow symmetric emission bands and high photostability. They preserve excellent stability of optical properties upon conjugation to biomolecules and different quantum dots can be excited by a single light source at the same time (Alivisatos et al., 2005; Calpp et al., 2006; Salata, 2004). The color and emission wavelength of QDs are determined by their size and composition. As such, their emission spectra can be quite narrow, by varying the core diameter (Figure 1.4) (Azzazy et al., 2007; Hermanson, 2008). The emission spectra of QDs usually range between 450 nm and 850 nm and QD can be controlled to have the desired wavelength, whereas their excitation spectra is very broad (Figure 1.5) (Yezhelyev et al., 2006). Thus, the narrow emission spectrum reduces spectral overlap, which enhances the possibility to distinguish various fluorophores at the same time. The vast separation between their emission and excitation spectra (known as Stroke's shift) makes the detection sensitivity be better as the whole emission spectra of QDs can be detected.

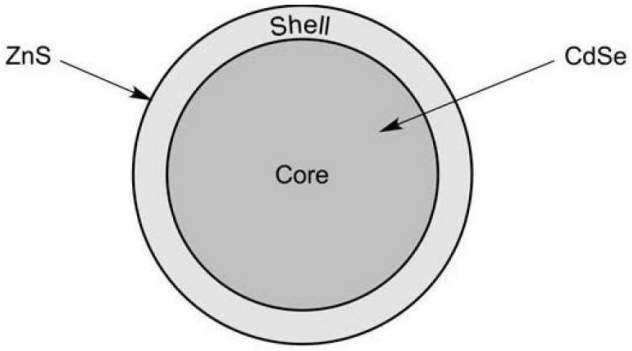

Figure 1.3 | The structure of a typical CdSe/ZnS QD: This includes a semiconductor core (in this case CdSe), surrounded by a shell of a different metal (ZnS). Many different composition can be used and are possible (adapted from Hermanson, 2008).

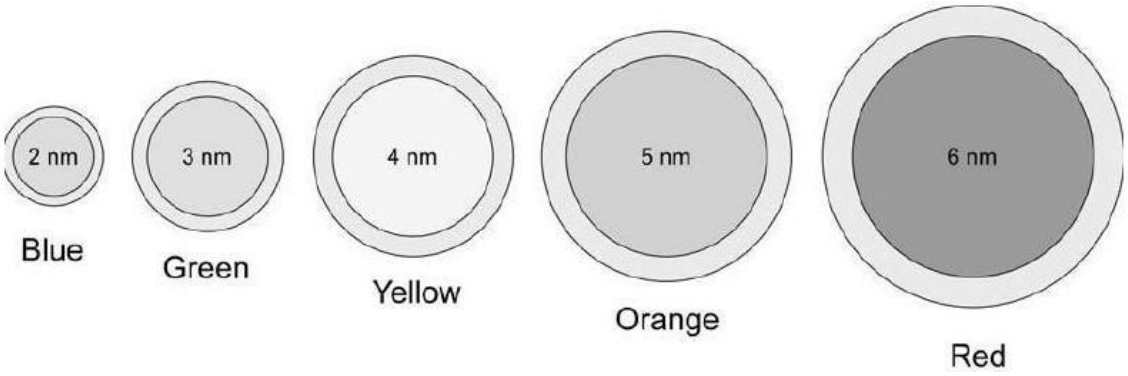

Figure 1.4 | The QD size proportionally affects its emission wavelength. By controlling the core size, it can develop a range of nanocrystals with distinct emission spectral characteristics. Therefore, larger nanocrystals absorb and emit in the red while smaller nanocrystals absorb and emit in the blue of the visible spectrum (adapted from Hermanson, 2008).

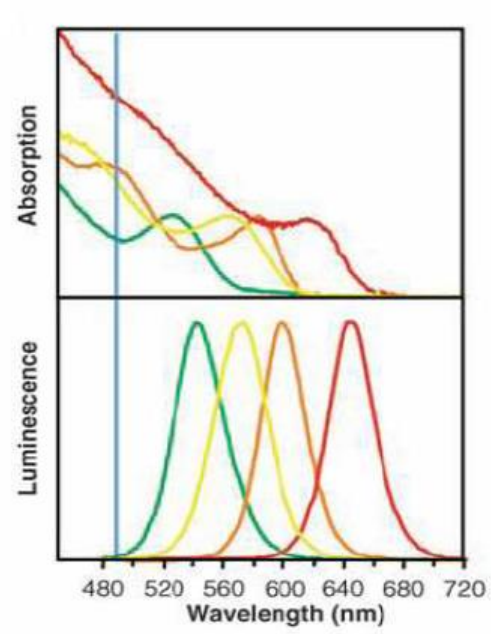

Figure 1.5 | Absorption and emission spectra of four CdSe/ZnS QD examples. The blue vertical line indicates the 488-nm line of an argon-ion laser, which can be used to efficiently excite all four types of QD's simultaneously (adapted from Santos, 2009).

These nanoparticles can be synthesized with different properties (in terms of crystalline grains and size distribution), depending on the intended applications (Parak et al., 2005; Azzazy et al., 2007). Usually, the synthesis of these monodisperse and stable particles such as CdSe, is carried out in organic solvents at high temperatures in the presence of surfactants. The size of QDs and their spectral properties are determined during the synthesis process by the reaction time (Hermanson, 2008). However, QDs produced by previous described method are by default hydrophobic and thus, they aren't appropriate for use in biological media (Alivisatos et al., 2007; Jaiswal and Simon, 2004). With the aim to use QDs in a biological environment, they need to become hydrophilic. This can be solved by substituting the surfactant layer or by coating with an additional layer, introducing electric charge or hydrophilic polymers and so controlling solubility in water (Parak et al., 2005).

1.3.2. Biocompatibility, Functionalization and Bioconjugation

As described above, QDs can become hydrophilic introducing, for example, bifunctional ligands with an electrical charge. A common bifunctional ligand used for this purpose are mono or dithiols. They have a hydrophilic group, such as carboxylic acid, which binds to the metal ions present at the surface of QDs (Medintz et al., 2005). The introduction of functional ligands is fundamental for achieving solubility of the QDs but also for the bioconjugation with affinity molecules. Thus, QDs can be adapted to the specific application through the conjugation with biomolecules such as antibodies, peptides, oligonucleotides or aptamers, or by coating with streptavidin to be used for specific binding with biotin. (Figure 1.6) (Azzazy et al., 2007).

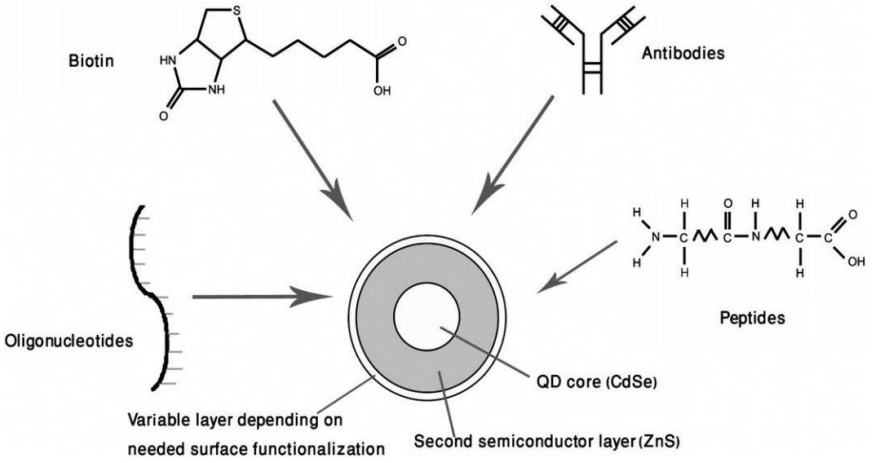

Figure 1.6 | Many antibodies, proteins and other target or affinity molecules can be conjugated to QDs for biological applications. For this purpose, the QDs must become biocompatible by coating with a hydrophilic layer that modifies the surface, preventing aggregation and non-specific binding (adapted from Azzazy et al., 2007).

There are several methods used for conjugation of QDs to the specific biomolecules, which include: electrostatic attraction, covalent linkage, adsorption and mercapto (-SH) exchange. The method to be used will depend on the features of the biomolecule of interest. Usually, the covalent binding of biomolecules to the functional groups on the surface of QDs is the most frequent used method because of its stability. For example, if the QD surface carries carboxyl groups, it can be conjugated to a biomolecule that has available amine groups via 1-ethyl-3-(3-dimethylaminopropyl)carbodiiamide (EDC) cross linker (Alivisatos et al., 2005; Lin et al., 2004).

The conjugation of an antibody to another protein or molecule is highly desired due to its large applicability in life science research, diagnostics and therapeutics. Antibody conjugates have been considered an important classes of biological agents because their use in target therapy for many diseases (Carter et al., 2004). The purified immunoglobulins are prepared by isolating them from antisera by affinity chromatography. Generally, immunoglobulin G structure (Figure 1.7) comprises symmetrical molecules, constituted of two similar glycosylated heavy chains and two similar non-glycosylated light chains, connected by noncovalent interactions even as a number of disuphide bonds. The heavy chains are linked to each other by disulphide bonds in hinge region and the light chains are

disulfide-bounded to the heavy chains in the C_L and C_{H1} regions respectively as represented in figure 1.7. The heavy chains of each immunoglobulin molecular are similar.

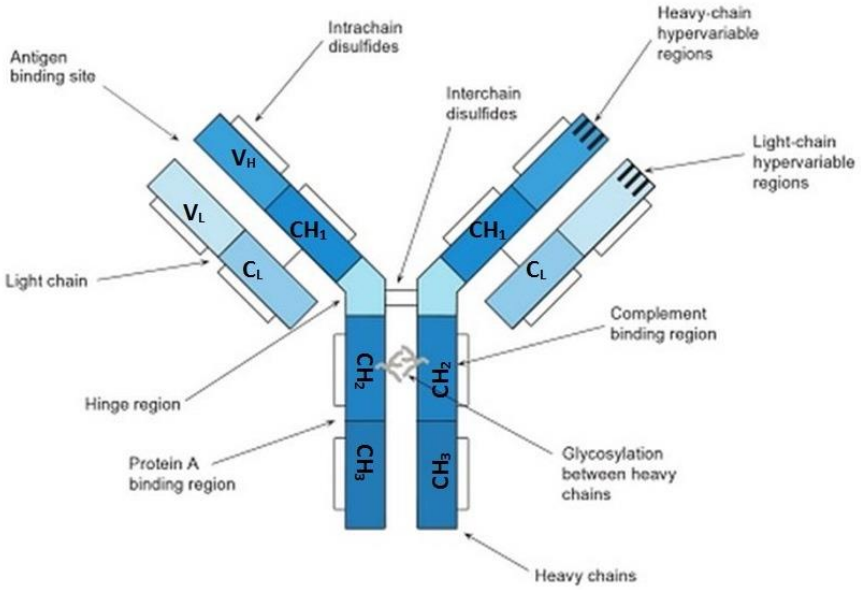

Figure 1.7 | Structure of an IgG molecule (Adapted from Hermanson, 2008).

According to the class of immunoglobulin, the molecular weight for the heavy chains varies from 50 to a 75 kDa and approximately 25 kDa for the light chains. The whole molecular weight which corresponds to all subunits ranges from 150 to a 170 kDa. The light chains play an important role in establishing the specificity of antibodies. However, it is the antibody's heavy chain variety that defines the individual class of immunoglobulin and all the master function of antibodies. The immunoglobulins can be divided into five main classes: IgA, IgD, IgE, IgG and IgM (Figure 1.8). Each class of antibodies has distinct sizes, structural constitution and different biological properties. For example, antibody classes IgD, IgE and IgG are constituted by elementary Ig monomeric structure consisting in two light and two heavy chains. In other hand, IgA molecules can present a basic Ig monomeric structure as a singlet, doublet or triplet while IgM molecules are large pentameric structure.

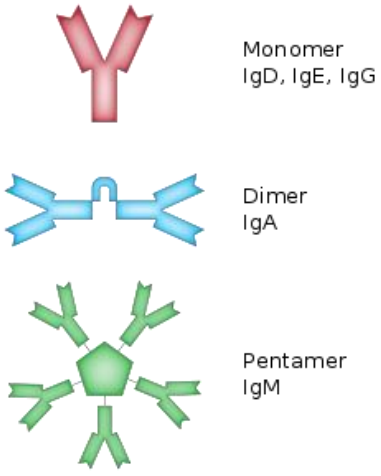

Figure 1.8 | General structures of five different classes of antibodies (adapted from https://en.wikipedia.org).

The heavy chains of immunoglobulin molecules are also glycosylated usually in CH_2 domain inside the Fc fragment region ("Fragment crystallisable") but also have two carbohydrates near the antigen binding sites. The Y-shaped unit is constituted by the two identical heavy chains and two identical light chains. The top of Y-unit contains the variable region also designated by antigen binding site. These sites have the suitable structural conformation to interact with complementary region of the antigen molecule. The binding site has affinity for a certain antigen because of 3D structural region of the molecule that complements the binding region of the antibody, involving the combination of van der Waals, ionic, hydrophobic and hydrogen bonding forces. Thus, antibodies possess functional groups in their structure that are appropriate for modification or conjugation processes (Hermanson, 2008).

For this purpose, effective approaches have been used to link biological molecules to QDs. There are several conjugation methods, like non-covalent conjugation of streptavidin coated QDs to biotinylated antibodies, covalent coupling between carboxylic acid coated QDs and primary amines of antibodies, site-directed conjugation via oxidized carbohydrates groups on the antibody Fc portion and conjugation to antibody fragments via disulphide reduction and sulfhydryl amine coupling (Xing et al., 2007).

The covalent strategy is reached through direct binding of the biomolecules to the QD surface coating with reactive groups such as a carboxylic acid or an amine or other cross-linker molecules. The procedures used consist on cross-linking reactions between carboxylic acid (-COOH) coated QDs and primary amines (-NH2) of antibodies which leads to a random bioconjugation, catalyzed by carbodiimide (Xing et al., 2007). A typical method to covalent conjugation uses the 1-ethyl-3-(3-dimethylaminopropyl)carbodiiamide (EDC) together with the presence of *N*-hydroxysuccinimide (NHS) to react the primary amino groups of biomolecules with carboxyl groups on the QD surface (Figure 1.9) (Pereira and Lai, 2008). One of the advantages of this method is related to the fact that proteins contain primary amines and do not need chemical modification (Xing et al., 2007). One limitation of the conjugation of proteins to QDs can be related to the functional sites accessible on the surface of a single QD. QDs can bind to the amine terminal groups in the antigen binding sites of the protein of interest and blocking them (Medintz et al., 2005).

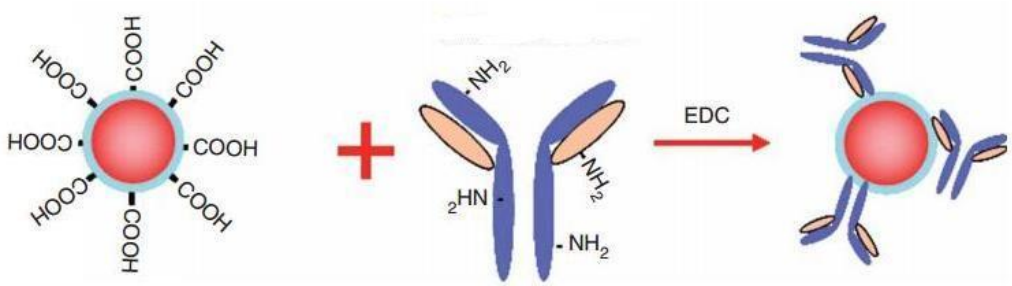

Figure 1.9 | Schematic diagram showing a method for QD-antibody (QD-Ab) bioconjugation: covalent coupling between carboxylic acid (-COOH) coated QDs and primary amines (-NH2) on intact antibodies using EDC as a catalyst (adapted from Xing et al., 2007).

1.3.3. Applications

QDs have physical and chemical properties that give advantages, like high photostability and bright fluorescence, in relation to classic fluorophores currently used. As such, they are often used in numerous

science applications like controlled drug delivery, imaging, cell labeling, biosensing, diagnosis, histochemistry and tissue engineered applications (Figure 1.10) (Chaudhuri and Paria, 2012).

Agrawal et al. have showed that QDs can be used for real-time detection of single molecules. They developed an immunoassay using antibodies conjugated to different QDs that would bind to different sites of the target biomolecules. If both QDs conjugated to antibodies bind at the same time, the signal is detected (Agraw et al., 2006).

Another important application is the molecular imaging *in vitro* and *in vivo*. Concerning the imaging, QDs are suitable for this due to their high photostability for extended periods of time and great resistance to phobleaching, without damaging the sample.

In cellular localization studies, QDs are used to clarify the dynamic properties of cell surface receptors (Dahan et al., 2003). Cellular labeling studies with QDs have been used as application in last years. It has been shown that cellular labeling with QDs take advantage to the standard fluorophores because it allows prolonged visualization of cells under continuous illumination just as multicolor imaging (Medintz et al., 2005).

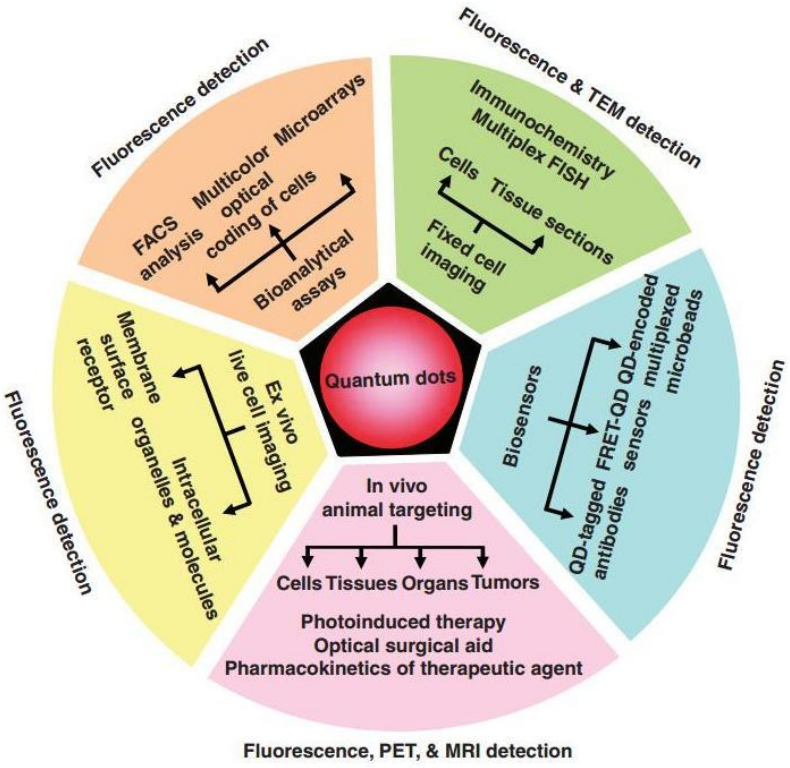

Figure 1.10 | Some applications of quantum dots as multimodal contrast agents in bioimaging (adapted from Michalet et al., 2005).

1.3.4. Cytotoxicity

The extensive use of QDs open questions about their toxicity. Quantum dots have raised concerns about their adverse effects in biological applications (cells and animals) because their chemical composition from highly toxic elements such cadmium and selenium (Smith et al., 2008) or presence of

alloys with unknown toxicological characteristics (Hermanson, 2008). To evaluate the utility of these nanomaterials, it's necessary to investigate their potential toxicity (Derfus et al., 2004).

QD toxicity depends on several factors that are related to their physicochemical properties and environmental conditions like size, charge, concentration, outer coating bioactivity (capping material, functional groups), oxidative state, photolytic and mechanical stability (Hardman, 2006; Male et al., 2008).

For QDs cores, the common used element is cadmium and studies have been done to quantify the amount of free cadmium ions (Cd^{2+}) in different biological systems (Derfus et al., 2004; Chang et al., 2006). Studies with cells exposed to QDs have shown that the cytotoxic effects come from the intracellular release of free cadmium ions from the QDs caused by the oxidative degradation of QDs (Kirchner et al., 2005). In fact, the cadmium has been reported as the main cause of cytotoxicity but there are other possible factors that contribute to the toxicity such as the catalysis for the formation of reactive oxygen species (ROS). To overcome these obstacles, an alternative solution is the addition of surface coatings. For this strategy, it has been used different kinds of coating comprising a semiconductor shell such ZnS or small ligands (Smith et al., 2008). The right capping of CdSe/ZnS QDs with hydrophilic coating demonstrated no adverse effects on cells in proliferation studies (Alivisatos et al., 2005; Jaiswal and Simon, 2004; Michalet et al., 2005).

Chang *et al* relates that is important to differentiate the origin of cellular toxicity, if it appear from the interaction of QD surface molecules with cell membranes or from the intracellular uptake of endocytosed QDs. Maysinger *et al* suggest two probable processes to elucidate why QDs lead to cell damage or/and death: leaching of constituent metals of the QDs core with comprised integrity (ions of Cd, Se, Pb, etc.) and/or formation of reactive oxygen species (ROS) as a consequence of cell-QD interaction (Maysinger et al., 2007).

It's obvious that QDs citotoxicity can be affected by several other factors but there are still others issues that need to be clarified and optimized, such as the diversity of surface coatings used, the differences in experimental conditions tested (like concentration used), the duration of QDs exposure to the cell or even the media chosen (Smith et al., 2008).

1.4. Intra-erythrocytic Parasite Infections

One area which is of clinical importance is the intra-erythrocytic infections and the way they affect red cells contents, function and membrane transport.

Parasites are microorganisms that live off other hosts to survive. They grow, reproduce and secrete toxins to the host that makes it sick. These parasitic infections are a big problem in tropical and subtropical regions. Malaria is an example of a deadly disease caused by an intra-erythrocytic parasite. Some of these infections propagated due to an insect which acts as a vector of the disease and transmits it while feeding the host (Cooke, B.M. et al., 2005).

Babesiosis is an infection caused by an intra-erythrocytic parasite of the genus *Babesia.* It is a common infection in mammalians that is propagated by ticks. Babesiosis is an emerging disease with a worldwide distribution. Despite the advances made in prevention of this disease, Babesiosis continues

to have a significant medical impact, so study towards diagnosis and treatment will be important to overtake that potential threat to the mammalians. In this disease the symptoms range from a silent infection until an acute, like malaria disease, resulting sometimes in death (Homer et al., 2000).

1.4.1. *Babesia ovis*

Plasmodium and *Babesia* are apicomplexan haemoprotozan parasites that infect red blood cells and cause severe diseases, namely malaria and babesiosis, with significant medical and veterinary importance. Comparing the cellular and molecular mechanisms, the pathogenesis of the diseases caused by these two organisms is notably similar. However, they are phylogenetically different. In the research of Malaria during the last years, various studies were concentrated on the parasites to comprehend the mechanisms that cause the parasite induced changes in red blood cells. Now, it's possible to apply this information to *Babesia* parasites. This relation can help to learn more about the biology of *Babesia* parasites, the way they cause infection and disease and how to develop novel therapeutic strategies or vaccines for these infections (Cooke, B.M. et al., 2005). Like *Plasmodium*, *Babesia* parasites can also be cultured *in vitro*. This characteristic together with the moderately short intracellular growth cycle time, becomes them ideal models to discover parasite red blood cell interactions (Jackson et al., 2001).

Similarly to Malaria, Babesiosis is a parasitic infection caused by haemotropic protozoa of the genus *Babesia*, family Babesiidae, order Piroplasmida, within the phylum Apicomplexa and is transmitted by the bite of an infected tick. These parasites infect the erythrocytes of an extensive diversity of wild and domestic animals. Along the years, *Babesia* has drawn attention as an emerging zoonotic problem because of the economic losses in cattle industry in various tropical and subtropical regions in the world (Silva et al., 2009; Horta et al., 2014). Normally, babesiosis reveals various symptoms such fever, extensive erythrocytic lysis leading to anemia, icterus, hemoglobinuria and death.

B. ovis is characterized by small round parasites, localized typically at the periphery of the red cell. This is transmitted by *Rhipicephalus bursa*. *B. ovis* is highly pathogen particularly in sheep. Mortality rates in vulnerable hosts vary from 30 to 50% in field infections (Aktas et al., 2005). This disease is considered economic important in terms of death cases, yield losses and the costs of treatment in the livestock industry (Sevinc et al., 2013). The RBC invasion is very similar to that for *B. bigemina* in which the parasite invades, grows and replicates asexually in erythrocytes of their vertebrate host, causing all the previously described symptoms.

As such, many studies have been done in order to control these diseases and various several diagnostic methods have been developed to identify early infections in whole blood. The standard diagnostic method of this kind of disease is based on visualization of the parasites in the erythrocytes in Giemsa stained blood smears by microscopic examination (Sevinc et al., 2013). In course of time, this method have been replaced by others methods in order to increase the sensitivity and specificity such as immunofluorescence assay (IFA), enzyme-linked immunosorbent assay (ELISA), polymerase chain reaction (PCR), reverse line blotting (RLB) and Flow cytometry too. (Bose et al., 1995; Homer et al., 2005; Costa-Junior et al., 2006; Schnittger et al., 2004; Wyatt et al., 1991).

Babesia parasites have a complex life cycle that can be divided into three main stages: gamogony, sporogony and merogony. When there is a bite from an infected tick, the sporozoites of *Babesia* can directly invade the host erythrocytes and suffer an asexual growth cycle in the erythrocytes stage as shown in figure 1.11 (Vial and Gorenflot, 2006; Yokoyama et al., 2006). Once already inside the erythrocyte of the host, the sporozoites divide into two or sometimes four merozoites which follow an asexual reproduction also known as merogony. Subsequently there is a rapid intracellular multiplication which leads to a destruction of the host erythrocytes with release of new parasites that will infect and lyse other erythrocytes (Vial and Gorenflot, 2006). However, the molecular interactions between *Babesia* merozoites and host erythrocyte and their biological roles are not totally understood (Yokoyama, 2006).

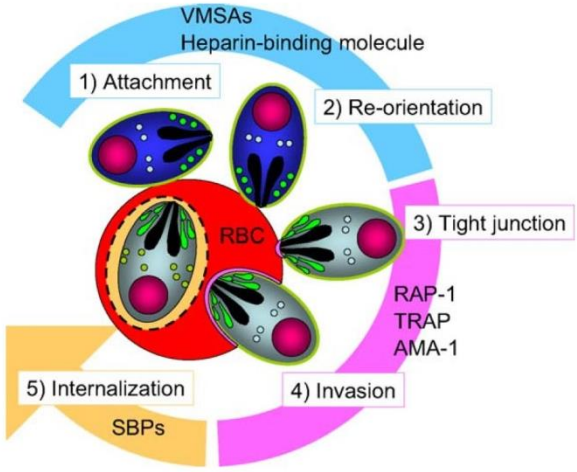

Figure 1.11 | Schematic representation of erythrocyte invasion by *Babesia* parasites. The whole process comprised essentially five steps: (1) Attachment of the parasite onto the host RBC. (2) Re-orientation of the parasite. (3) Formation of tight-junction between the the apical part of parasite and erythrocyte surface. (4) Invasion. (5) Internalization of the parasite within the infected RBC (adapted from Yokoyama et al., 2006).

Apicomplexans utilize several molecules (ligands) in their invasion process. In the stage of erythrocyte invasion, the *Babesia* parasites coat the extracellular merozoites, using their surface molecules, promoting the attachment to RBCs. During the invasion process and after their attachment, apicomplexan parasites secrete proteins from their apical organelles onto the merozoite membrane or into the environment outside the parasites. For *Babesia* parasites, these proteins are situated in the anterior end of the parasites also denominated apical complex and includes the rhoptries and micronemes proteins and spherical body. After the intracellular internalization of protozoan parasites in the host cell environment, some proteins are liberated into the cytoplasm of the infected erythrocytes with the view to promote an optimal environment for the parasites (Yokoyama et al., 2006; Gohil et al., 2010).

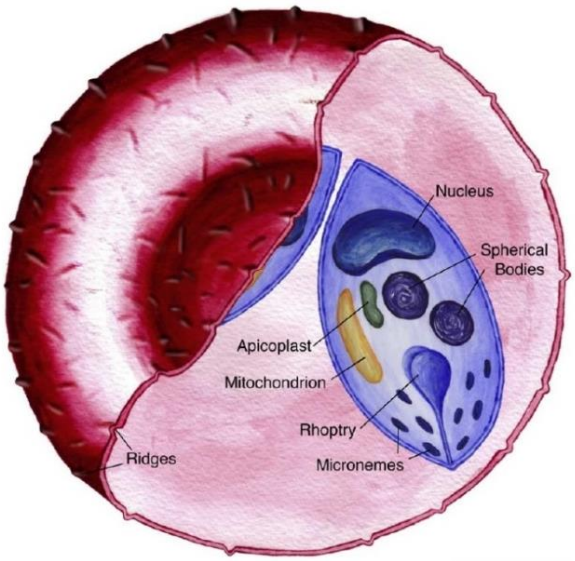

Figure 1.12 | Schematic representation of a bovine RBCS with *Babesia bovis* parasite. Apical organelles and different proteins within the parasite that are involved in erythrocyte invasion are also shown as well as the formation of ridges on the surface of the infected RBC (adapted from Gohil et al., 2010).

Micronemes are small, cigar-shaped organelles that cluster at the apical end of protozoan body and their number is different according to the species and the development stages (Figure 1.12). There are two invasion molecules considered in micronemes products (in *B. bovis* too merozoites): The apical membrane antigen 1 (AMA-1) and the other, thrombospondin-related anonymous protein (TRAP), with 82 and 75 kDa respectively. The AMA1 is expected to be implicated in RBC invasion and TRAP in recognition and possible attachment and invasion of host erythrocytes (Yokoyama et al., 2006; Gohil et al., 2010).

AMA1 is a type I transmembrane protein that is found on the surface of the invasive forms of parasites. It is an asexual blood-stage protein expressed in the invasive merozoite from Apicomplexan parasites (Triglia et al., 2000). The development of a vaccine is an urgent priority because is knwown that methods used to control the clinical signs, leave carcinogenic substances in sheep and goat milk (Carletti et al., 2016). The study of the protein molecules expressed on the surface of merozoites is relevant for the development of potential vaccine candidates. AMA1 might be a key vaccine candidate because it is expressed in the asexual life cycle of this parasite (Narum and Thomas, 1994) because it was observed that antibodies which target the extracellular domain of AMA1 block the invasion of erythrocytes (Thomas et al., 1984).). Due to the involvement of AMA1 in the invasion process by parasite, the study of this protein and the RBCs with microfluidic, open new possibilities to continue a detailed investigation in order to achieve the treatment of this disease.

1.5. Membrane Proteins

Membrane is a physical barrier that separates a cell from its surrounding environment. It plays an important role regulating the exchange of materials between cells and exterior. Red blood cell membrane is composed by a lipid bilayer (41%), membrane proteins (52%) and carbohydrates (7%).

Membrane proteins are divided into peripheral proteins and integral proteins. Peripheral proteins are located on cytoplasmic surface of lipid bilayer and anchored via integral proteins. They are responsible for membrane elasticity and stability. Integral or transmembrane proteins (TP) are embedded in membrane via hydrophobic interactions with lipids. These proteins are involved in such important biological cell functions, like virus binding, cell surface antigenicity, cell-cell recognition and communication, cellular transformation, transport, energy transduction etc. In red blood cell membrane, there are three types of TPs: Band 3, Glycoproteins and Aquaporins.

Glycoproteins are proteins with covalently bounded carbohydrates. They were classified into sialoglycoproteins which are a combination of sialic acid and glycoprotein, i.e, a combination of sugar and protein. These sialoglycoproteins are rich in sialic acid which give the erythrocytes a very hydrophilic charged coat. Approximately 10% of erythrocyte membrane is covered by sialoglycoproteins and their sialic acid content gives negative charge on the cell surface, preventing adherence of RBCs to each other and to vessel walls (Viitala and Järnefelt, 1985).

Membrane cells are constituted by several target proteins of currently available drugs for treatment of diverse disorders. So, studying this cell component, is possible to develop new tools to label the known targets or even identify new ones.

1.5.1. Glycophorin A

Sialoglycoproteins are also known as Glycophorins (GP). They are composed of 60% carbohydrate including sialic acid and 40% protein. The existence of glycophorins in erythrocyte membrane was discovered by Fairbanks et al. There are four different types of glycophorins and they comprise approximately 2% of the total RBC membrane protein (Fairbanks et al., 1971). These include Glycophorin A (GPA), B (GPB), C (GPC) and D (GPD) which belong to a group of important transmembrane proteins that play an important role in cell-cell interactions (Tomita and Marchesi, 1975).

Table 1.1 | RBC membrane glycophorins (adapted from: Chasis and Mohandas, 1992).

	GPA	GPB	GPC	GPD
Copies per cell ($\times 10^3$)	500-900	80-30	50-100	20
Molecular mass (kDa)	36	20	32	23
RBC specific	Yes	Yes	No	Unknown

Glycophorin A is the most abundant, constituting approximately 75% of the total sialoglycoproteins in erythrocyte membrane (Furthmayr et al., 1975) with 5 to 9 × 10^5 copies per cell. GPA was the first membrane protein to be isolated and sequenced and has been used as a model for topology of receptors and other transmembrane glycoproteins in surface cells (Tomita and Marchesi, 1975) (Table 1.1). This glycophorin is exclusively expressed in erythroid cells (Gahmberg et al., 1978; Yurchenco and Furthmayr, 1980).

Initially, the hematologic interest in glycophorins was restricted to blood bank serologists and the characterization of blood group antigens situated on these type of proteins. Nevertheless, with more recent functional studies, it is become notorious that some glycophorins also play different but important roles in regulating RBC membrane mechanical properties and in maintaining RBC shape. As well as play a crucial role in modulating RBC-RBC interactions, they also modulate the RBC interactions with vascular endothelium and other circulating blood cell, avoiding the RBC interaction (Figure 1.13) (Dahr, 1986).

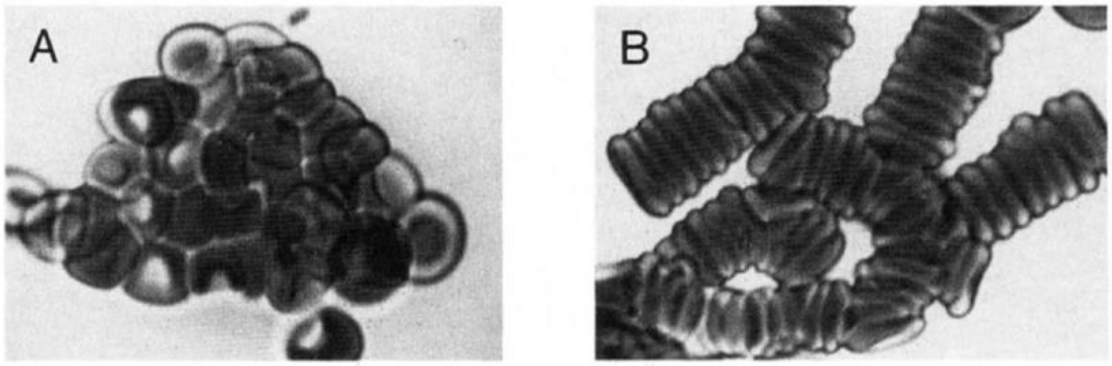

Figure 1.13 | Red blood cells interactions. (A) RBC aggregation due to strong associations, for example such as those originated by Ig binding. This type of aggregation needs much bigger forces for cell dissociation. (B) Aggregation resulting from weak cell to cell interactions, which occurs physiologically and overcome the repulsive negative charge of the surface but are easily dissociated (adapted from: adapted from: Chasis and Mohandas, 1992).

RBC membrane have glycophorin variants and deficiencies that were initially discovered by serological and immunochemical assays and later, characterized at a molecular level. These different phenotypes have some particular interest due to the functional role of glycophorin in the membrane. In pathological genetic conditions where GPA is not present, cells appear to exhibit normal physiologic properties. As such, individuals with this different phenotype are clinically healthy showing no observable changes in erythrocyte morphology and do not present anemia (Chasis and Mohandas, 1992).

An interesting and relevant data is the discovery that GPA also works as a receptor for infective agents like *P. falciparum* and may function as a chaperone which is a protein that assists the assembly or disassembly of other macromolecular structures. This function enables the targeting of specific transmembrane proteins to the cell membrane. A protein from malarial parasite was isolated and it was verified that it combines in a specific way with glycophorin A, showing that this glycoprotein has a receptor function for malarial parasite and in this process the sialic acid content of glycophorin A are involved since this interaction is inhibited by sialic acid. Therefore, GPA is a likely RBC surface attachment site for *P. falciparum* (Vanderberg et al., 1985). Due to the presence of GPA in erythrocytes and its involvement in RBC invasion by malarial parasite which is notably identical to Babesiosis, the intra-erythrocytic disease under study, make this glycoprotein a good model for the following assays.

Moreover, glycophorin A works as a major receptor for encephalomyocarditis virus, influenza virus and *M pneumoniae*. This protein is also involved in some red blood cell diseases such as leukopenia and thrombopenia. It's possible that it play a role in the aging mechanism of the red cell even as in

binding of some important metal ions for example, Mg^{2+} and Ca^{2+} to the red cell membrane. It's also a receptor for enterotoxigenic *E.coli* (Tayyab and Qasin, 1988).

1.6. Nanotoxicology

An important area of the nanotechnology field of knowledge is the nanotoxicology. It refers to the study of the concentration of nanomaterials with biological entities. This study is centered on the relationship between the physical and chemical properties (e.g. size, shape, surface chemistry, compositions and aggregation) of nanostrcutures with the induction of toxic biological responses. This type of information is important to characterize the nanomaterial applications in areas like biotechnology, biomedical applications and toxicity screening.

Quantum dots are composed by metallic elements like cadmium and selenium and their impact in cells and tissues is subject of study. Due to their chemical composition, they rise concerns about their biological interaction. As a result, their cytotoxic effect through the induction of oxidative stress was evaluated (Santos, 2009; Qu et al., 2013).

1.6.1. Reactive Oxygen Species

The term ROS (Reactive Oxygen Species) is used to characterize forms of oxygen that are energetically more reactive than molecular oxygen. ROS are an essential component in stress responses and its level defines the type of response (Shao et al., 2008).

Cells are sensitive to ROS and when their production exceeds the antioxidant defense, cellular redox balance is shifted and the cells are then in a state of oxidative stress. This sensitivity to ROS is dependent on the cell type, the level and the duration of oxidant production, the species of ROS originated and the specific site where ROS are produced (Maysinger et al., 2007).

These species are constantly produced within red blood cells, as a consequence of their physiological role. The main function of erythrocytes is to transport large amount of oxygen (O_2) and mediation of carbon dioxide (CO_2) production during their lifetime, resulting in oxidative stress. Studies indicate that many physiological and pathological conditions such as inflammation or eryptosis for example, are developed through ROS action (Çimen, 2008).

The interest in ROS have increased as agent of pathological state. Even without mitochondria, ROS are constantly produced in erythrocytes due to the high O_2 tension in arterial blood and their rich heme iron content (Baynes, 2005). These species are formed by the one or two electron reduction of O_2. They are oxygen-centered molecules which contain non-radicals hydrogen peroxide (H_2O_2) and singlet oxygen even as radicals superoxide anion ($O_2^{\bullet-}$), hydroxyl radical ($HO^{\bullet}$) and nitric oxide (NO). They are formed in small amounts through the normal metabolic processes. The addition of one electron to O_2 produces the $O_2^{\bullet-}$ while the addition of two electrons origins H_2O_2 (Figure 1.14). H_2O_2 can react with $O_2^{\bullet-}$ and ferric ions to produce the highly reactive $HO^{\bullet}$ (Cheesman and Slater, 1993). Under pathological conditions, ROS are formed with high concentration and can oppress cellular defenses leading to cellular damage, acting as both oxidizing and reducing agents (Al-Omar et al., 2004). Many factors can generate oxidizing radicals in erythrocytes. The source of ROS in red blood cells is the oxygen carrier protein Hgb that suffers autoxidation to produce $O_2^{\bullet-}$.

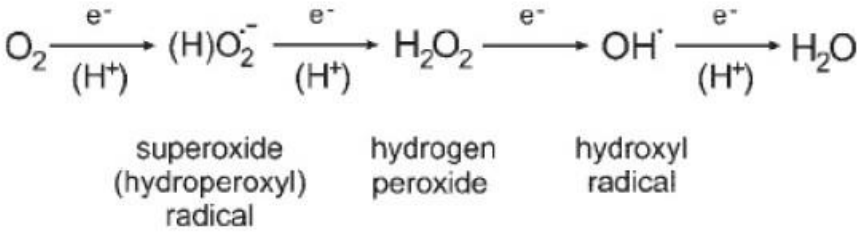

Figure 1.14 | Representative scheme of ROS generation through the reduction of molecular oxygen (adapted from Gechev et al., 2006).

High levels of ROS can result in non-controlled oxidation of a variety of cellular structures, including membrane damage (Apel and Hirt, 2004) and can provoke apoptosis or necrosis according to the level of damage (Maysinger et al., 2006). RBCs are constantly exposed to both endogenous and exogenous source of reactive oxygen species (ROS) and studies have demonstrated that oxidative stress plays an important role in damaging the RBC membrane and improving its deformability (Mohanty, J.G. et al., 2013). So, this study can be used as a model for the oxidative damage of RBCs functions during their long journey in the blood stream.

RBCs were incubated with chosen QDs to evaluate their cytotoxic effect. The induction of oxidative stress is an important toxic feature of nanomaterials (Hoet and Boczkowsky, 2008). QDs are redox active nanoparticles (effective donors and acceptors) and can generate highly reactive free radicals with exposure to light. Since this technology is to be used in live cells, its potential cytotoxic effects is an essential factor to be considered because it may affect the cell physiology. The size, charge and concentration of the QDs, their outer shell bioactivity and oxidative, photolytic or mechanical stress are all factors that, collectively and individually, can determine their cellular toxicity. The literature on toxicity of QDs is a mix of reports of numerous type of QDs with widely varying physicochemical parameter, making comparisons a quite difficult. So it is imperative to test the used QDs in our cell model to evaluate its toxicity because the unknown interferences of these nanoparticles with physiological processes could lead to misinterpretation of the results, whatever the application for.

1.7. Microfluidic

Microfluidic is characterized by the study and control of the fluidic behavior in microstructures (Zare et al., 2010). It deals with fluid flowing inside narrow channels (< 100µm) with external control devices. This approach allows reduced reagents, high efficient template concentrations in small volumes, scalability, easier automation, improved cell manipulation and multi-step integration (Lecault et al., 2012). Usual microfluidic channels have dimension between tens and hundreds of microns that are comparable to the size of single cell (Schmid et al., 2010). The area of microfluidics has emerged as a powerful tool to investigate the complexity of cellular systems (Whitesides, 2006). To not disturb the biochemical pathways or molecules of interest, cells must be manipulated gently before analysis. Microfluidic devices (Figure 1.15) are platforms which allow the rapid analysis of single cells. These devices enable the integration and automation of cell and high efficiency separations (Roman et al., 2007). Even more, microfabricated devices for sample preparation would open new opportunities by

enabling comprehensive genomic and proteomic analysis from small homogeneous subpopulations down to single cells (Toner and Irimia, 2005).

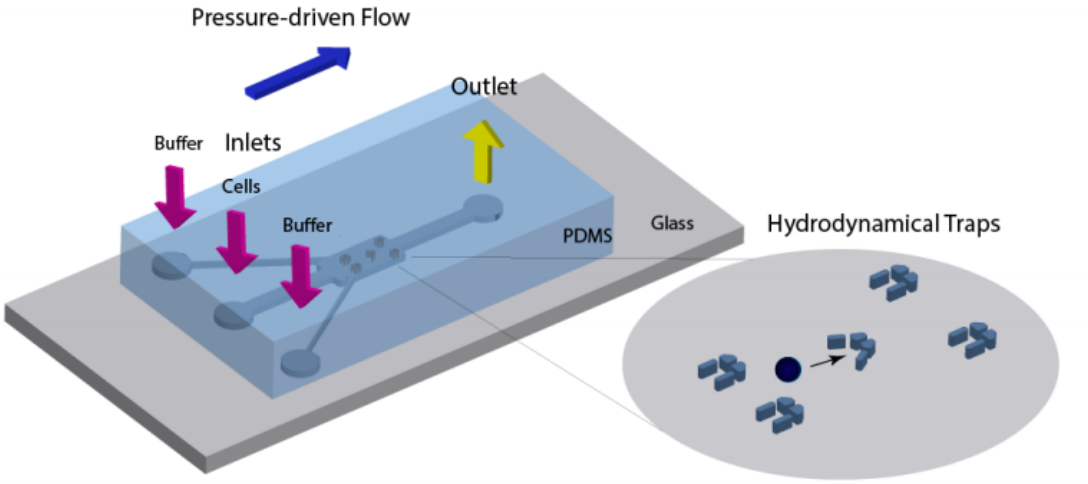

Figure 1.15 | Representation of a microfluidic device: a PDMS chip consisting of microchannels containing arrays of V and U chapped hydrodynamical traps.

1.7.1. Blood-on-a-chip

Blood sampling and analysis are of great interest for medical and science applications and play a crucial role in diagnosis of various physiologic and pathologic conditions (Toner and Irimia, 2005). However, this requires a deep understanding of the biology involved and the use of appropriate techniques.

In the early steps of blood research, the observation of the cells was made by microscopes. Later, tissue-staining techniques were developed enabling the initial characterization of populations. Even nowadays, the analysis of cell morphology of the peripheral blood is done with Wright-Giemsa staining protocols and the full blood count are the most basic and used techniques in investigations in hematology (Bauer, 1999). Flow cytometry techniques used nowadays offer higher capability because of its advanced details and higher throughput, representing a major advance in cell identification and separation. Nevertheless, the complexity of this technique needs higher specialization of the operator. To reduce the possible errors, it is necessary to reduce the time from blood collection to analysis. The availability of analysis techniques at the site where blood is collected is considered a challenge that would need faster, cheaper and simpler approaches (Toner and Irimia, 2005). For these reasons, a microfluidic chip was developed to trap red blood cells.

1.7.2. Microfabrication

Microfabrication is characterized by the process of producing systems with micrometric structures. This platforms fabrication can be obtained through several approaches, such as photolithography, replica molding, micro contact printing, micro machining and hot embossing (Meira, 2015). Microchips

fabrication is based on photolithography. It is a modeling method that uses irradiation to transfer a pattern to a substrate. This technique allows the obtention of direct replica of a plastic, glass or silicon wafer. This replica can be repeated several times for obtaining a functional micro-device (Meira, 2015). The irradiation through a mask with photoresist layer allows the selective removal of resist in the development (Franssila, 2010). Photoresists are photosensitive polymeric materials that are used to create a patterned coating on a surface. These type of materials allowed the reduction of structures downwards to 100nm. Photoresists can be positive or negative, property which define their susceptibility to UV rays. In case of positive photoresists, the exposed zones become soluble in the developer and consequently, the unexposed areas remains insoluble. On the other hand, with negative photoresists, the exposed areas are insoluble to the developer and the unexposed become soluble (Franssila, 2010). Among the photoresist frequently used in microfabrication are negative SU-8 or P-50100. There is also a positive variant, the novolac resin SPR 220-7 (Meira, 2015).

The crucial step in whole chip microfabrication is the production of the SU-8 mold to create PDMS replicas because PDMS replicates with very precision all the features of the master mold so any defect will affect the PDMS chip structure. PDMS (Polydimethylsiloxane) is a silicon based elastomer and it presents a hydrophobic surface. This is the most used material in microfluidics due to its transparency, elasticity, and low cost. In addition, it can be bonded without adhesives and it can be easily structured by molding with nano-precision but for this purpose, it requires a mold. For this, Si wafer is coating with SU-8 to originate a mold (Figure 1.16: A – E). A master consists of a positive relief of photoresist on a silicon (Si) wafer and serves as a mold for PDMS (Figure 1.16: E). The master is covered with this silane derivative to simply the peeling of the replica (F and G). SU-8 is a thick photoresist i.e. a polymer which can be patterned using light and it's the most used material for high and narrow microstructures. This photoresist has excellent chemical, optical, mechanical and thermal properties. So, the SU-8 and PDMS is the most used combination in microfluidic.

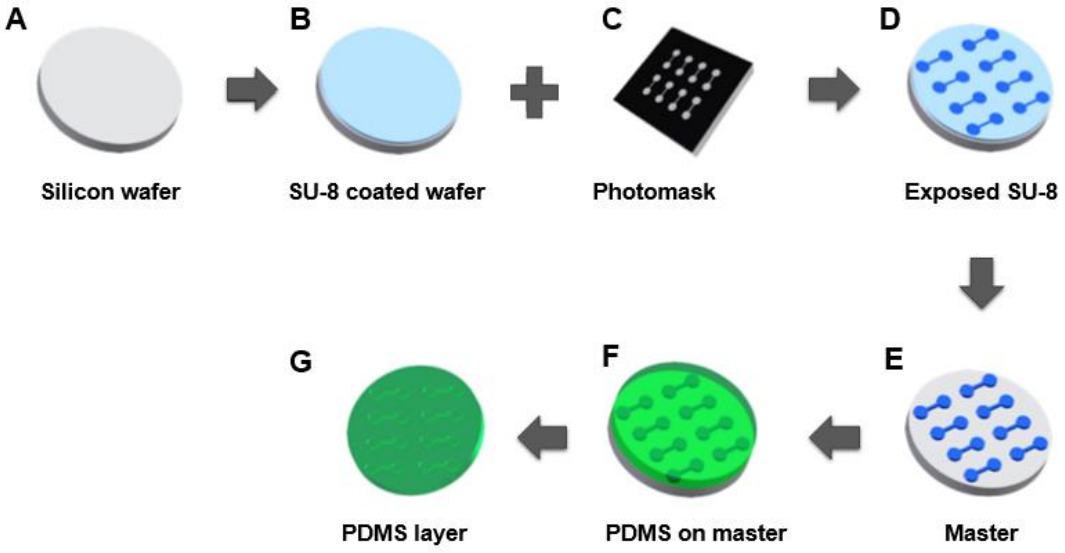

Figure 1.16 | Representative scheme of PDMS microfludics fabrication. (A) A cleaned silicon wafer is the substrate on which features will be patterned). (B) SU-8 epoxy photoresist is spin coated onto the wafer and a photomask will define the features to be patterned (C). (D) The SU-8 photoresist is exposed to UV light to become the patterned area insoluble in developer solution. (E) Unexposed regions are removed by a developer solution leaving a negative 3D image of the final PDMS pattern. (F) PDMS is mixed and poured onto the master into the desired pattern. (G) PDMS layer is peeled off of the master and can be used to make devices. The master can be reused (adapted from: https://cleanroom.soe.ucsc.edu/microfluidics).

The process of microfabrication of a microfluidic chip starts with the design of a system of channels in a CAD program. A commercial printer uses the CAD file to produce a high resolution transparency mask. This transparency is used as a photomask in contact photolithography to produce a master and here, the replica molding process starts.

In turn, soft-lithography is a low cost production method based on elastomeric stamps, allowing the creation of three-dimensional patterns at room temperature. This process include some methods and one of the most common is the replica moulding (casting), i.e, the transfer of a pattern from a master into replica by solidifying a liquid precursor against the master (Elhadj et al. 2010). It is considered one of the main techniques in microfluidic production due to its lower coast (Figure 1.17).

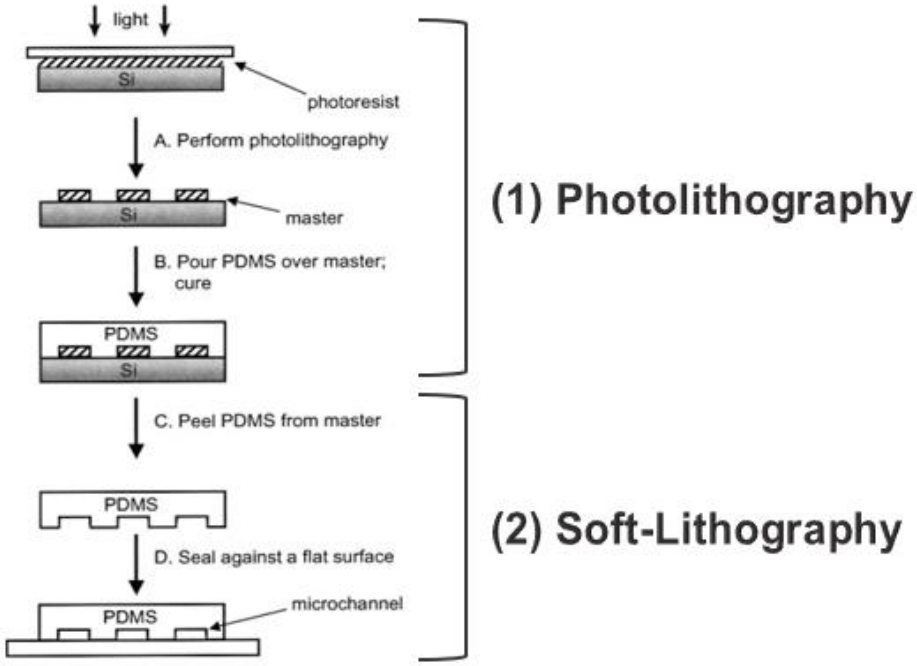

Figure 1.17 | Representative scheme of photolithography and soft-Lithography process. Photolithography (1) followed by soft-lithography (2) allow to obtain a direct replica of the inverse mask (negative resist) (A), (B) and (C), after the UV exposure and development. At the right time, deposition and etching can be performed through the addition and subtraction to achieve the desired pattern (D) (adapted from Meira, 2015).

After crosslinking, the replica is peeled off the mould. Finished this step, the replica can be used directly to produce chips, or for the casting of subsequent chips, to prevent damage of the master. Here, it is common to use an epoxy mould from PDMS mould. The use of epoxy allows an increase of the number of replicas. Finally, the replica is cut into individual chips and access holes for inlet and outlet are made through a sharp tip. In the end of the process, chips are sealed to a glass slide, closing the cannels from the bottom.

Chapter 2 | Materials and Methods

2.1. Blood collection

For studies with intra-erythrocytic infections, in particular *Babesia ovis* culture *in vitro* and identification of AMA1 protein, ovine blood was collected and subsequently processed. In trials to identification of Glycophorin A protein and to investigate the oxidative stress produced by cells when incubated with QDs, human blood was used.

2.1.1. Uninfected ovine RBCs for subculturing

Desfibrinated ovine blood (Oxoid) was collected from healthy ovine donors. The blood was separated in two falcons of 50mL for packed RBCs and it was centrifuged during 20 min, 2500 rpm at 4ºC. The supernatant was collected to another falcon and this is the serum. Then, the RBCs were washed in VyM (Vega et al., 1985) to reach the final volume of 50mL. Two more centrifugations were made and the final RBCs are stored at 4ºC.

2.1.2. Human Blood

The human blood samples were obtained following the standard international rules of WMA Declaration of Helsinki – Ethical Principles of Research Involving Human Subjects. A few drops of blood was collected by pricking the finger of volunteers and then the sample was preserved in 200 µL of 2.1% sodium citrate to not coagulate. The blood was centrifuged (10 min, 2500 rpm at 4ºC) and the supernatant was discard. Pellet was washed in 1x PBS. The final sample was stored at 4˚C.

2.2. Quantum Dots

The ability to bioconjugate QDs makes them suitable for applications as biological label, immunostaining or as live cells markers. Their chemical composition can be determinant for subsequent assays. Preliminary experiments are necessary to choose the appropriate type of these nanoparticles before their use with cells. As such, three types of water soluble CdSe/ZnS quantum dots were bought from Ocean Nanotech manufacturer in order to assess which ones were suitable for the cells being studied.

2.2.1. Characterization of Electrophoretic Mobility and pH stability

The QDs were tested at different pH conditions in agarose gel to evaluate changes in fluorescence intensity and to observe their migration profile. It is a technique suitable also for estimation of the nanoparticle size

In terms of pH, 50nM solutions of each type of QDs were diluted from their corresponding stock solutions (1.6µM for all of them) in 10mM Na-P buffer in the pH range between 5 and 8. An agarose gel electrophoresis was done in 1x TBE pH 8.4 (containing Tris base, boric acid and

EDTA 0.5M) diluted from the 5x stock solution with bidistilled water. The 1% agarose gel was prepared by dissolving under heating 0.5g of agarose (Thermo Scientific) in 50mL of 1x TBE and 2.5µL of SYBR® safe DNA gel stain (Thermo Scientific) were added. 5µL of each QD solution previously prepared were mixed with 2µL of 6xDNA loading dye (Fermentas), before loading onto the gel. 4µL of 1kb and 5µL of 100bp DNA ladder (Fermentas) were loaded onto the gel for estimation of the size of each type of QDs. The gel ran at 100V during 90 minutes using a Mini-Sub Cell GT system (Biorad) and was visualized under blue sample tray (suitable for gels stained with SYBR® stain) using Gel Doc™ EZ Imager and Image Lab™ software.

2.2.2. Bioconjuagtion of antibodies to QDs

The QD conjugation was performed by direct conjugation of antibodies to carboxy-QDs through amine-carboxylic acid coupling using EDC/NHS chemistry. This protocol is divided into three steps: the QDs activation with EDC and NHS solutions, the bioconjugation of activated QDs with antibodies and the purification and concentration of final bioconjugates.

EDC and NHS stock solutions were prepared to a final concentration of 2.2mM for EDC (Thermo Scientific) and 4mM for NHS (Acros Organics) both dissolved in Na-P buffer, yielding a final volume of 1mL. To QD activation, 0.1nmol of carboxy-QDs (Ocean NanoTech) from a 2µM stock solution of COOH-QDs (50µL) were mixed with 10µL of a 2.2mM EDC solution and the mix was slowly shaken during 30 minutes at room temperature and in dark. 10µL of a 4 mM NHS solution and 30µL of buffer (to reach a final volume of 100µL where QD concentration is approximately 1µM) were added and once again, the solution was slowly shaken for another 30 minutes under the same conditions. Then, 900µL of buffer were added to activated QDs diluting them to a final concentration of 100nM and subsequently they are purified by dialysis (Medicell Membranes Ltd, MWCO: 12-14000 Daltons cut-off) overnight, without shaking, at 4°C in dark, against Na-P buffer to remove the excess of EDC and NHS reagents. To link the activated QDs to antibodies, 0.4nmol of antibody (Mouse anti-Glycophorin A, Diagnostics BioSystems and Rabbit anti-AMA-1) i.e, 318µL from a ~1mg/mL stock solution and 136µL from ~0.5 mg/mL stock solution, of yielding a QD/Ab molar ratio of approximately 1:4, were mixed with previously dialyzed overnight activated QDs solution following the addition of buffer for a final concentration of QDs around 50nM. This final reaction was incubated 4 hours at room temperature, with slowly shaking and in the dark. To eliminate any activated carboxy groups that are not linked to antibodies, 1µL of a 100mM stock solution of ethanolamine (Sigma) was added (using a QD/ethanolamine molar ratio approximately 1:940) and the final solution was incubated overnight at 4°C, with slowly shaking and in the dark. After incubation, the solution was purified against buffer to remove the excess of ethanolamine added by dialysis (Medicell Membranes Ltd, MWCO: 12-14000 Daltons cut-off) under same conditions. For purification and concentration of the final bioconjugates, the final solution was purified using centrifugal filtering devices (Vivaspin 500, cut-off 100 kDa). The bioconjugated samples were washed by centrifuging (Heraeus Sepatech, model Biofuge 13) at 2000g, 5 minutes at room temperature. This procedure was repeated three times to guarantee

the total removal of possible free antibody in solution. The final QD-antibody sample can be diluted to a desired concentration.

2.2.2.1. Characterization of conjugated QDs

Agarose Gel Electrophoresis

The characterization of the QD-Ab conjugates was performed by agarose gel electrophoresis. Free COOH-QDs and free antibodies were used as control.

The procedure followed this protocol: 2µL of each bioconjugation resulting sample as well as 2µL of 50nM free COOH-QDs and 2µL of free antibody solutions were mixed with 2µL of 6xDNA loading dye, making a final volume of 10µL with 10 mM Na-P buffer. The final samples were loaded onto the gel. The 1% gel was previously prepared by heating 0.5 g of agarose in 50 mL of 1x TBE buffer, without adding SYBR® safe DNA gel stain. 6µL of 1kb DNA ladder was also loaded onto the gel to possible estimate the molecular weight. The electrophoresis was conducted at voltage ranging 45 to 90V during 2h15min because the high molecular weight of the final bioconjugates. The gel was visualized under UV sample tray (suitable for gels using ultraviolet illumination) using Gel Doc™ EZ Imager and Image Lab™ software.

SDS-PAGE Electrophoresis

Samples of antibody-QD conjugates, free antibodies and free QDs were analyzed by SDS-PAGE electrophoresis (Bolt and Mahoney, 1997), in reduced and non-reduced conditions. In the non-reduced conditions, 5µL of each bioconjugate sample were used. Then, 5µL of Loading Dye non-reduced (10% v/v glycerol in water and bromophenol blue to the desired coloring) were mixed. 3µL of 50nM COOH-QDs control was mixed with 3µL of Loading-dye non-reduced while 2µL of each antibody control was mixed on the same proportion as the loading dye. For the reduced conditions, the same number of samples were prepared in the same way but mixed with Loading-dye mixed with Dithiothreitol (DTT, Sigma) at a concentration of 0.1M (1:1, 2.5µL of DTT+2.5µL of Loading dye). All the samples were loaded into the 4-15% gradient precast gel (Biorad) as well as the 5µL of protein ladder (MW 20-250 kDa, NZYTech) to estimate the protein molecular weight. The gel was run for 1h30 minutes at a constant voltage of 120V in Tris-Glycine 1x Running Buffer diluted from a 10x stock solution (250 mM Glycine, 1.92 mM Tris-base and 1% SDS) previously prepared. In the end, gel was visualized using a gel imaging instrument Gel Doc™ EZ Imager with UV Tray.

Western Blotting

The Western Blot analysis was carried out following the standard western protocols (http://www.abcam.com/ps/pdf/protocols/WB-beginner.pdf). Three filters and one filter paper (Thermo Scientific) were soaked in Transfer buffer pH 8.3 (Tris base 25mM, Glycine 192mM, 0.1% w/v SDS and 10 % v/v MeOH all purchased from Sigma) previously prepared. A 0.45 µm PVDF blotting membrane with low auto-fluorescence (Immobilon™-FL, Millipore) with the same size of the gel to be blotted (10 x 10 cm) was cut and wetted in a plastic box with approximately 5mL of 100% MeOH and equilibrated for 5 minutes with Transfer buffer. The previous soaked

three filters and one filter paper as well as the gel and the membrane were placed in the semi-dry system (Xcell II™ Blot Module, Life Technologies). One more filter paper and three more filters were placed in the same semi-dry system in this order over the remaining pieces for membrane transfer. The transfer was performed for 1 hour at 30V at room temperature. After the transfer, the membrane was softly washed with approximately 20 mL of TBS 1x pH 7.6 (Tris-buffered saline: Tris-HCl 10mM and NaCl 150mM) with constant agitation at room temperature. Then, the membrane was blocked with 40mL of freshly prepared Blocking buffer (5% w/v non-fat milk and TBS 1x) overnight at 4ºC with slowly agitation. The membrane was cut and incubated with secondary antibody anti-mouse IgG and anti-rabbit with HRP conjugate (R&D Systems), previously diluted in Blocking buffer (1:5000) for 2 hours at room temperature under shaking conditions. Then, it was washed twice with approximately 20mL of T-TBS (TBS 1x containing 0.05% Tween 20, Sigma) for 5 minutes each time with slowly agitation at room temperature, followed by one more wash with just 20mL of 1x TBS under the same conditions. To visualize the immunoreactive proteins, a detection reagent was used (Western Lightning ECL Pro, Perkin Elmer Life Sciences) and the images were obtained in a molecular imager ChemiDoc, using the Quantity One software, in Chemiluminescence mode and the bioconjugated QDs was visualized under the UV-Light in the same molecular imager.

2.3. *Babesia ovis* infected cultures

One goal of this work was to create a label tool to identify the AMA1 in the RBC membrane through the conjugation of QDs with a specific antibody for this transmembrane protein. As previously described, AMA1 is expressed on the surface of erythrocytes invaded by *Babesia* parasites. As such, it was necessary to use an *in vitro* culture in order to obtain infected erythrocytes to test with bioconjugates obtained by the process described in section 2.2.2.

2.3.1. *In vitro* cultivation of *Babesia ovis*

Portuguese strain of *Babesia ovis* was isolated and cryopreserved in a tank of liquid nitrogen. For each isolated cryotube, 46mL of complete culture medium were prepared according to the table 2.1. The sera used was commercial (Gibco). From Portuguese *B.ovis* collection available in the lab, the used parasite was from the cryotube number 620 collected from the field in 16.4.2014 with a 5% of parasitemia.

Table 2.1 | Complete medium prepared with commercial serum

Complete medium	mL (x1)	mL (x46)
TES buffer 1M (1:50) (Sigma)	0.02	0.92
Ovine sterile serum (20%) (Life Technologies)	0.2	9.2
Medium M199 (Gibco)	0.767	36
Antibiotic/Antimycotic (1:500) (Gibco)	0.002	0.092
Bathocuproinedisulfonic acid 0.02M (Sigma)	0.01	0.46
L-cysteine 1mM (Sigma)	0.001	0.046

The HEPES-buffered medium M199 is composed by L-glutamine and L-aminoacids. To start the culture, each cryotube was thawed, placing it inside a goblet with warm water and agitated. When the cryotube content started to melt, it was transferred to a 50mL falcon filled with 46mL of complete medium. Next, the cryotubes were centrifuged at 1300 rpms, during 15 minutes at 4ºC and the, the supernatant was discarded and replaced by 2mL of RBCs with complete medium with 10% of RBCs, collected as described in section 2.1.1.

Lastly, 2mL of each culture was placed in a plate of 24 wells and placed inside the inoculation chamber and filled with a mixture of gases 5% CO_2, 2% O_2 and 93% N_2 at 37ºC (NuAIRE, Nu4750E).

Changing the culture medium

To continue the cell culture growth, new fresh culture medium had to be prepared every 48 hours and changed every single day. 6mL of fresh culture medium was prepared using the sera of the blood, according to Table 2.2.

Table 2.2 | Fresh culture medium composition

Complete medium	mL (x1)	mL (x6)
TES buffer 1M (1:50)	0.02	0.12
Ovine sterile serum (20%)	0.2	1.2
Medium M199 (Gibco)	0.767	5
Antibiotic/Antimycotic (1:500)	0.002	0.012
Bathocuproinedisulfonic acid 0.02M	0.01	0.06
L-cysteine 1mM	0.001	0.006

From the culture wells, 1mL of old medium was discarded and replaced by new fresh complete medium. The 24-well plates were placed again inside the incubation chamber and with the same gases mixture and temperature as before. When parasitemia reaches 1%, is necessary to split the culture 1:2 for two wells.

Preparation of smears

2µL of culture was pipeted and put on a clear microscope slide to prepare the smear. With assistance of another microscope slide at a 45˚ angle, creating a thin film of infected blood spread over the glass slide. The smears were stained by Giemsa (Merck). For this purpose, the microscope slide was placed for a minute inside a glass staining box filled with methanol. Next, the slides was taken off and dried in the air. Then, the Working Giemsa staining solution was prepared: 40 mL of Working Giemsa buffer were added to 1 mL of commercial Giemsa stain (previously filtered) and to 20µL of Triton X-100 (USB). The slides with smears were immersed in that solution during 15 minutes. In the end, they rinsed cautiously with running water and dried in the upright position. The parasites presence was observed in the inverted microscope using the immersion oil objective 100x. The parasitemia was calculated as it follows, using the ImageJ software. All the samples were handled in a laminar flow chamber (NuAIRE, class II Type A/B3).

2.3.2. Immunofluorescence Assays

Immunofluorescence assays were performed to detect AMA1 antigenic protein in *B.ovis* infected RBCs. QD-Ab conjugates (COOH QDs-AMA1) and infected ovine smears prepared as described in sections 2.2.2 and 2.3.1 respectively, were used. These assays were accomplished with indirect immunofluorescence assay on slide, using the infected culture, as described below.

Indirect Immunofluorescence Assay

Aliquots (4mL) of *B.ovis in vitro* culture containing 2-3% infected sheep erythrocytes were centrifuged (10 min, 2500 rpm at 4˚C) (Heraeus Sepatech, model Biofuge 28RS), suspended in 1x PBS+Fetal Bovine Serum (1:1, v/v) and smeared on glass slides. The glass slides were dried and stored at -80˚C until use. These smears were brought from -80ºC (NuAIRE) to r.t. for 20 minutes following the immersion in ice-cold methanol (Carlo Erba Reagents) to fix for 10 minutes and then dried with compressed air. Slides were washed with 1x PBS for 5 min and blocked with 1% BSA (Roth) in 1x PBS for 1h at r.t, with shaking. Three slides were incubated with: 1x PBS, 1:50 dilution of control rabbit serum and anti-AMA-1 rabbit serum in humid dark chamber, for 30 min at 37˚C. The slides were washed with PBS-T (PBS+0.05% Tween-20, Sigma), 1x PBS and with double distilled water, for 5 min each with shaking and dried with compressed air. A secondary anti-rabbit IgG antibody conjugated with FITC produced in goat (Sigma) was used and incubated for more 30 min at a 1:2000 dilution in a humid dark chamber, at 37˚C. Slides were washed twice with PBS for 5 min. DAPI (Roche Applied Science) nuclear stain was added at a 1:1000 dilution and incubated for 30 min, at 37˚C in a humid dark chamber. Slides were washed again, dried with compressed air and mounted with glycerol+PBS (1:1, v/v). These preparations

were maintained in the dark until observed in microscope at 1000x magnification with immersion oil, using FITC and DAPI filters (Zeiss AxioImager Upright). Images were obtained using Axiocam MRmAxioVisionRel 4.8.2 software.

Direct Immunofluorescence Assays Using QD-Ab Conjugates

Smears prepared as previously described, were brought from -80ºC (NuAIRE) to r.t. for 20 minutes following the immersion in ice-cold methanol (Carlo Erba Reagents) to fix for 10 minutes and then, they were dried with compressed air. Slides were washed with 1x PBS for 5 min and blocked with 1% BSA (Roth) in 1x PBS for 1h at r.t, with shaking. Three slides were incubated with: 1x PBS, 1:2000 dilution of control secondary anti-rabbit IgG conjugated with FITC and with anti-AMA-1 antibody conjugated with COOH-QDs, in humid dark chamber, for 30 min at 37˚C. Slides were washed with PBS-T (PBS+0.05% Tween-20), 1x PBS and with double distilled water, for 5 min each with shaking and dried with compressed air. DAPI nuclear stain was added at a 1:1000 dilution and incubated for 30 min, at 37˚C in a humid dark chamber. Slides were washed again as before, dried with compressed air and mounted with glycerol+PBS (1:1, v/v). The preparations were maintained in the dark until observed in microscope at 1000x magnification as in indirect immunofluorescence.

2.4. Detection of Glycophorin A transmembrane protein

Immunofluorescence assays were performed to detect GPA transmembrane protein in human erythrocytes. QD-Ab conjugates (in this case, COOH QDs-GPA) and RBCs solution prepared as described in sections 2.2.2 and 2.1.2 respectively, were used. These assays were accomplished with indirect immunofluorescence assay also in solution, as described below

Indirect Immunofluorescence Assay

A 5µL aliquot of erythrocytes was prepared and washed three times with 95µL of 1x PBS by centrifugation (5 min, 2500 rpms at 4ºC). After centrifugation, the supernatant was discarded and the pellet was suspended in 95µL of 1% BSA in 1x PBS for 1h at r.t. with gentle agitation. Then, the solution was centrifuged (5 min, 2500 rpms at 4ºC) and the pellet was suspended in 1x PBS and incubated with primary antibody (Monoclonal mouse anti-Glycophorin A, 1:50) for 30 min at 37ºC without shaking. The supernatant was discarded and the solutions were washed with 1x PBS. The incubation with secondary antibody was performed adding anti-mouse IgG-FITC (1:500) produced in sheep (Sigma) for 30 min at 37ºC in the dark. The supernatant was discarded and the solution washed again with 1x PBS. A control was prepared, using only the secondary antibody incubated with blood. A 20µL of each solution were observed in a microscope slide, using an inverted microscope with the B2E-C filter (Exc: 465-495 nm, Em: 515-525) filter and Image ProPlus 7.0 software (Image-Pro® Plus Version 7.0 for Windows™, Start-Up Guide).

Direct Immunofluorescence Assays Using QD-Ab Conjugates

The human samples were collected as described in 2.1.2. A 5µL aliquot of erythrocytes was prepared and washed three times with 95µL of 1x PBS by centrifugation (5 min, 2500 rpms at 4ºC). After centrifugation, the supernatant was discarded and pellet was suspended in 95µL of 1% BSA in 1x PBS for 1h at r.t. with gentle agitation. The solution was centrifuged (5 min, 2500 rpms at 4ºC) and the pellet was suspended in 1x PBS following the incubation with QDs-GPA bioconjugates for 30 min at 37ºC without shaking. Supernatant was discarded and the solutions were washed with 1x PBS. A control was prepared, using only the COOH-QDs incubated with blood. A 20µL of each solution were observed in a microscope slide, using an inverted microscope with the B2A filter (Exc: 450-490 nm, Em: 520-∞) filter and Image ProPlus 7.0 software.

2.5. Cytotoxic Assay: Oxidative Stress

To investigate the oxidative stress produced by the presence and interaction of the QDs with erythrocytes, 2',7'-Dichlorodihydrofluorescein diacetate (H_2DCFDA) was used. This reagent allows to determine cellular oxidative stress as described by Ortega-Villasante *et al*. (2005), with small modifications. The assays were performed on slide and using a microfluidic platform. The experimental procedures for the different assays tested were carried out as described below.

The used RBC solution was prepared according to section 2.1.2. A few microliters of erythrocytes were washed and suspended in 1x PBS at pH 7.4, to a final hematocrit of 5% (50µL of erythrocytes in 950µL of PBS) and incubated with QDs at a final concentration of 50nM at 37˚C for 30 min. Erythrocytes suspended in 1x PBS at physiological pH (7.4) were used as a control. Then, cells were washed once and suspended in 1x PBS at pH 7.4. H_2DCFDA was added both to control and erythrocytes with QDs at a final concentration of 20µM. Samples were incubated again at 37˚C in the dark. Slides were mounted and maintained in the dark until observed in inverted microscope (Nikon Eclipse TE2000-S), using the B2A filter (Exc: 450-490 nm, Em: 520-∞) and Image ProPlus 7.0 software (Image-Pro® Plus Version 7.0 for Windows™, Start-Up Guide).

2.6. Microfluidic Platform

Microfluidic platforms specific for blood assays, in particular to trap red blood cells, were designed and fabricated. By using a microfluidic chip, oxidative stress conditions produced in cells were tested. In brief, the process of microfabrication and the assembly of microchip developed for the biological experiments are described.

The process starts with the design of microfluidic patterns and correspondent modelling and optimization. This procedure includes: the design of mask comprising the microstructures, the COMSOL simulation to optimize the chips dimensions and geometry, the production of final mask and its projection for later casting in PDMS mould. Posteriorly, the microchips were fabricated in a temperature controlled clean room. The process of microfabrication described in section 1.7.2 is divided into six steps: the wafer preparation, the SU-8 processing, the casting of PDMS and epoxy mold, the casting of PDMS chips and for last, the sealing of final PDMS chips.

As described above, the first step of whole microfabrication process is the design of a photolithography mask with specific characteristics. The suitable designs were developed in order to get single-cell trapping and quantification, foreseeing the behaviour of the erythrocyte cells within the chip. For this purpose, AutoCAD software (2015) was used to design the micro-structures to capture the RBCs dimensions, considering a diameter of about 5-7µm (Figure 2.1). To test the efficiency of the microfluidic chips design, computational simulations were done using COMSOL Multiphysics (v5.1) software. Characteristics such as traps localization and width of chamber were adjusted in previous designs, considering the evaluation of simulations. Moreover, giving the information about the values of pressure to be used in the inlets and outlets for best efficiency during the experiment.

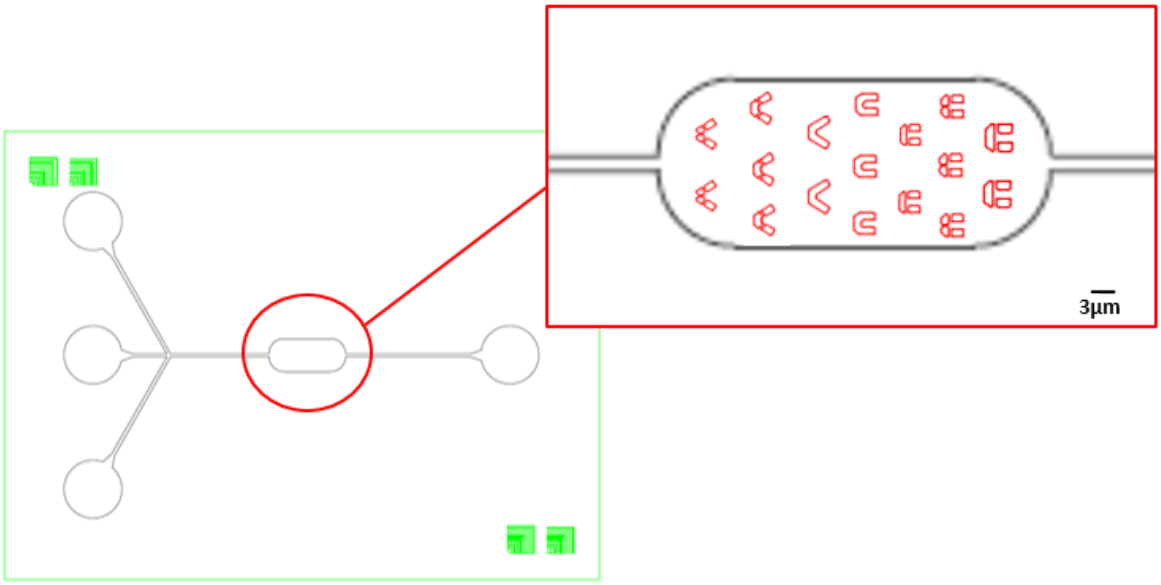

Figure 2.1 | Schematic diagram of the chip top view used for RBC trapping. This specific chip contains only one inlet and outlet and comprises a single chamber. (A) Top view image of the whole chip containing three inlets and one outlet, comprising a single chamber. (B) Detail of the cell trapping arrays with gaps of 3µm between posts.

The fabrication process starts with the silicon wafers (Si wafer) cleaning with acetone and isopropanol. The Si wafers supplement the SU-8 deposition. In SU-8 processing step, a thin layer of this photoresist (MicroChem, SU-8 2010) was spin-coating over Si wafer. After SU-8 deposition was completed, the wafer is exposed to the UV radiation of approximately 400nm, using the mask aligner, through the chromium mask with the chip structure imprinted. To finish the SU-8 processing, after the post-baking of the exposed wafers, a developer (PGMEA) was used to chemically dissolve and remove the unexposed regions covered by the photoresist. Taking in account the dimensions of a single erythrocytes (~5-7µm), the aimed thickness of the channels inside the chip was of 20µm. Then, the production of PDMS chips using the SU-8 molds is performed by a soft-lithography process. In this process, a PDMS (Sylgard 184, Dow Corning, Spain) replica of the original SU-8 master was obtained, decanting the liquid PDMS over the SU-8 mold. The PDMS was cured at 65˚C and then was peeled from the SU-8 master by cutting and gently pulling the formed layer upon the wafer. As mentioned above, a processing technique using

epoxy as an intermediate mold was included in fabrication process. This mold was obtained in similar way that PDMS mold, following the soft-lithography principle and by peeling it from the PDMS mold. The final PDMS chips were casted from the epoxy mold by soft-lithography process. The inlets and outlets were acquired by piercing the PDMS with a blunt needle. Finally, the last step of microfabrication process is the sealing of PDMS chips to glass by UV light or O_2 plasma to avoid fluid escape during the experimental assays. The devices were manufactured with resource to the CEMOP (Centre of Excellence in Microelectronics Optoelectronics and Processes).

2.6.1. Assembly for biological experiments with Microfluidic Chips

The biological assays that were performed with resource to a microfluidic platform include microchip itself and the whole structure in the course of the experiment. The setup of the complete assembly used in this project is shown in figure 2.2.

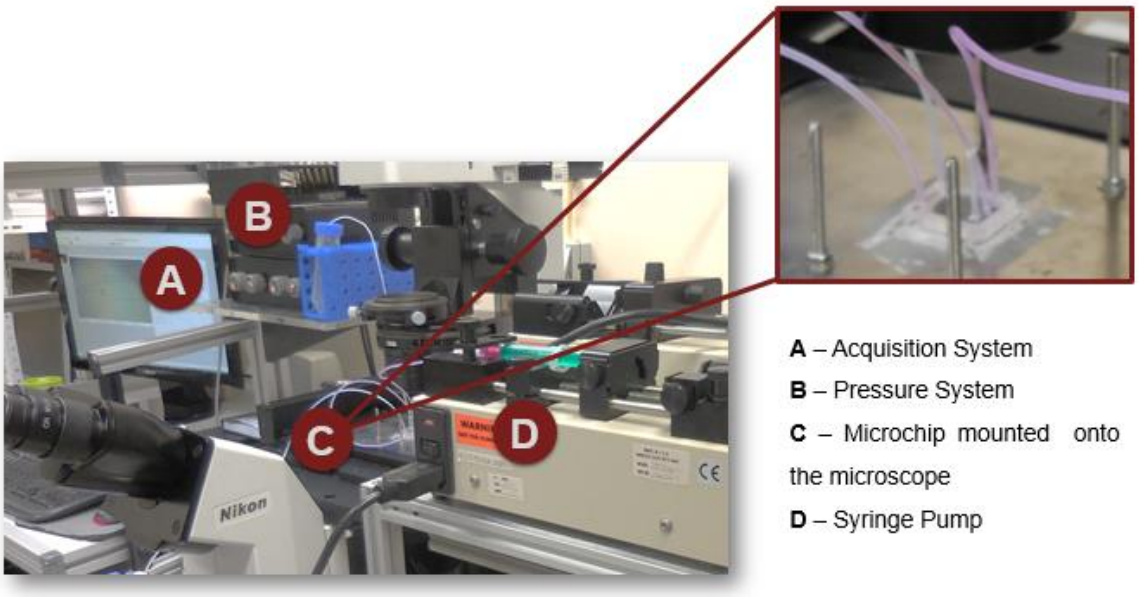

Figure 2.2 – Display of the complete assembly setup used during the microfluidic assays.

To manipulate the reagents and cells inside the microfluidic chips a syringe-pump was used coupled to the system, consisting in tubes directly inserted in the inlets/outlets of the chip. To control the fluid flow, syringes of 1mL with a filter and a rubber fitting which connect the filter to the tubing were used. However, when cells are injected, no filter is used.

The microfluidic chip is attached to the microscope platform, which was cleaned before starting the biological experiment. First, the surface of microchip is cleaned and treated with 70% Ethanol for 10 minutes, through the connected syringe. The ethanol from the chip was dried connecting it to a pressure supplier through the inlets and outlets. The pressure was controlled using the LabView Software. A second treatment is given to the chip with PEG for 1 hour. Then, the chip was washed with a continuous flow of cell medium used in the experiment, in this case PBS for about 2/3 minutes.

After this cleaning and surface treatment, the cells prepared as described above in section 2.5, were introduced in the chip and observed in inverted microscope (Nikon Eclipse TE2000-S), using the B2A filter (Exc: 450-490 nm, Em: 520-∞) and Image ProPlus 7.0 software (Image-Pro® Plus Version 7.0 for Windows™, Start-Up Guide).

.

Chapter 3 | Results and Discussion

3.1. Characterization of Quantum Dots

To characterize the appropriate work conditions of the QDs nanoparticles and to evaluate their behaviour under different conditions, preliminary assays were performed in order to choose which one compatible for the purpose of this work. The electrophoretic mobility and the pH stability of QDs were observed.

3.1.1. Electrophoretic Mobility and pH stability

The bioconjugation of QDs to biomolecules could be affected by pH because nanoparticles could form large aggregates, preventing a possible posterior bioconjugation. These differences lead to changes in mobility of the nanoparticles. The three types of QDs (PDDA, PEG and COOH) were evaluated before conjugation with antibodies in terms of pH stability and electrophoretic mobility. To achieve the characterization, an agarose gel electrophoresis was prepared and the three QDs were run at a pH range from 5 to 8, in 1x TBE buffer to observe their migration profile and to assess if there are differences in fluorescence intensity. The image of gel electrophoresis of three different surface ligands of QDs is shown in figure 3.1.

Gel electrophoresis is a technique to separate and analyze macromolecules and their fragments, based on their size and charge. The molecules are separated through the application of an electric field to move the negatively charged molecules through the agarose gel. Smaller molecules move faster than larger because they migrate more easily through the pores of the gel. Gel electrophoresis can also be applied to separate nanoparticles. Water-solubilization of CdSe/ZnS core shell QDs involves the exchange of ligand on this nanoparticles surface. The hydrophilicity of QDs is obtained by the charged groups (such carboxylic acid, amines, etc.) or by the poly(ethylene glycol) (PEG) polymers that surrounds the nanoparticles. Those ligands form a solubilization layer that highly influences the surface charge and the mobility of QDs. This aspect is important for defining the bioassay design, regarding the delivery and migration of the QDs.

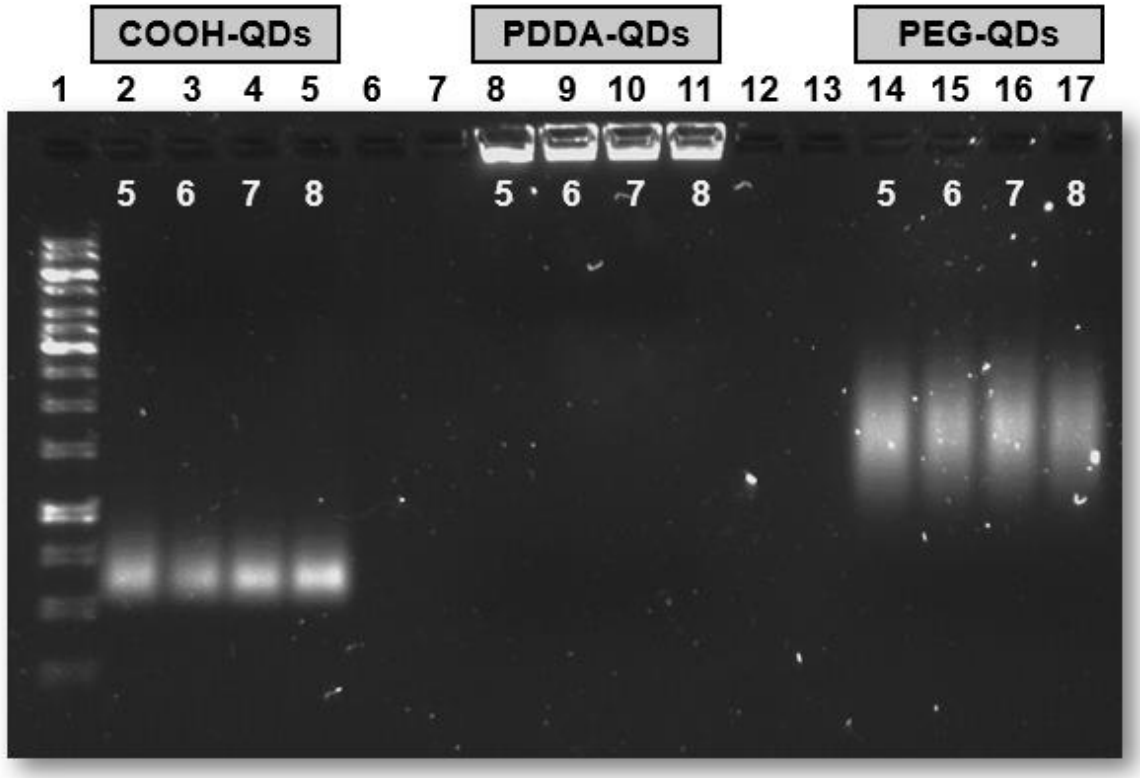

Figure 3.1 – Comparison of Electrophoretic Mobility and pH stability of three different QDs. The electrophoretic mobility and pH stability of QDs was evaluated. pH values are in range from 5 to 8. 1% Agarose gel electrophoresis in TBE 1x buffer (pH 8.4) after running 3h at 50 V. The gel was visualized under GelDoc Ez Imager using Blue tray.

The images of the gel show that the QDs coated with PDDA that remained in the well (Figure 3.1, wells 8-11). This can be due because PDDA-QDs have a positive charge so they can't migrate from the negative electrode to the positive, being retained in the wells, where is the cathode. The COOH-QDs (Figure 3.1, wells 2-5) easily migrates towards to the pores of the gel, observing a well-defined band, due to its negative charge allowing an easy movement to the positive electrode. The PEG-QDs (Figure 3.1, wells 14-17) exhibit a smear instead a well-defined band. The long length of PEG molecule increase the QD size and consequently, its electrophoretic mobility is lower than COOH-QDs. Furthermore, the exhibited smear can also indicate that these type of QDs are constituted by several agglomerates.

Such as electrophoretic mobility, the characterization of the pH stability of QDs is also important to control and optimize the performance in biological assays. Figure 3.1 also shows QDs functionalized with COOH, PEG and PDDA ligands in Na-P solutions whose pH ranges from 5 to 8 because pH's lower than 5 and higher than 8 are not suitable for biological applications. The results demonstrated that there are no differences in fluorescence of QDs functionalized with different ligands, concluding that they are stable in a wide pH range from 5 to 8. So the following assays with biomolecules can be performed using experimental conditions within this pH range, not affecting the experimental procedure.

In brief, it was possible to demonstrate that COOH-QDs are well dispersed in a wide pH range, compared with PDDA-QDs, which are retained in the wells, and PEG-QDs, being constituted by several aggregates. The study shows that stability and migration behavior of QDs depend on the nature of the functionalized ligand.

As a consequence of this assay, it can be concluded that COOH-QDs are suitable for the bioconjugation assay due to the better charges distribution and their smaller size.

3.2. Characterization of QDs-Ab conjugates

A common method for coupling QDs to antibodies is the covalent approach of the reactive amine groups present in the antibodies to carboxylic acid coated QDs using EDC/NHS as a non-selective reagent. This is a simple procedure with some advantages related to water solubility of EDC reagent which allows direct bioconjugation without prior organic solvent dissolution. The excess of these reagents can be easily removed by dialysis. In addition, this procedure doesn't implies chemical modification of antibodies due to the amine groups that are present in proteins and are very reactive (Xing et al., 2007; Puertas et al., 2011). However, this strategy implies working at pH values below 8 which can lead a randomization of crosslinking sites of the antibody on the nanoparticle surface (Miguel, 2012). EDC/NHS chemistry is the most used technique for bioconjugation however, the search for new and optimal experiment conditions is still a constant. This covalent bond can be formed at any pH or salt condition (Puertas et al., 2011). Taking account this fact, the coupling of monoclonal antibodies with carboxy-coated QDs through EDC/NHS chemistry was performed using sodium-phosphate buffer 10mM (NaP buffer) as working media ranging the pH from 6 to 8. It was observed (in section 3.1.1) that QDs are stable in range of pH between 5 and 8, not affecting their fluorescence or their migration profile.

One of the double bonds of EDC reacted with the OH groups of the carboxylic acid present on the surface of QDs, originating an active ester (O-acylisourea) (Figure 3.2). This intermediate could directly react with a primary amine of the Ab, but the reaction rate would be low and the intermediate can hydrolyse in aqueous solution (Figure 3.2 – a). In order to originate a more stable intermediate able to react with primary amines of antibodies, NHS reagent was used to support the EDC active complex. Therefore, a NHS intermediate was formed as a result of the reaction of the hydroxyl group of NHS with EDC active ester and thus increasing the rate of amide bond formation (Figure 3.2 - b). This two steps are intended to lead to higher bioconjugation yields in relation to a single-step EDC reaction (Hermanson, 2008).

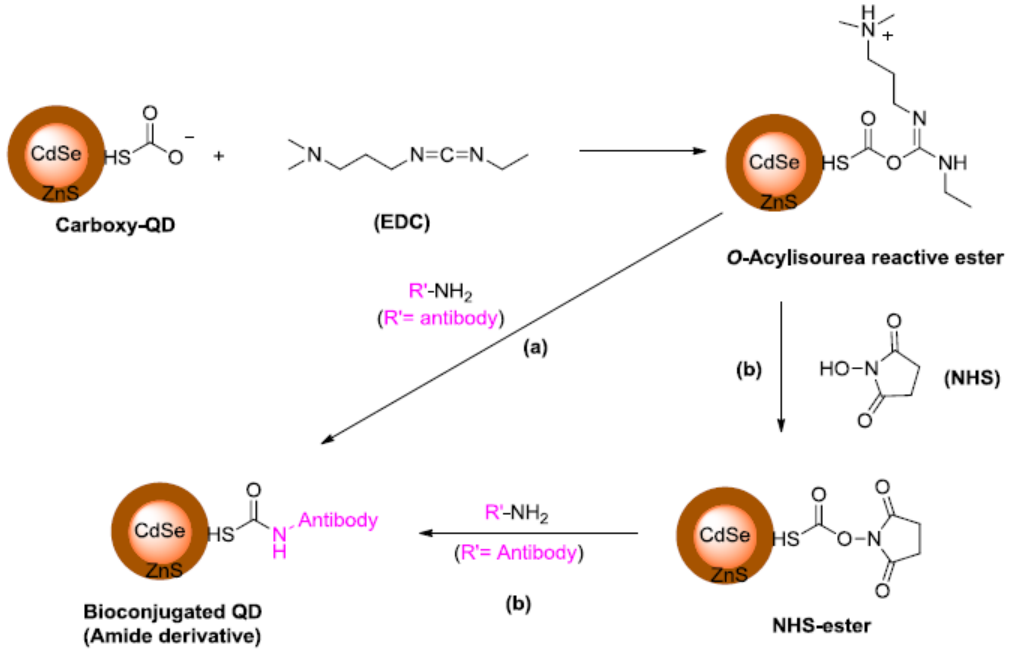

Figure 3.2 - Conjugation of Antibodies to Carboxy-QDs using EDC or EDC/NHS. Coupling of QDs containing carboxylate groups with amine-containing biomolecules using (a) EDC single-step reaction or (b) EDC/NHS two-step reaction to form bioconjugated QDs (amide derivative) (adapted from: Miguel, 2012).

To start the bioconjugation procedure, it is necessary to activate the COOH-QDs for subsequent coupling with antibodies. This was performed by two-step EDC/NHS reaction as described above. QDs were activated using different concentrations of EDC and NHS (1:2 respectively) towards maximization of NHS ester formed and consequently preventing the formation of undesired surface secondary products. The activated COOH-QDs were then purified by dialysis overnight to eliminate the excess of EDC and NHS. Sodium phosphate buffer was used to bioconjugation process tested by previous work of Miguel, 2012. The activated QDs were used to couple with antibodies using an estimated proportion of (one QD for four Ab molecules). In the obtained QDs-Ab conjugates, the surface of the nanoparticles should be inert to avoid unwanted interactions with other components of the sample. Incubating the samples with an excess of ethanolamine overnight, the remaining activated carboxyl groups on the QDs surface are blocked. The unreacted ethanolamine was eliminated by a purification dialysis. The final step of the bioconjugation protocol is a purification, to eliminate possible free antibody in samples. This was achieved by using a centrifugal filtration with a 100kDa cut-off, keeping the supernatants.

3.2.1. Analysis of Bioconjugation Protocol by Agarose Gel Electrophoresis

A quick way to evaluate if the bioconjugation had occurred is the analysis by an agarose gel electrophoresis (Figure 3.3). In this technique, the migration of the nanoparticles immersed in the electric field is dependent on both total charge of particles and their size. Thus, it is possible to observe different electrophoretic profiles of QDs with antibodies on their surface. In figure 3.3, the image of the electrophoretic run shows the possible conjugation between QDs and antibodies, which is consistent with theoretical predictions. The analysis of QD-Ab conjugates was performed using a negative control, comprising a 50 nM of non-activated COOH-QDs solution (well 1) to compare with the final bioconjugate samples. The voltage of electrophoresis ranged between 45 and 90V during 2h15 hours because the high molecular weight of the bioconjugate samples.

Regarding the differences in electrophoretic mobility, it can be observed that the QD-anti GPA and QD-anti AMA1 samples (wells 3 and 5) were both slower than free COOH-QDs (well 1). This behavior can be explained by the greater diameter of the QDs-Ab complexes and the reduction of the total charge resulting from positively charged amino groups present in the antibodies.

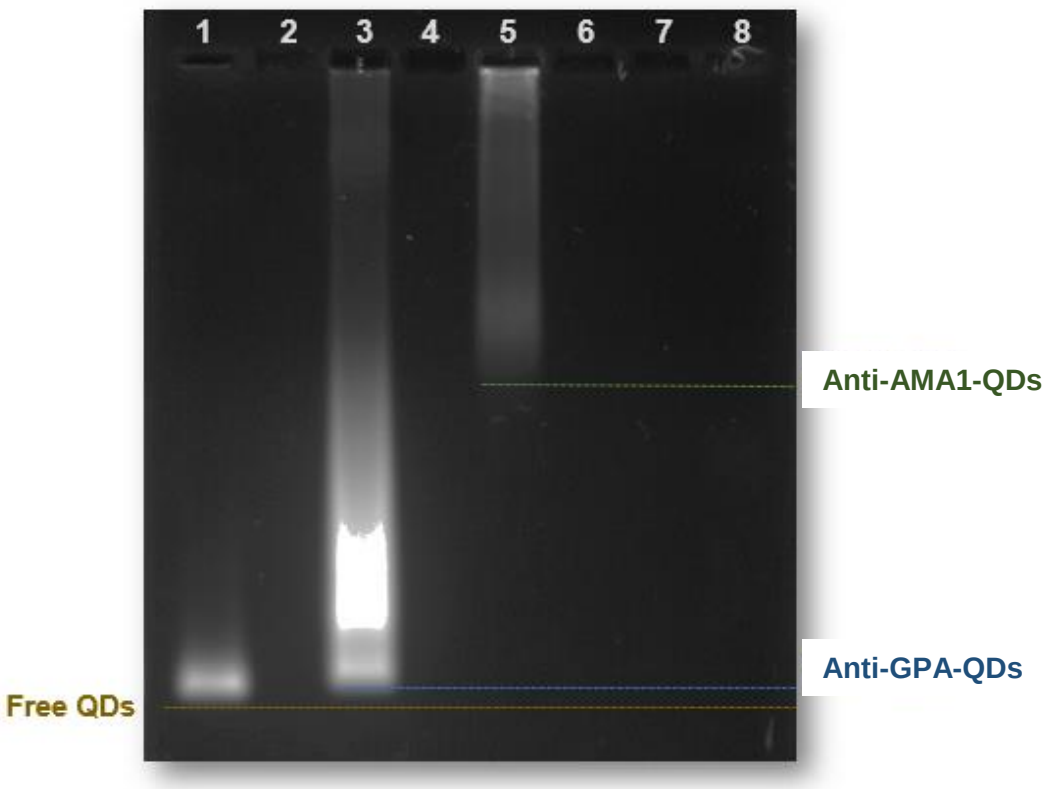

Figure 3.3 - Analysis of bioconjugation protocol by agarose gel electrophoresis. Comparison of a control 50 nM non-activated COOH-QDs (well 1) with activated QDs after conjugation (well 3 and 5). Controls with respective free antibodies were also used with free GPA-IgG (well 7) and free AMA1-IgG (well 8). Agarose gel electrophoresis was run in 1% agarose gel with TBE 1x running buffer (pH 8.4) for 2h15 at ranging 45 to 90V. The gel was visualized under GelDoc EZ Imager using the UV Tray.

Analyzing the fluorescence intensity of the bands, it can be observed that it is more intense due to no addition of SYBR® safe DNA gel stain which influences the fluorescence of QDs and bioconjugate samples. About the quantity of Ab-QDs complexes, it seems that the reaction

between QDs and AMA1-IgG produced a larger quantity of bioconjugates than the reaction between QDs and GPA-IgG (Figure 3.3 – lanes 3 and 5). In addition, it is important to note the formation of aggregated samples that can be visualized across the gel. In general, these initial results indicate that the conjugation between antibodies and QDs had occurred. However, it was necessary a confirmation by performing a detailed characterization of bioconjugate samples.

3.2.2. Characterization of Ab Conjugates to QDs by SDS-PAGE Electrophoresis

To confirm if antibodies were indeed covalently bound to the QDs, QDs-Ab complexes were run in a sodium dodecyl sulfate polyacrylamide gel electrophoresis (SDS-PAGE), with and without Dithiothreitol (DTT) to separate the functional components of conjugated antibodies from the QDs.

Disulfides are frequently the point of attachment for subunits in a protein molecule. IgG molecules hold together the two heavy chains as well as disulfides holding the light chain-heavy chain pairs together. Reductants such as DTT can be used at low concentrations to perform a partial cleavage of disulfide bonds. DTT limited cleavage of disulfides in antibody molecules can mean the reduction essentially the bonds between the heavy chains of the immunoglobulin. This will causes two-half antibody molecules where each half contains one antigen binding site and free sulfhydryls in the hinge region (de Rosario et al., 1990). Thus, when antibodies are reduced with DTT, in addition two distinct fragments, one more fragment could be created and they are differentiated by their molecular weight: the light chain which comprises half of the specific antigen binding site and has a 25 kDa, a heavy chain which includes the other half of the specific binding antigen site and has 50 kDa and a 75 kDa incompletely cleaved chain which is a heavy and a light chain held together by an unreduced disulfide bond (Figure 3.4).

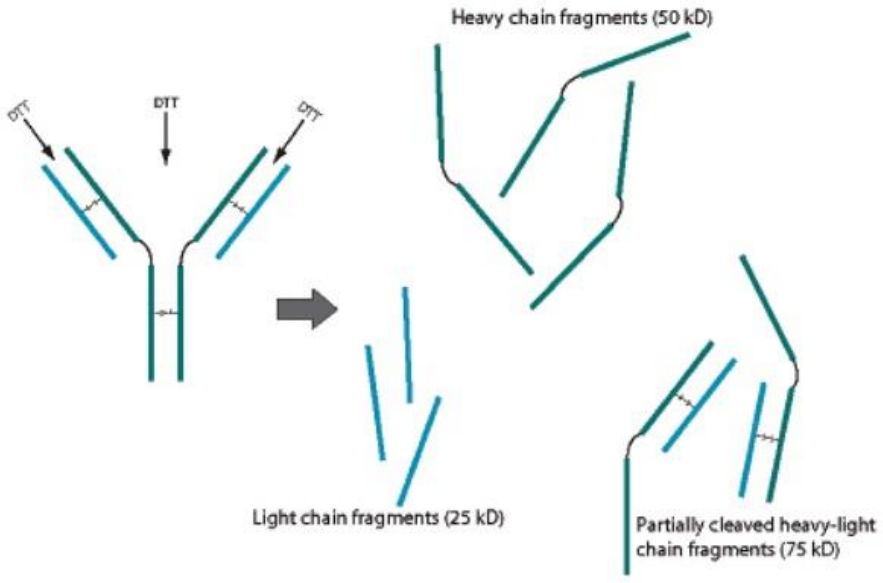

Figure 3.4 - Antibody reduction with DTT. Schematic representation of antibody cleavage sites by DTT at disulphide linkages (adapted from: Pathak et al., 2007).

The SDS-PAGE gel electrophoresis has run under reduced and non-reduced conditions and the gel was observed with UV light (Figure 3.5).

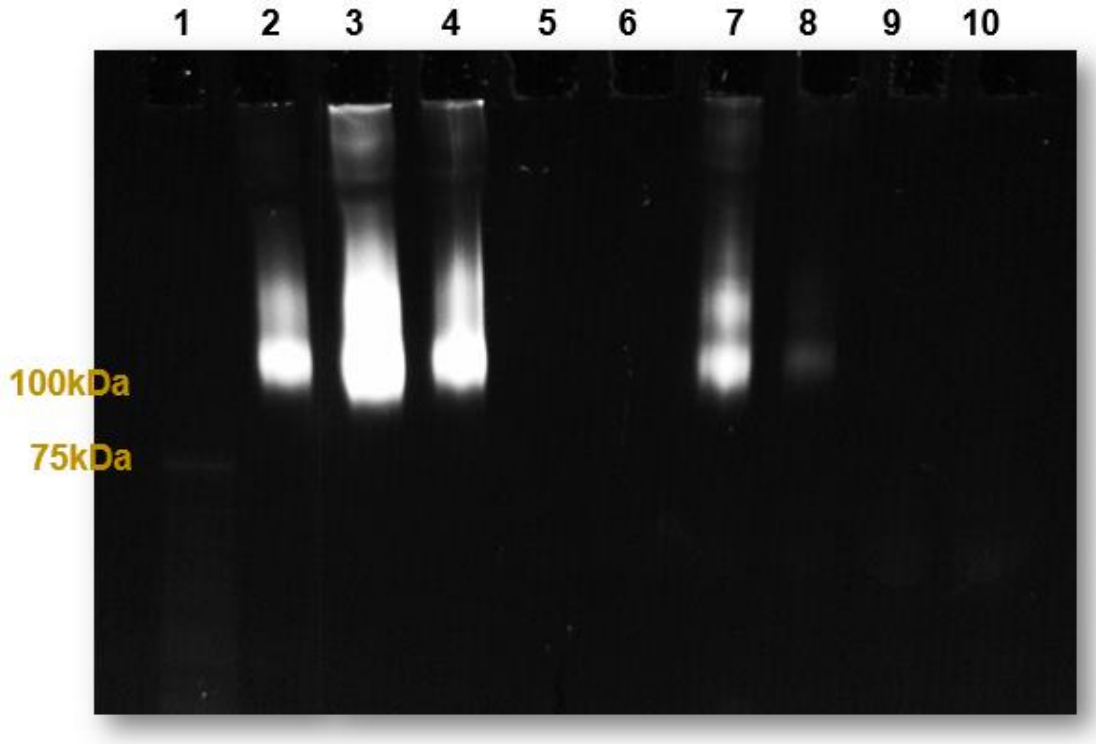

Figure 3.5 - Separation of Ab-QDs complexes into fragments by SDS-PAGE electrophoresis. Comparison of a control 50 nM non-activated COOH-QDs (well 2) with activated QDs after conjugation (wells 3, 4, 7 and 8). Controls with respective free antibodies were also used with free anti-GPA IgG (wells 5 and 6) and free anti-AMA1 IgG (wells 9 and 10). The SDS-Page elecytrophoresis was run in 4-15% Precast gel with 1X Running buffer for 90 minutes at 150V. The gel was visualized under GelDoc EZ Imager using the UV Tray with GelDoc EZ Imager using the UV tray.

Making an initial analysis, these results apparently demonstrate that bioconjugation had occurred and that the Ab was linked to the QDs since bioconjugated QDs which migrated in SDS-PAGE gel (Figure 3.5 – lanes 3, 4, 7 e 8), exhibit a different migration behavior in relation to the control sample which contain just free QDs (Figure 3.5 – lane 2). It can be observed a smear across the gel in all samples but in lanes 3 and 4, the smear is longer when compared with control. It is also visible that some bioconjugated QDs remained in the wells (lanes 3, 4 and 7). Considering that bioconjugation had occurred, the presence of smears can be due to aggregation or high molecular weight of the QDs-Ab complexes which limits their mobility in the pores of the gel. In case of free QDs (lane 2) the present smear can be explained by aggregation between the nanoparticles.

For DTT reducing conditions (lanes 4 and 8), it is evident the loss of fluorescence. Antibodies are linked to water-soluble QDs which are functionalized with carboxylic acid. Carboxylic acid is bounded to the CdSe/ZnS core-shell QDs surface by a single and weak sulphur bridge (Miguel, 2012). If DTT could cleave the sulphydryl bond in proteins and antibodies, it is also possible to disrupt these bonds in other molecules. This can be indicate that some of antibodies linked to QDs were split into light and heavy chains because the sulphur bridge between ligand and the

ZnS shell from free QDs was first reduced with DTT. It's known that after treatment with reducing reagents such DTT, in general each antibody molecule is fragmented into heavy and light chains which have a molecular weight of 50kDa and 25kDa respectively in SDS-PAGE electrophoresis. This information could be used to evaluate the orientation of antibodies coupled to quantum dots (Miguel, 2012) because according to Puertas et al (Puertas et al., 2011), when the conjugation is done with a site-selective orientation using, for example, the Fc portion of antibody (which is constituted by CH_2 and CH_3 chains as demonstrated in Figure 1.7) only the heavy chains fragments should be attached to the quantum dots and after reduction only the light chains of the QDs could be released. By contrast, if antibody is randomly conjugated, after treatment with DTT both light and heavy chains could be liberated. It is important to understand if separation had occurred. Just analyzing the SDS-PAGE gel under UV light, it is not clear if separation between heavy and light chains happened.

Generally, it can be said that the conjugation between CdSe/ZnS QDs capped with carboxylic acid and antibodies has occurred. The results suggest that antibodies are probably covalently linked because the partial QDs-Ab complexes in non-reduced conditions travel through the gel. It is evident that some of bioconjugates, mainly the non-reduced samples, remained in the wells because of their large size. For more detailed conclusions, a western blot was performed in order to verify if fluorescence of conjugates is coincident with the protein band on membrane.

3.2.3. Evaluation of immunogenicity of Ab-QDs complexes

Western Blotting, also known as immunoblotting, is a technique that uses antibodies (or other specific ligands in related techniques) to identify antigens among a number of unrelated protein species. The identification of protein target is performed via antigen-antibody (or protein ligand) specific reactions. Proteins are firstly separated by SDS-PAGE electrophoresis and transferred onto a membrane. The membrane is overlaid with primary antibody for specific target and then, with a secondary antibody labeled, for example, with enzymes.

Immunoblotting was performed to qualitatively analyze the attachment of QDs to antibodies and to evaluate the functionality of the QDs-Ab complexes, confirming if these probes are able to recognize their antigen. After running SDS-PAGE gel, QDs-Ab complexes under reduced and non-reduced conditions, free QDs as well as the anti-Glycophorin A and anti-AMA1 antibodies (as described in section 3.2.2) were blotted onto a low auto-fluorescence Polyvinylidene difluoride (PVDF) membrane. The membrane was next incubated with secondary antibody conjugated with horseradish peroxidase (HRP) enzyme, to perform the immune-detection of QDs-Ab samples. The samples were visualized under UV-light, to observe the natural fluorescence of QDs, checking for an immunofluorescence reaction (Figure 3.7) and using the chemiluminescence HRP substrate to reveal the interaction between anti-IgG and IgG (Figure 3.6).

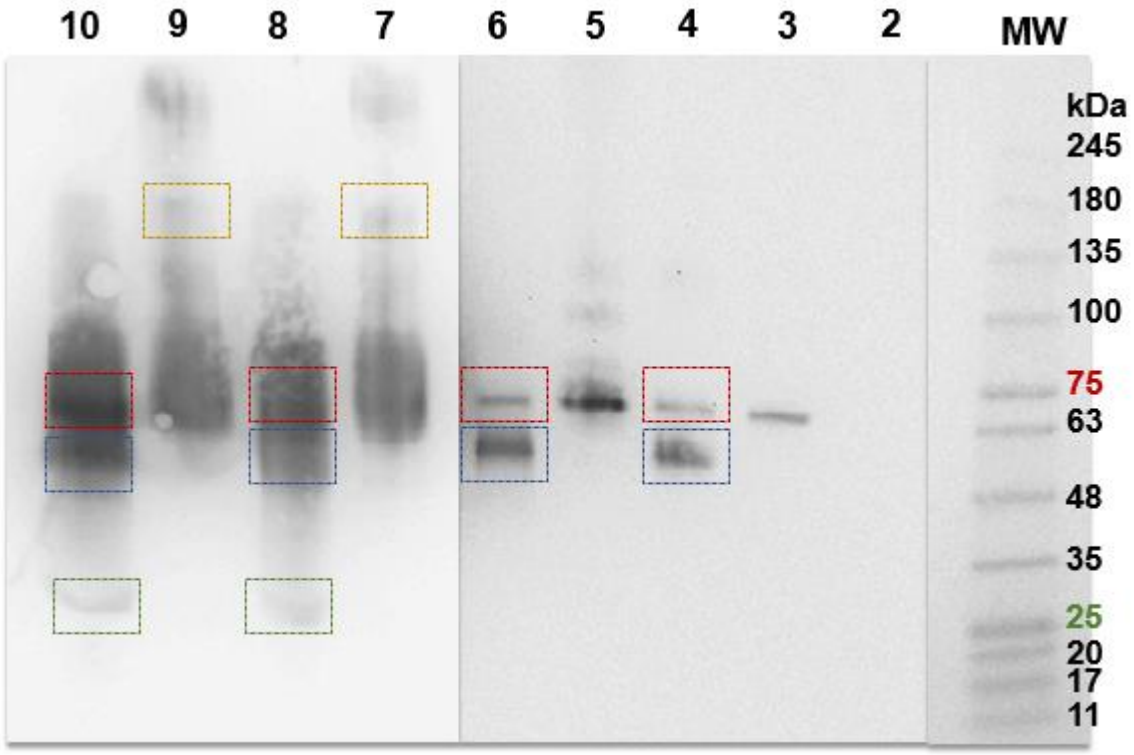

Figure 3.6 – Separation and functional activity of Ab-QDs complexes. The image shows the capacity of Ab-QDs complexes to recognize their antigen. The samples were prepared in blocking buffer containing 5% (w/v) of non-fat milk and the images were acquired with ChemiDoc equipment. In the left image, the detection method used was the chemiluminescence HRP substrate.

In lanes treated with DTT (lanes 4, 6, 8 and 10) it is possible to observe the reduction of samples. This is evidenced by the presence of bands at 75kDa (highlighted by a red box). The bands with this molecular weight correspond to incompletely cleaved chains. In same lanes, it can also be seen the presence of bands at 50kDa (indicated inside the blue box). This means that samples were also fragmented into heavy chains. At 25kDa which characterize the molecular weight of light chains, it is only possible to visualize bands in samples with anti-AMA1 primary antibody (lanes 10) and in anti-AMA1 conjugated with QDs (lane 8), as can be seen in green box. Thus, it can be concluded that in case of samples 8 and 10, there was a complete reduction while in samples 6 and 4, the reduction was partial. In relation to samples with anti-AMA1 antibody under non-reduction conditions (lanes 7 and 9), a band at approximately 170kDa was visualized as expected due to the absence of reducing reagent because this is the molecular weight of a whole IgG molecule (highlighted by a yellow box). In contrast, in the non-reduced anti-Glycophorin A antibody (lanes 3 and 5), band is not present. The behavior of samples in lanes 3 and 5, suggests a degradation of this antibody, due to the presence of one single band in lane 3 (QDs-anti-GPA complexes) and the non-defined bands in lane 5. Monoclonal antibodies are prone to a variety of physical and chemical degradation pathways. Like other proteins, they are particularly susceptible to temperature and pH changes and other factors like oxidation or light ionic content for example. These factors can affect their potency, purity and quality. The two major pathways

of physical instability are denaturation and degradation of antibodies (Nebija et al., 2014). One factor that may have contribute for the possible degradation of anti-Glycophorin A antibody is the running buffer which is constituted by 1% of SDS. SDS is an ionic detergent and it has the ability to linearize the proteins. The stability and aggregation behavior of antibodies, can vary significantly between different types of them, which can justify the degradation of anti-Glycophorin A and the non-degradation of anti-AMA1 antibodies (Schaefer and Plückthun, 2012).

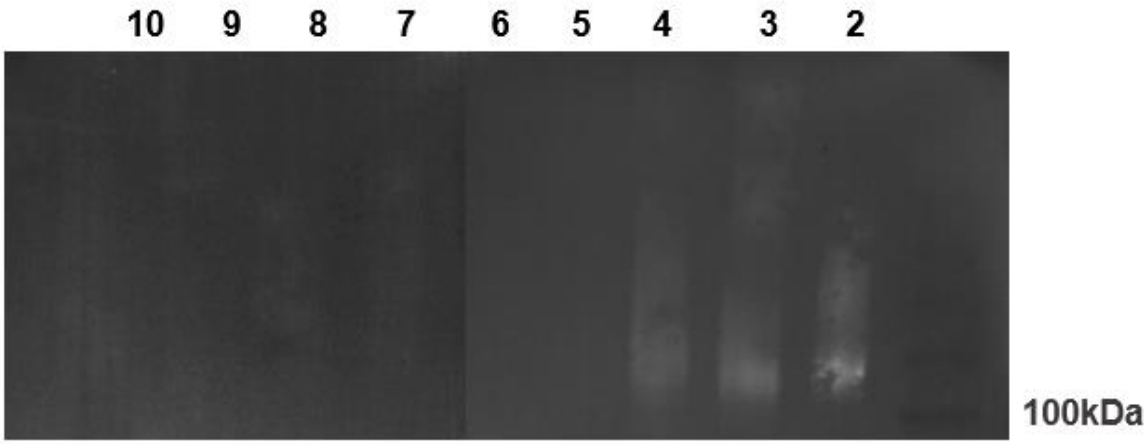

Figure 3.7 – Visualisation of western membrane under UV-light. The fluorescence of QDs were observed in different strips containing antigen protein. 50nM of COOH-QDs control (lane 2) and Ab-QDs complexes (lanes 3, 4, 7 and 8) were prepared in blocking buffer containing 5% (w/v) of non-fat milk. The detection method used was chemiluminescence HRP substrate and image was acquired in ChemiDoc equipment.

The resulting image visualized in western membrane also reflect the antigen recognition by the antibodies attached to QDs, suggesting that antibodies present in Ab-QDs samples are functional and specifically recognize the antigen. This can be observed as the immunoreaction detected with the collared reaction of the HRP with the substrate. However, it is not clear if these antibodies are really attached to quantum dots or are free in solution. Just looking for figure 3.6 it can not be conclude if bioconjugation had occurred because the profile of conjugated samples (lanes 4, 8 and lanes 3, 7) under reduction and non-reduction conditions respectively, is similar when compared with samples that only contain the primary antibodies (lanes 6, 10 and lanes 5, 9) under the same conditions. To clarify these doubts, the membrane was also observed under trans-UV light. No immunofluorescence has been observed in antibodies control samples (Figure 3.7 – lanes 5, 6 and 9, 10). On the other hand, it is possible to observe that COOH-QDs in their natural form strongly interact with the antigen immobilized in the membrane (Figure 3.7 – lane 2).

During the performance of Western Blot, TBS and TTBS were used in different steps along the procedure and both are prepared to have a pH of 7.4, close to the physiological pH. At that pH, an interaction between the antigen and non-conjugated QDs can be occurred. In figure 3.7 – lane 2, it can be observed a polar interaction between the protonated amine groups present in the antigen and the carboxylate groups present on the QDs surface is possible. If is possibly that COOH-QDs in their natural form interact directly with the antigen, the antibody in QDs-anti-AMA1 complexes must be attached to the QDs because if QDs were free in solution, at least one weak fluorescent band or smear should have appeared in lanes 7 and 8. In case of QDs-anti-GPA

complexes, the results suggest that antibody is not linked to the QDs because the fluorescence profile of lanes 3 and 4 is identical to the lane 2, meaning that QDs are just free in solution and that they interact with the antigen on the membrane.

3.3. Detection of AMA1 Antigenic Protein in Infected *Babesia ovis* Erythrocytes

3.3.1. *Babesia ovis in vitro* culture

Babesia ovis is a tick-transmitted intraerythrocytic protozoan parasite which reproduces asexually within sheep and goat erythrocytes, originating two pear-shaped merozoites (Carletti et al., 2015).

In vitro Babesia cultivation allows to produce the quantities of parasites needed for infection studies and to develop methods for detection of the parasite. Studying the process of infection, it is possible to examine the basic biology of the organism as well as host-microbe interactions, immune factors triggered by the parasite, factors involved in innate resistance of animals to infection and the anti-microbial susceptibility (Schuster, 2002). Thus, allows the opportunity to obtain information for diagnostics of infections and for studies on phylogenetic relations between several *Babesia* species. Multiplied protozoan parasite in erythrocytes, can be used as a source of vaccine antigens applied in animal immunization (Spencer et al., 2006).

Cultures were initiated from small amounts (0.5mL) of packed erythrocytes infected with *B. ovis* parasites in processed fresh ovine blood. To identify the intra-erythrocytic parasites in *in vitro* culture suspensions, the common method is the Giemsa stained blood smears in microscope slide (Figure 3.8). This culture was cultivated for 15 days and its parasitemia level did not exceed the 5%.

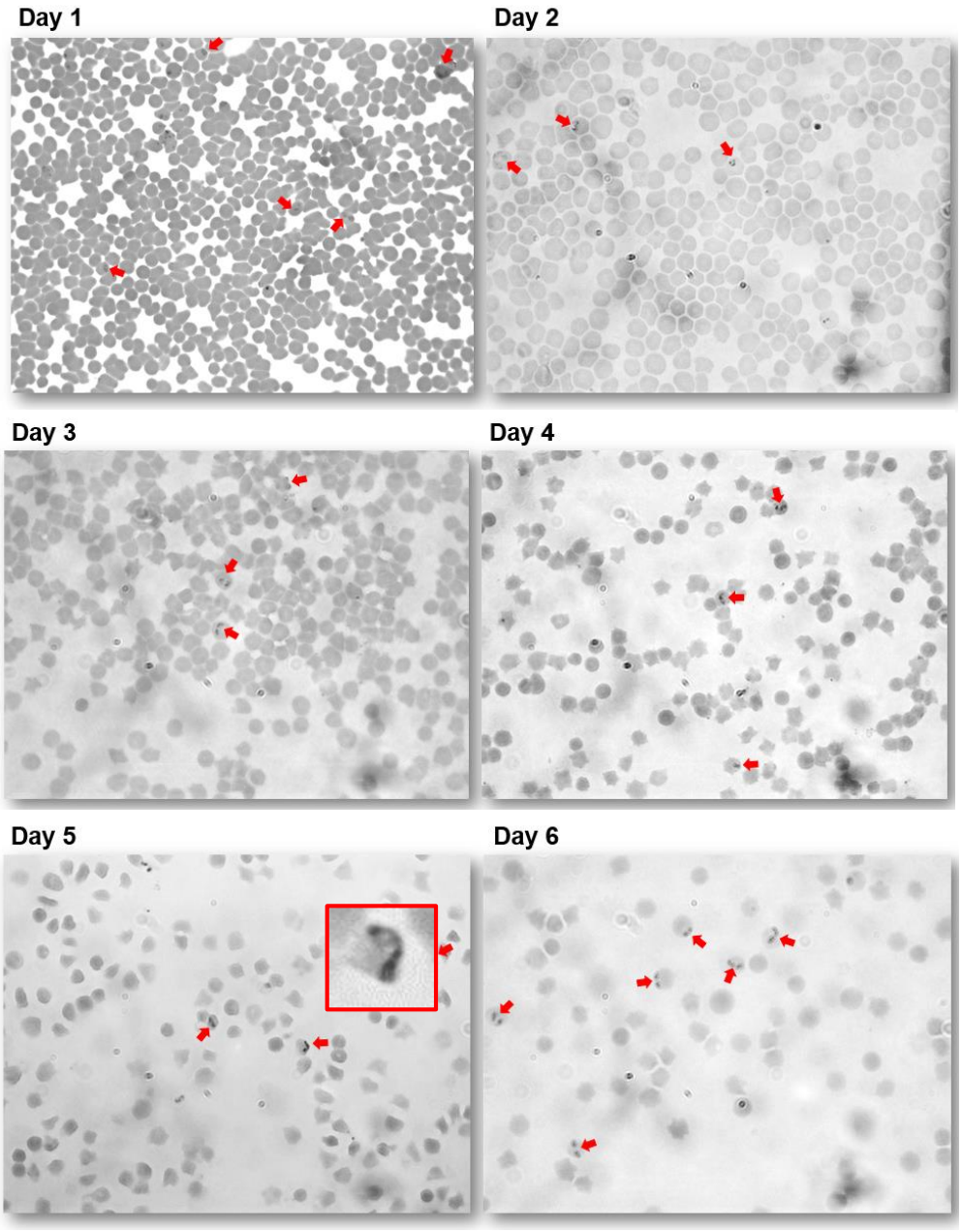

Figure 3.8 - Identification parasites in *B.ovis* infected cell of in *vitro* culture suspensions. The images demonstrate the evolution of cell culture growth from day 1 to day 6. During the experiment, the percentage of parasite infected erythrocytes was measured observing blood films stained with Giemsa under microscope with a magnification of 1000x. The cells were counted using the ImageJ program. Different days of cells growth represent different percentages of parasite infected erythrocytes: Day 1 – 0.28%; Day 2 – 0.9%; Day 3 – 0.42%; Day 4 – 1.1%; Day 5 – 2.15%; Day 6 – 2.4%. The red arrows indicate the parasites inside the erythrocytes.

However, the procedure to cultivate *B. ovis in vitro* is a complex process dependent on several variables for like temperature, pH of the medium, percentage of CO_2 and nutrient gradients. Moreover, these protozoan parasites have complex life cycles as they have different morphological stages within the life cycle (since is not possible to synchronize like Malaria). *In vitro* culture of parasites at any one of these stages within the life cycle implies a number of

variables including parasite stage, host site, host temperature, host immune responses, parasite species and/or strain and parasite protective mechanisms.

The standard laboratory technique to diagnose the parasitemia level of *Babesia* infections is based on observation of infected cells. This is achieved by preparing blood smears following the microscopic examination of the films stained with Giemsa at pH of 7.2 to highlight the parasite inclusion in erythrocytes. This examination of a stained thin blood film is typically realized by observing the number of parasitized RBCs (in a standard microscope using the 100x oil immersion objective) and expressing it as a percentage. Consequently, a 1% parasitemia for example, will contain 1 parasite per 100 RBCs.

Generally, there are small (diameter 1.5 to 3μm) to large (diameter 3 to 5 μM) *Babesia* species, although the parasite size may reflect the size of host's erythrocytes (Kain et al., 2001). The presence of pairs of parasites in stained erythrocytes constitutes the diagnostic of babesiosis. In this case, it's possible to observe the pairs of parasites (highlighted by a red box in figure 3.9) concluding that erythrocytes are indeed infected with *Babesia ovis*.

The period of exponential growth is dependent of the initial percentage of parasitized erythrocytes, i.e, the lower the initial number, the shorter the period of exponential growth. Then, the medium has to be replaced daily because if not, the rate of growth decreases. It can be explained by the accumulation of metabolites that directly influences replication, so by a daily change of the medium daily decreases the concentration of these inhibitory products enough to permit continued growth. However, when the absolute number of parasites reaches a threshold level (for example, 1%), daily change of medium is not enough to permit constant replication. The percentage of parasitized erythrocytes is comparable to the concentration of erythrocytes present in the culture. When this threshold level is reached, a percentage of fresh erythrocytes (10%) are added. This can be observed when the culture supporting growth turned dark red to black because the utilization of oxygen by the parasites and deoxygenation of hemoglobin, with the pH of the culture rising to 7.2 from its initial pH of 7. So, when cultures have a bright red color this means that it doesn't support parasite reproduction (Schuster, 2002).

Another factor which has influence in growth of *B. ovis* is the pH. If the culture medium becomes too acidic, the rate of growth starts to decrease and the organisms begin to die. So it's evident that there is an inverse relation between the percentage of parasitized erythrocytes and the pH of the culture medium. The type and concentration of the buffer is crucial to maintain the optimal pH for culture growth. To preserve an adequate buffering in our culture, it needed 20mM TES buffer because if the buffering capacity is increased by greater concentration, it's possible that the culture growth is affected (Goff and Yunker, 1988). After several studies (Goff and Yunker, 1988), the TES is the best pH buffer because the infectivity of the parasites is maintained.

The culture was grown in M199 medium supplemented with ovine sterile serum (20%) which is used as medium supplements for *in vitro* growth of babesia species. This represents a variable factor which is necessary to support cultures with higher parasitemias.

The culture was subcultured when the percentage of parasitemia reaches the 1% given rise to propagation of the cultures. When this procedure is done, it's normal to observe a decrease of

parasitemia percentage (Figure 3.8, day 3) when compared with the culture before splitting. This is expected because the percentage of parasitized erythrocytes declines when concentration of erythrocytes present in culture increases. However, this process is reversible after few hours of cultivation and culture normal growth was achieved when complete medium was re-supplied.

This culture was placed with a mixture of gases 5% CO_2, 2% O_2 and 93%N_2 at 37ºC because according to some studies (Goff and Yunker, 1988), the optimal temperature for endocytosis in erythrocytes is 37ºC. A low-O_2 atmosphere is essential to initiate *B. ovis* growth in erythrocytes cultures, starting with a small number of parasites (Scheibel et al., 1979) (with parasitemia percentage between 0.1 and 0.2% as shown in figure 3.8). The CO_2 concentrations seem to play an important role in parasite growth and in many cases is the reason of early unsuccessful experiences.

3.3.2. Detection of AMA1 Antigenic Protein

Apicomplexans utilize several molecules (ligands) in their invasion process. The AMA1 is one protein expected to be implicated in RBC invasion (Gohil et al., 2010).

To identify early infections of *B. ovis*, there are several methods. One of the most used is the indirect immunofluorescence test (IFAT). This method consists in using two antibodies: the primary antibody, which is unlabeled, specifically binds the target molecule and the secondary antibody, typically an anti-IgG, which contains a fluorophore, identifies the primary antibody and binds to it (Indirect Immunofluorescence detection - Figure 3.9). The advantage of this method compared with the direct immunofluorescence is related to the diversity of secondary antibodies and various detection techniques (for example, flow cytometry, ELISA and immunohistochemistry) that can be used. In terms of sensitivity, the use of several secondary antibodies can result in an amplified signal (for example due to enzymatic amplification). However, this protocol has the disadvantage of the number of additional steps that add more complexity and time needed for each assay. There is also the possibility of secondary antibodies cross-react with other species present in the samples provoking a high background.

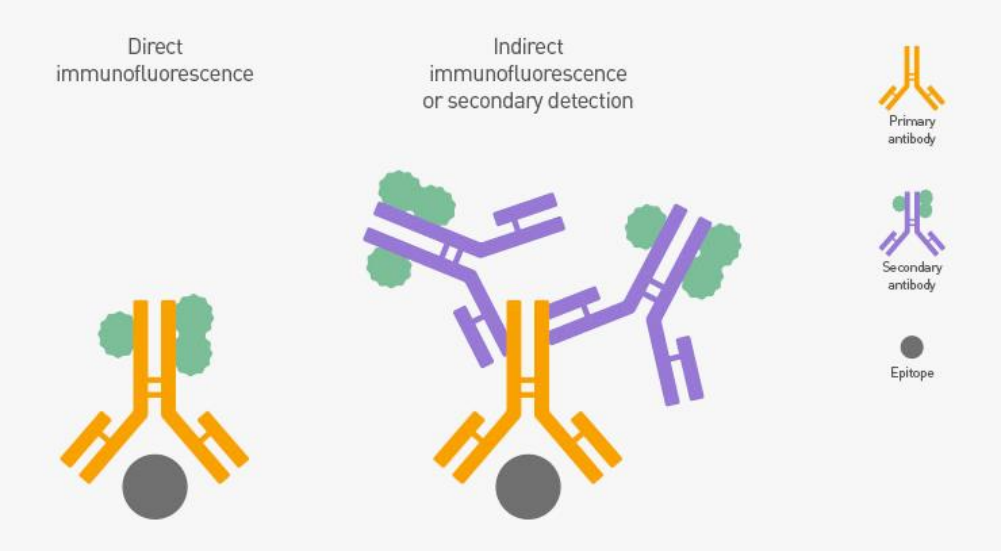

Figure 3.9 - Schematic representation of direct and indirect immunofluorescence assay (adapted from: thermofisher.com).

In the direct immunofluorescence assay it is used only a single antibody, chemically linked to a fluorophore that binds to the target molecule. After the immunoreaction, the fluorophore can be detected by fluorescence microscopy (Figure 3.9). Protocols for this method are usually simpler as fewer steps are needed for the assay. In addition, species cross-reactivity is minimized using conjugated primary antibodies. As disadvantages, can be outlined that conjugated primary antibodies are more expensive and less flexible and the signal obtained may seem weak when compared with indirect methods.

COOH-QDs were conjugated with anti-AMA1 antibody (section 2.2.2) and tested to detect the presence of AMA1 antigenic protein in *Babesia ovis* infected erythrocytes, as an alternative to standard immunofluorescence assays. Cultured infected RBCs samples were incubated with AMA1-QDs conjugates using smears with infected blood on slide as described in section 2.3.2. As a positive control, the assay was realized with the standard IFAT, using the anti-AMA1 and a FITC anti-rabbit IgG produced in goat as primary and secondary antibodies respectively. It is important to notice that all the preparations were mounted with media containing 4′, 6 diamidino-2-phenylindole dihydrochloride (DAPI) solution. This reagent has the capability to bind to the A-T regions of parasites DNA, originating a fluorescent compound under UV light. DAPI allows to easily identify the parasites presence in infected cells. All preparations were observed using a microscope and the results obtained can be observed in figure 3.10 for assay with QDs-AMA1 and in figure 3.11 for positive control with FITC.

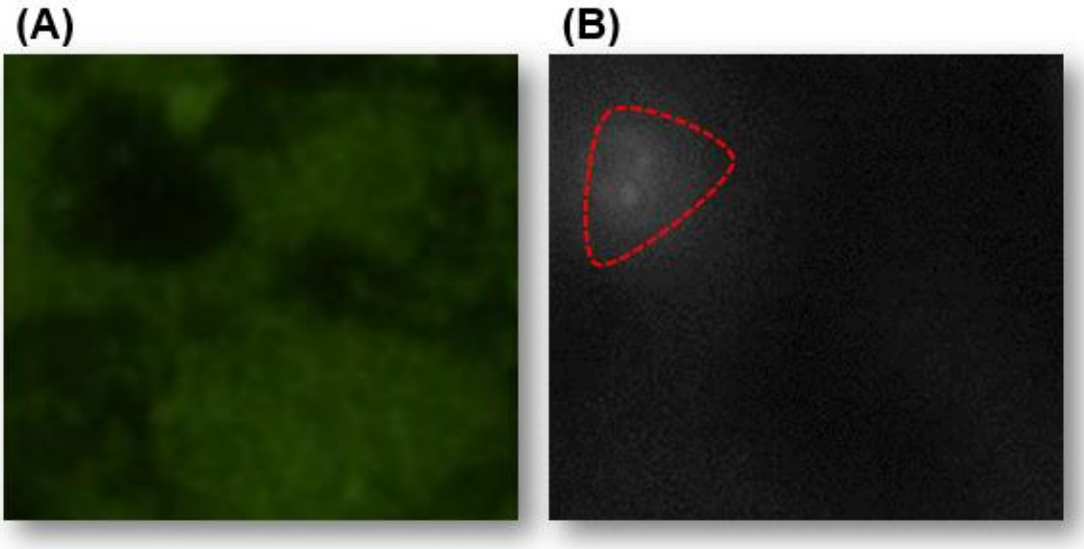

Figure 3.10 – **Immunofluorescence assay using anti-AMA1-QDs conjugates.** Smears of *B. ovis* infected ovine erythrocytes were incubated with conjugates of anti-AMA1 antibody and COOH-QDs followed by observation by epifluorescence (1000× magnification), with filters to detect QDs (A) and contrast micrograph to identify the parasite (B). The same result was observed when infected ovine erythrocytes were incubated with COOH-QDs.

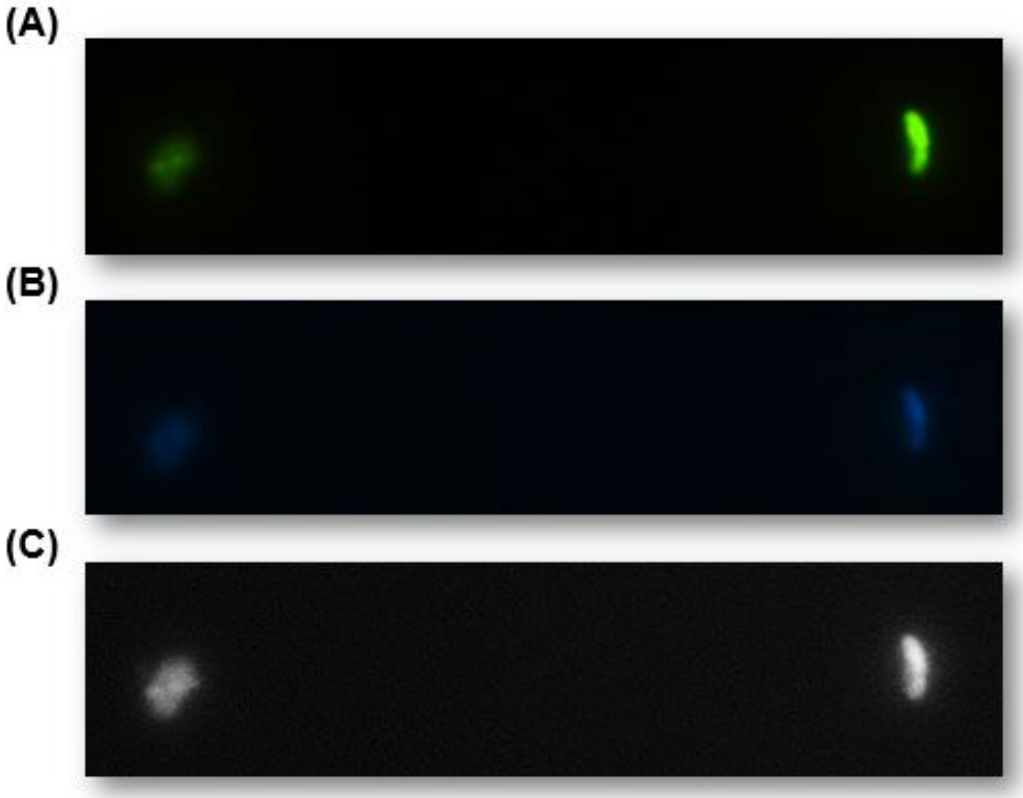

Figure 3.11 – Positive control by Indirect Immunofluorescence Assay. Smears of *B. ovis* infected ovine erythrocytes were incubated with DAPI and rabbit anti-AMA1 antibody; followed by detection with FITC-labeled anti-rabbit IgG and observation by epifluorescence (1000× magnification), with filters to detect FITC (A) and DAPI (B). (C) is the corresponding phase contrast micrograph. No fluorescence was detected when control rabbit serum was used (not shown).

Figures 3.10 and 3.11 show the images of the immunofluorescence assays on slide containing smears of *Babesia ovis* infected erythrocytes incubated with QDs-AMA1 bioconjugates. It is possible to identify the presence of parasites seen as fluorescent spots in both positive control (Figure 3.11 – B) and represented in direct assay with QDs-AMA1 conjugates (Figure 3.10 – B). Moreover, in figure 3.11 – A, it can be seen the labelled parasite, which means that the anti-AMA1 antibody recognizes the antigen AMA1 in *Babesia ovis* infected erythrocytes. However, in immunofluorescence assay using QDs-Ab complexes (Figure 3.10 – A), aggregation of QDs is observed but not specific to the antigenic protein. The origin of nanoparticles aggregation may be due to the fact that the experiment was performed on slide in a static way, in other words, without any homogenization of the bioconjugated samples during the incubation time at 37˚C. One possible solution to reduce the aggregation is to perform this assay with agitation to provide a better distribution of the bioconjugated sample during the incubation with infected erythrocytes. This non-specificity of QDs-Ab complexes to the AMA1 antigenic protein, supports the idea discussed above (in section 3.2.3) about the orientation of bioconjugates. The used conjugation procedure often results in random orientation of the antibody in QDs bioconjugates, blocking the antigen-binding sites. Another point is, once prepared, the QDs-Ab conjugates has to be stored at 4˚C. The problem is that the most antibodies needed to be stored at -20˚C while QDs samples at 4˚C. If the QDs-Ab conjugates are stored at 4˚C for too long, the antibodies lose binding affinity and specificity (Xing et al., 2007). It is important to notice that the immunofluorescence assay with a standard method confirm the recognition of AMA1 antigenic protein in infected erythrocytes by anti-AMA1 primary antibody. However, the use of bioconjugated samples did not show a positive response for the detection of AMA1 protein. Other clear observation is that the intensity of fluorescence emitted by FITC fluorophore conjugated to the secondary antibody is lesser than the fluorescence emitted by QDs. It is the background of the image of figure 3.10 – A (assay with QDs-Ab complexes) compared with figure 3.11 – A (assay with FITC labelled parasite) is lower. This can be due to the poor photo-resistance demonstrated by the standard organic dyes when excited for long periods of time (Hermanson, 2008). This observation is in accordance with the QDs as an useful label for biosensing and labelled applications, due to their exclusive photoluminiscent properties and their high resistance to photobleaching (Dabbousi, 1997). In conclusion, the indirect control assay shows the recognition of AMA1 protein by primary antibody but when QDs-AMA1 complexes are used, no cell staining is observed maybe due to the QDs disruption from antibody or Ab lost its affinity during the conjugation process.

3.4. Detection of GPA Transmembrane Protein in Erythrocytes

COOH-QDs were conjugated with anti-Glycophorin A to identify the presence of this protein in erythrocytes membrane. RBCs solution were incubated with anti-GPA-QDs conjugates and observed in microscope. A positive control was performed with the traditional IFAT method, using the anti-GPA and a FITC anti-mouse IgG produced in rabbit as primary and secondary antibodies respectively. The acquired images can be observed in figure 3.13 for the direct assay with anti-GPA-QDs complexes and in figure 3.12 for positive control with FITC.

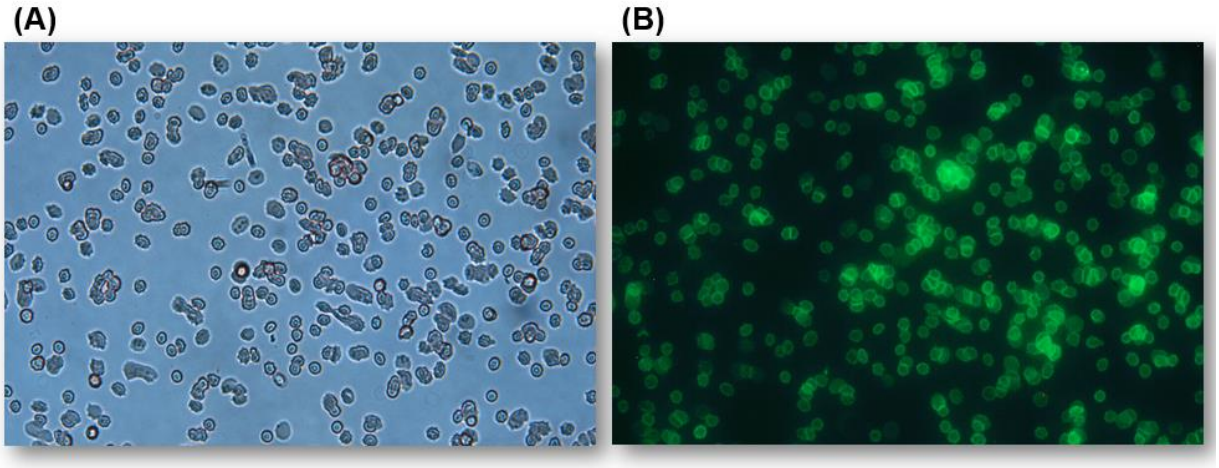

Figure 3.12 – Detection of Glycophorin A transmembrane protein in human erythrocytes. Human blood was incubated with mouse anti-GPA antibody followed by detection with FITC-labelled anti-mouse IgG. The images were observed with 400x amplification under B2E-C filter (Exc: 465-495 nm, Em: 515-525) (B) and bright field (A). No fluorescence was observed in control when erythrocytes were incubated with FITC-labelled anti-mouse IgG (not shown).

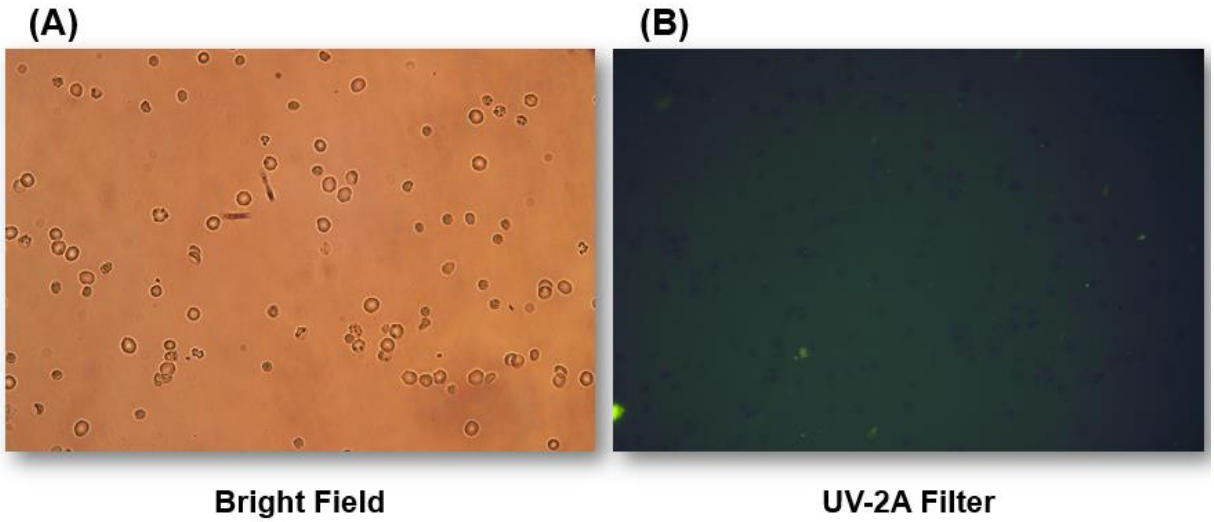

Figure 3.13 - Immunofluorescence assay using anti-GPA-QDs conjugates. Erythrocyte cells were incubated with conjugates of anti-GPA antibody and COOH-QDs. The images were acquired with a magnification of 400x in bright field (A) and under UV-2A filter. The same result was observed when erythrocytes were incubated with COO-QDs.

Glycophorins represent approximately 2% of the total RBC membrane proteins. These proteins are also known as sialoglycoproteins due to its sialic acid content which is the contributor to the net negative charge of erythrocyte membrane. The negative charge produces the electrostatic repulsive energy, minimizing the RBC-RBC interactions and allowing the circulation of blood cells on the vessels, preventing the aggregation between them. The function of this protein also enables the targeting of other specific transmembrane proteins to the cell membrane. Therefore, due to the abundant presence of GPA in RBC membrane (as can be seen in positive control in Figure 3.12), the incubation of anti-GPA-QDs complexes with RBCs would be an ideal model to evaluate the binding efficiency of the produced bioconjugates.

The positive control confirms the antigen recognition of the anti-GPA antibody in erythrocytes membrane represented by an intense green fluorescence in all cells, meaning that the anti-GPA antibody is specific to its target.

However, anti-GPA-QDs complexes appear to be non-specific to GPA protein. This can be due to some reasons discussed in section 3.2.3 such as the random orientation of antibody in QDs bioconjugates because the antigen-binding sites may be blocked. Another discussed point is the loss of binding affinity by storing the final conjugates at 4˚C for too long. The results also raised hypothesis that some factors like small variations in temperature, pH or physically instability during the bioconjugation procedure can affect the quality of Ab and lead to its degradation.

3.5. Evaluation of ROS formation

The use of QDs in cells raises concerns about their potential cytotoxic effects due to their chemical structural composition such as cadmium and selenium. Several factors can influence their cellular toxicity like size, charge, concentration and their outer shell bioactivity, leading to the formation of ROS. Hence, it is important to test the QDs to be used with our cell model to evaluate their interference on cell life.

To perform this experiment, the microfluidic platform was used. In this case, a measurement at a single cell level will be advantageous to individually observe the effect of QDs in the cells. Microfluidic technology is the suitable technique because it can allow a collection of cells trapped in a microchamber with a controlled environment. This technique facilitates the miniaturization of precise analytical measurements as well as low reagent consumption and allows a fast analysis in real-time. However, a preliminary assays were done on slide.

3.5.1. Evaluation of ROS production on slide

To evaluate the induction of oxidative stress characterized by free radicals formation, the fluorinated compound H_2DCFDA was utilized. 6-carboxy-2',7'- dichlorodihydrofluoresceine diacetate (H_2DCFDA) is a sensitive and largely compound used for the detection of intracellular oxidants production. It is a marker that can determine hydrogen peroxide, hydroperoxides and nitric oxide and for studies of oxidative stress at the cellular level too (Bukowska, 2007). H_2DCFDA diffuses through the cell membrane and then is hydrolysed by intracellular estereases to 2',7'-dichlorodihydrofluorescein (DCFH). This is a non-fluorescent product but it is converted into DCF (2',7'-dichlorofluorescein), a high fluorescent product by reaction with reactive species, which can easily be visualized by fluorescence at 525nm when excited at 488nm (Figure 3.14) (Santos, 2009).

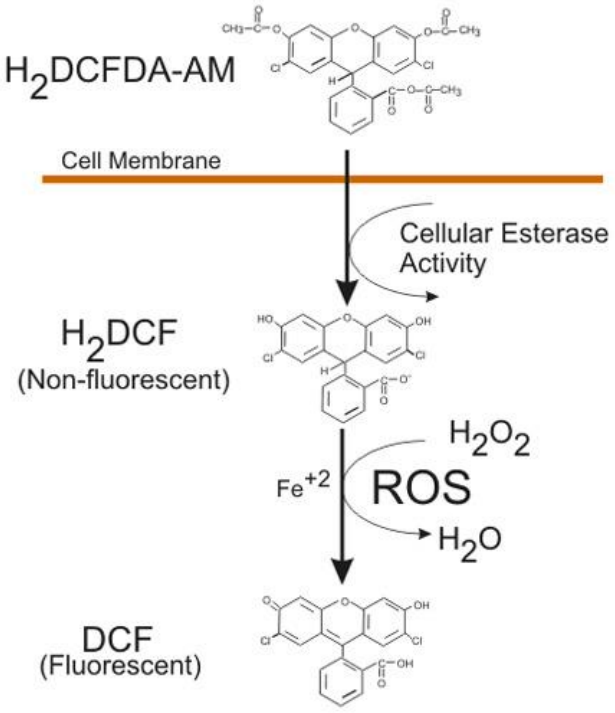

Figure 3.14 - Conversion of 2',7'-dichlorodihydrofluorescein diacetate (H_2DCFDA). H_2DCFDA is hydrolysed by cellular estereases to 2',7-dichlorofluorescein (H2DCF) which is converted to fluorescent 2'7-dichlorofluorescein (DCF) (adapted from: https://seallab.wordpress.com).

When H_2DCFDA enters cells it accumulates mostly in the cytosol. To avoid any cytotoxicity from this compound, cells are incubated with low concentrations of reagent. After several assays and based on literature, it was found that the optimal loading of 20μM for 30 minutes, which is suitable for the intracellular ROS experiment.

H_2DCFDA is widely used to measure the formation of reactive species within cells. However, it is not clear which species are the cause for oxidation of DCFH to DCF in cells. To determine the cellular oxidative stress of erythrocytes with QDs, cells were incubated with 10, 50 and 100nM of PDDA, PEG and COOH-QDs concentration and treated with H_2DCFDA to explore the effect of different QDs concentration in formation of oxidative stress by erythrocytes. As controls, erythrocytes at pH value of 6.2 and cells treated with just H_2DCFDA were used. The assays were done on slide and after optimization of protocol, the experiment was performed using a microfluidic chip to analyse the oxidative stress at a single-cell level. Observing the interaction between cells and these nanoparticles with different charges, is important for determination of intracellular uptake, morphological localization and their relative cytotoxicity (Zucolotto, 2013).

Three types of QDs were available to be tested. All three had the same chemical composition which is: a cadmium selenide (CdSe) core, a zinc sulphide (ZnS) shell and a dilayer coating composed of an OctaDecylAmine (ODA) monolayer and an Amphiphilic Polymer (APM) monolayer. The main difference between them was the outer monolayer coating which presented different types of surface functionalization: one is composed by carboxylic acid ($COOH^-$) which confers a negative charge to the nanoparticles. Another one has a PolyEthylene Glycol (PEG)

dilayer, being neutral QDs and finally, the other type of QDs is composed by PolyDiallyDimethyl-Ammounium ($PDDA^+$) which means that these QDs have a positive charge.

For all samples incubated with different type of QDs (Figure 3.15, 3.16 and 3.17) it is visible a DCF signal accumulated in cells which get stronger by increasing QDs concentration. In general, it can be assesses that QDs presence/interaction with RBCs induces a cellular oxidative stress. It is also noted that the fluorescence intensity of DCF signal decreased with exposition time. This can be due to sensitivity of H_2DCFDA to the light, being susceptible to degradation.

In incubation of RBCs with PDDA-QDs it is difficult to observe a response of isolated cells because the overlap of DCF signal (which is green) and natural fluorescence of QDs (which is yellow) (Figure 3.15).

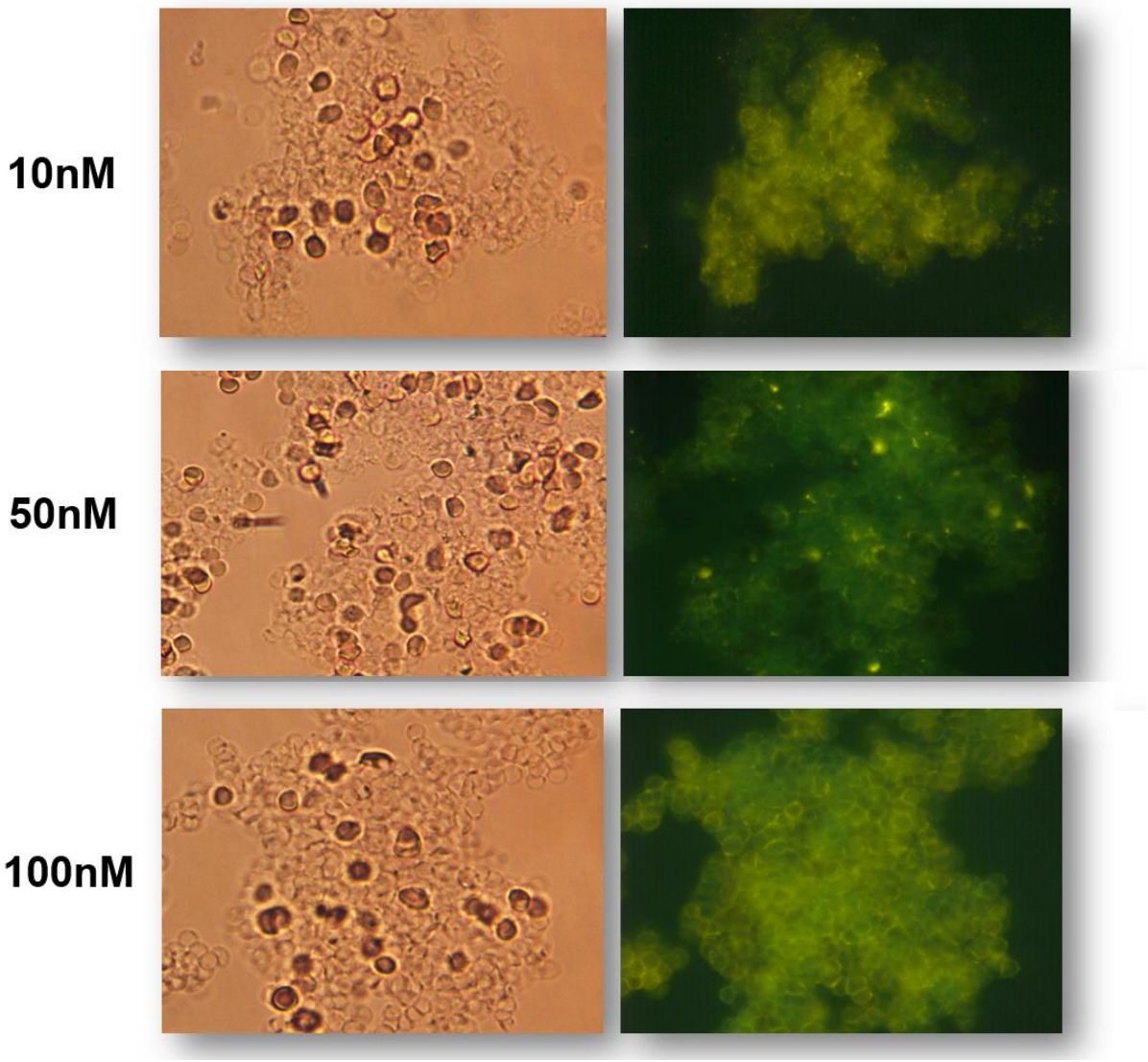

Figure 3.15 - Determination of cellular oxidative stress in erythrocytes cells incubated with PDDA-QDs. Erythrocyte cells were incubated with 10nM, 50nM and 100nM of PDDA-QDs for 30 minutes and treated with H_2DCFDA. Cells were observed with a magnification of 400x in bright field and in B-2A filter (Ex: 450-490nm; Em: 520-∞).

The PDDA-QDs interact with erythrocytes membrane provoking the aggregation of cells. Erythrocytes have a negative charge membrane which can lead to positive nanoparticle attraction by electrostatic forces. This explains why PDDA-QDs (with positive charge) interact with RBCs, indicating that nanoparticles with positive surface charge, in *in vitro* assays, are taken up faster by cells.

The fluorescence observed in RBCs incubated with PEG-QDs (Figure 3.16) and COOH-QDs (Figure 3.17) is due to the conversion of H_2DCFDA into DCF, emphasizing the production of reactive oxygen species by incubated cells which is proportional to the increasing of concentration of QDs. In contrast with PDDA-QDs, these two types of QDs do not interact with cells due to charge repulsion forces between the surface charge of these nanoparticles and cells membrane.

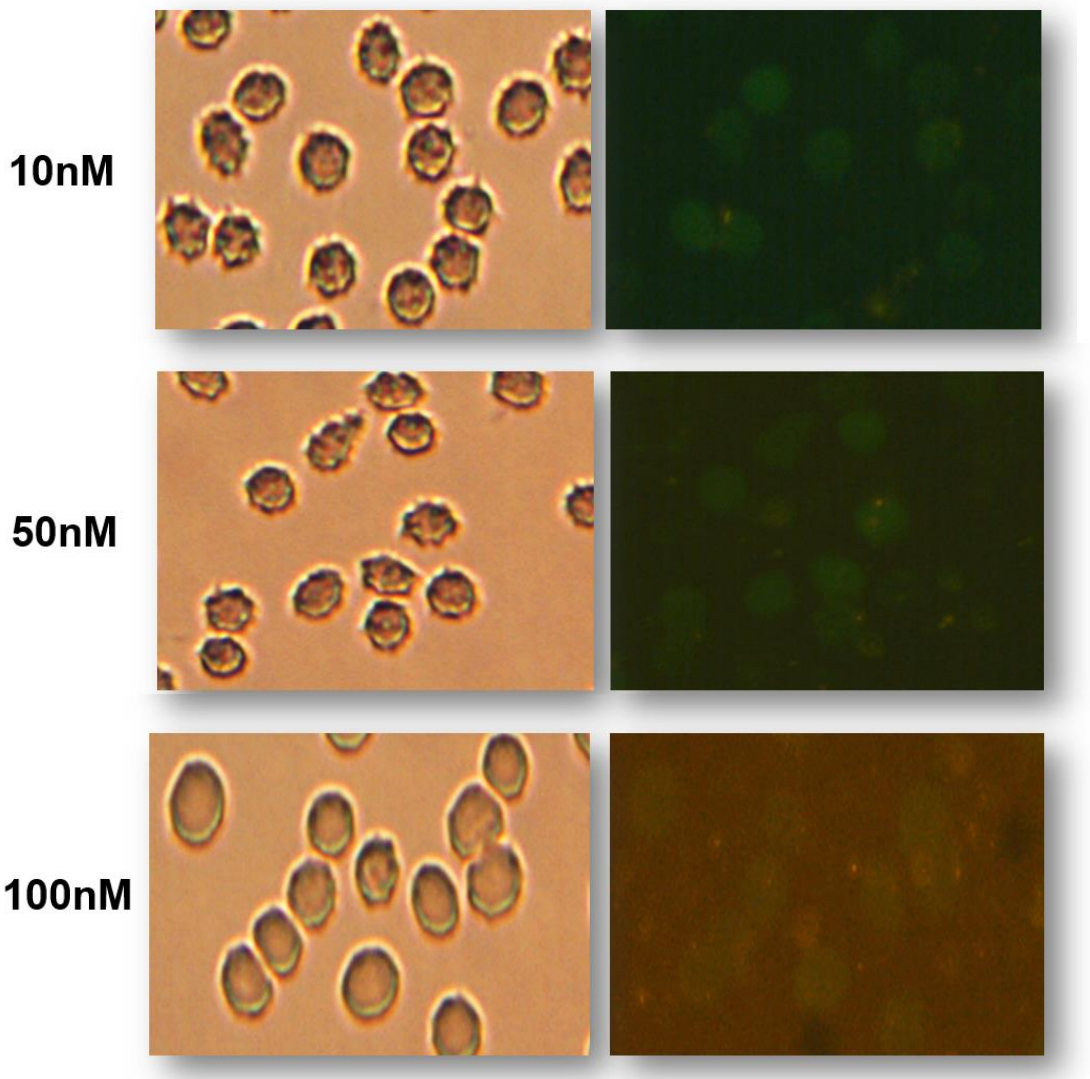

Figure 3.16 - Determination of cellular oxidative stress in erythrocytes cells incubated with PEG-QDs. Erythrocyte cells were incubated with 10nM, 50nM and 100nM of PEG-QDs for 30 minutes and treated with H_2DCFDA. Cells were observed with a magnification of 400x in bright field and in B-2A filter (Ex: 450-490nm; Em: 520-∞).

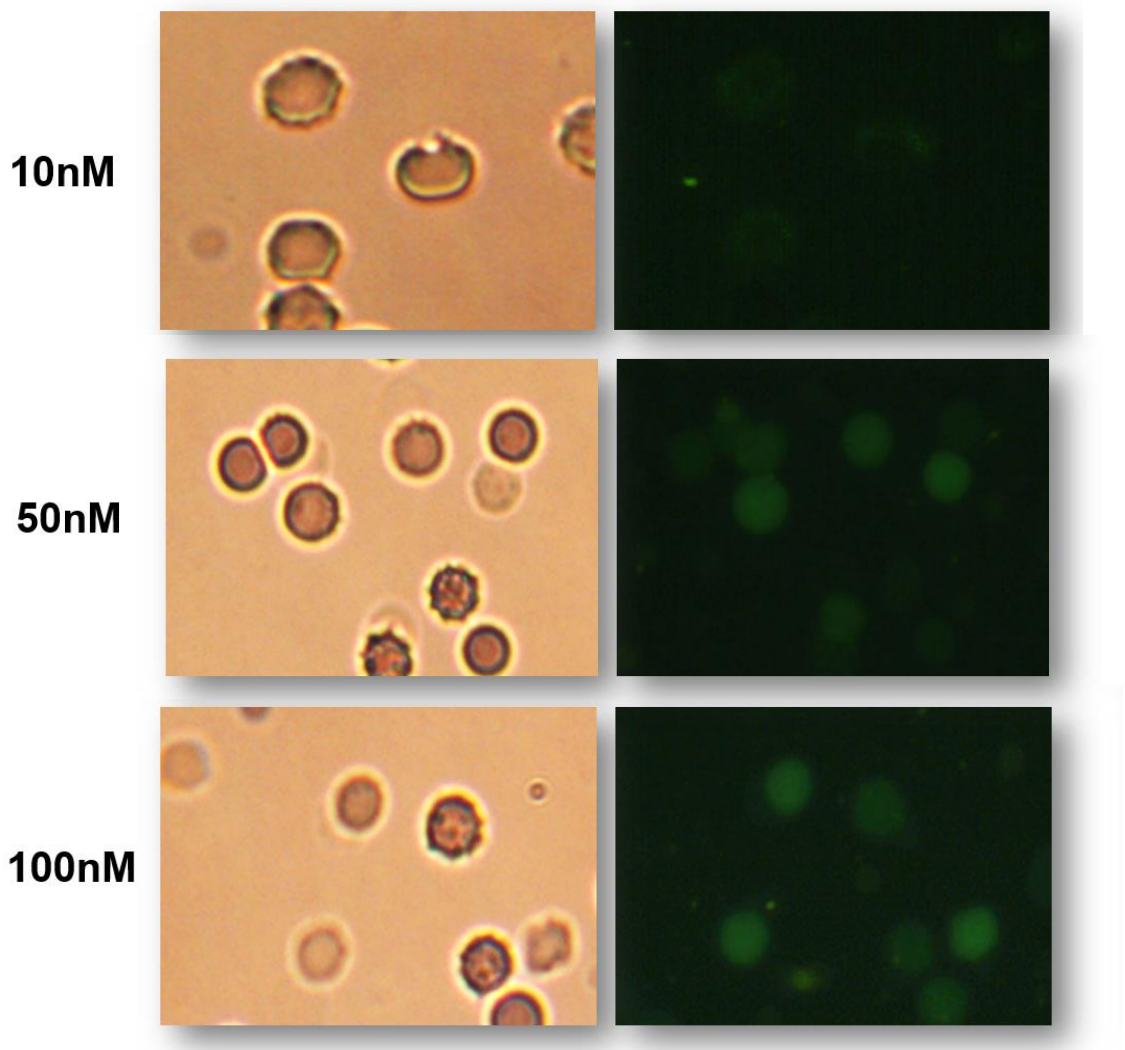

Figure 3.17 - Determination of cellular oxidative stress in erythrocytes cells incubated with COOH-QDs. Erythrocyte cells were incubated with 10nM, 50nM and 100nM of COOH-QDs for 30 minutes and treated with H_2DCFDA. Cells were observed with a magnification of 400x in bright field and in B-2A filter (Ex: 450-490nm; Em: 520-∞).

A control with erythrocytes at pH value of 6.2 was done in order to compare the level of fluorescence intensity with cells incubated with QDs. Normally, blood is slightly basic, with a pH range of 7.35 to 7.45. Decreasing the value of pH to 6.2, oxidative stress produced by erythrocytes is induced and comparing the response of cells subjected to different pH with those that were incubated with QDs, it is possible to estimate the level of oxidative stress due to the presence of QDs. In erythrocytes at pH value of 6.2, the DCF signal is significantly higher than in cells incubated with QDs (Figure 3.18), suggesting that the variation of pH leads to a high level of oxidative stress.

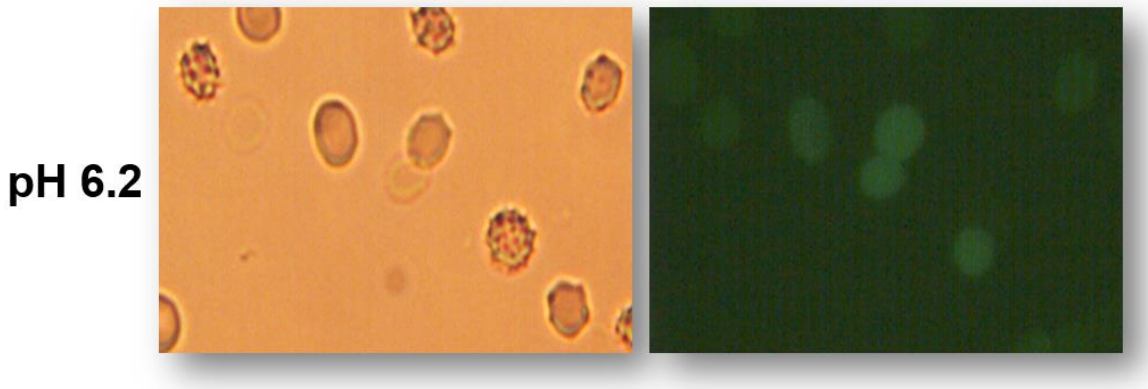

Figure 3.18 - Determination of cellular oxidative stress in erythrocytes cells induced by pH variation. Erythrocyte cells were subjected to a pH value of 6.2 for 30 minutes and treated with H_2DCFDA. Cells were observed with a magnification of 400x in bright field and in B-2A filter (Ex: 450-490nm; Em: 520-∞).

The control assay was prepared by incubating RBC just with H_2DCFDA. After incubation, H_2DCFDA shows a basal level DCF signal accumulated in whole cell area. This basal level of fluorescence is normal because despite the absence of mitochondria, ROS are constantly produced in erythrocytes due to their function as oxygen carrier protein haemoglobin that suffers autoxidation to produce $O^{2\bullet-}$. Moreover, erythrocytes are sensitive cells and are continuously exposed to both endogenous and exogenous sources of oxidants products. (Baynes, 2005). Other possible reason for this basal level of fluorescence is the chosen method to quantify the oxidative species in cells. Fluorescent microscopy is used to observe the produced fluorescents. This method has the problem of inducing photo-oxidation of H_2DCFDA to DCF at intracellular level caused by microscope light during the observation. It is difficult to control the time of light exposure when trying to locate, focus and photograph cells under the microscope (Wang and Joseph, 1999).

A normalized graphic representation of the measured fluorescence was acquired. To quantify the fluorescence in terms of average pixel intensity, an image processing program (ImageJ) was used. The fluorescence intensity was determined by multiplying the area of selected cells with mean of background and subtracting this value to their intensity value.

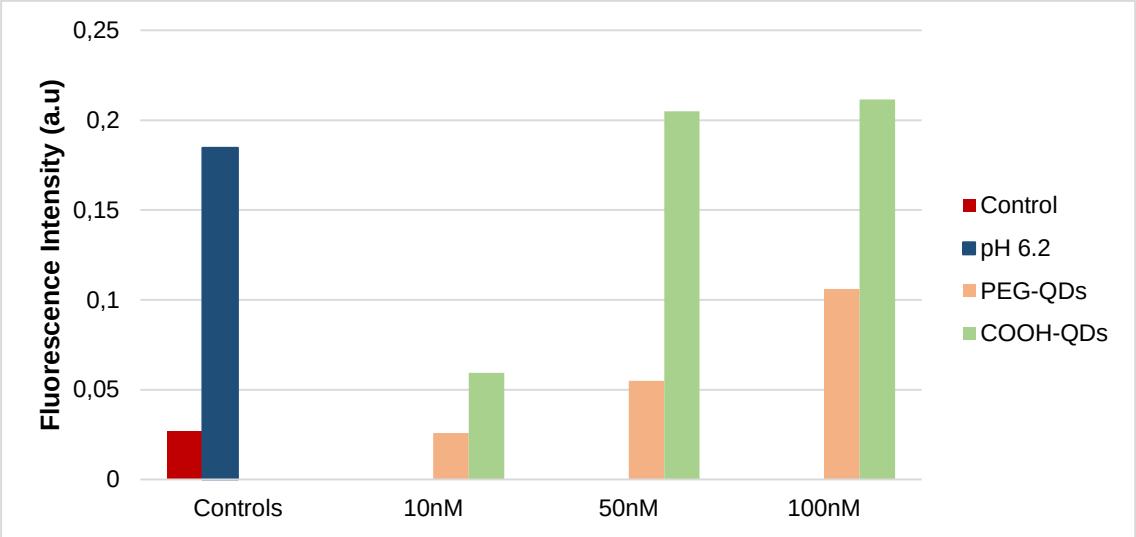

Figure 3.19 – Graphic representation of the fluorescence intensity of pictures from erythrocytes incubated with PEG and COOH-QDs and H_2DCFDA. The fluorescence intensity of erythrocyte cells incubated with 10, 50 and 100nM of QDs and treated with 20µM of H_2DCFDA was measured and compared with fluorescence intensity of control sample (erythrocytes treated with 20µM of H_2DCFDA) and cells with oxidative stress induced by pH at 6.2. The fluorescence was quantified in terms of average pixel intensity, using ImageJ program.

Figure 3.19 shows a graphic representation of pictures from: RBCs with H_2DCFDA, cells at pH of 6.2 and H_2DCFDA and RBCs incubated with PEG and COOH-QDs at three different concentrations: 10, 50 and 100nM for 30 minutes and further treatment with H_2DCFDA. Due to the interaction of PDDA-QDs with erythrocytes membrane, which forms a large quantity of cell aggregates and difficult the analysis of isolated cells, the quantification of fluorescence intensity was performed by using just PEG and COOH-QDs.

It can be observed that the cells at pH of 6.2 and incubated with QDs, present higher values of intensity in relation to the control. Comparing the intensity results obtained, while the control (RBCs and H_2DCFDA) maintained a value below 0.03 a.u. of intensity, RBCs incubated with QDs at three different concentrations demonstrate a higher fluorescence intensity with the increase of QDs concentration, which means that ROS production is intensified. When RBCs treated with QDs are compared with cells at pH value of 6.2, it is evident that changes in pH of cells medium induces an intense ROS production.

It is also notable the difference of oxidative stress produced by cells when they are incubated with PEG-QDs and COOH-QDs. At 10nM of concentration, PEG-QDs induce a stress response close to control. The fluorescence intensity increases with concentration but shows lower values than COOH-QDs. It has been reported that the coatings increase their solubility and reduce the cytotoxicity of QDs. Moreover, coatings bearing hydrophilic spacer such PEG on the nanoparticle surface. Could decrease the level of cytotoxicity by QDs in different mammalian cells (Miguel, 2012).

3.5.2. Design and Performance of Microfluidic Chip in Oxidative Stress Assays

The objective of this process is to create a sealed PDMS structure on glass that could trap single erythrocyte cells for consequently studies of oxidative stress produced by these cells. Erythrocytes are regular size cells with 5-7µm of diameter so the photolithography mask designs was consistent with this specific size of the cells. The traps were designed with different conformations, to evaluate the more efficient arrangement to capture the cells.

After the photolithography mask, the microfabrication process was initiated by transferring the pattern of the mask into the silicon wafer with SU-8 through UV-radiation. To make sure that the erythrocytes cells can easily pass through the microchambers, 20µm height channels were defined. After exposition to UV light, SU-8 mold for PDMS replica production was obtained. The PDMS mold allows the production of microfluidic chips. In addition, an intermediate epoxy mold using first PDMS replica as reference was fabricated in order to prevent the destruction of the original SU-8 mold due to several PDMS productions using the same wafer. That epoxy was spread over the PDMS mold previously obtained for production of PDMS microfluidic chips. The inlets and outlets of chips were then punched to allow the entry and exit of samples and reagents to the device.

To study the oxidative stress produced by erythrocytes at a single-cell level when incubated with QDs, cells were prepared using the same procedure of experiments on slide. Cells were incubated with COOH-QDs at three different concentrations: 10nM, 50nM and 100nM following the treatment with H_2DCFDA. The samples were injected in a microfluidic chip (previously treated with Ethanol and PEG) containing 1x PBS. Trapped cells were observed in microscope in bright field and using the fluorescence light. Results show that erythrocytes are retained in traps (Figure 3.20 – 1A, 2A and 3A) and for the three different concentrations of QDs, emitting fluorescence due to the conversion of H_2DCFDA non-fluorescent compound into DCF, which is fluorescent (Figure 3.20, 1B, 2B and 3B).

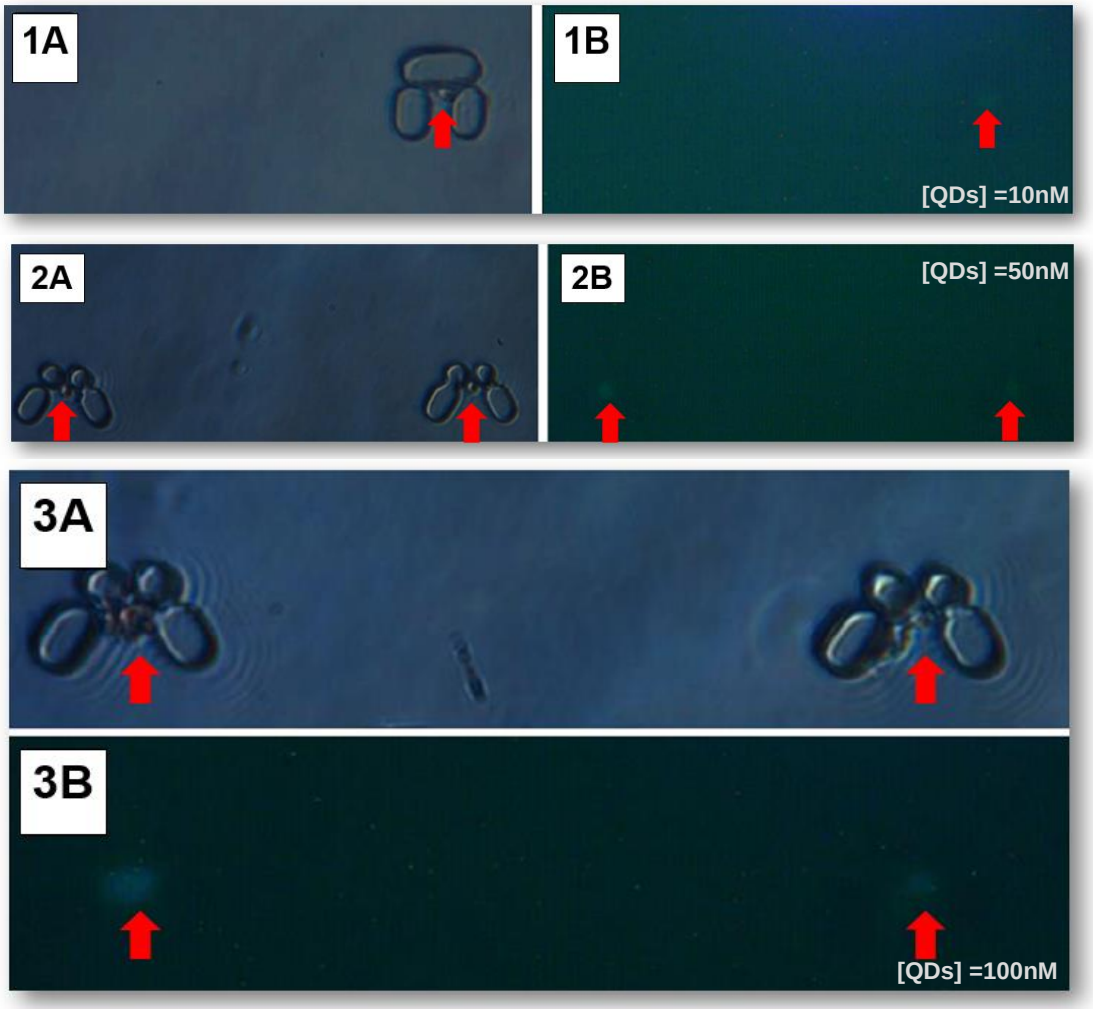

Figure 3.20 – Visualization of oxidative stress produced by trapped erythrocytes in microfluidic chip. Cells were incubated with 10nM (1A - 1B), 50nM (2A - 2B) and 100nM (3A - 3B) of COOH-QDs and treated with H2DCFDA at a concentration of 20µM. Images were acquired with a magnification of 400x in bright field (1A, 2A and 3A) and in B-2A filter (Ex: 450-490nm; Em: 520-∞) (1B, 2B and 3B).

However, difficulties in maintaining the cells attached to the traps for a period of time have been noted during the experiments, complicating the single-cell analysis. The parameters to construct traps in order to capture erythrocytes are in the resolution limits of the microfabrication process, due to the small dimensions and flexible characteristics of these cells. This can lead to production of defective traps (as can be seen in figure 3.21) limiting their ability to catch and hold the captured cells. In addition, the success of trapping process is also dependent on the conformation of traps.

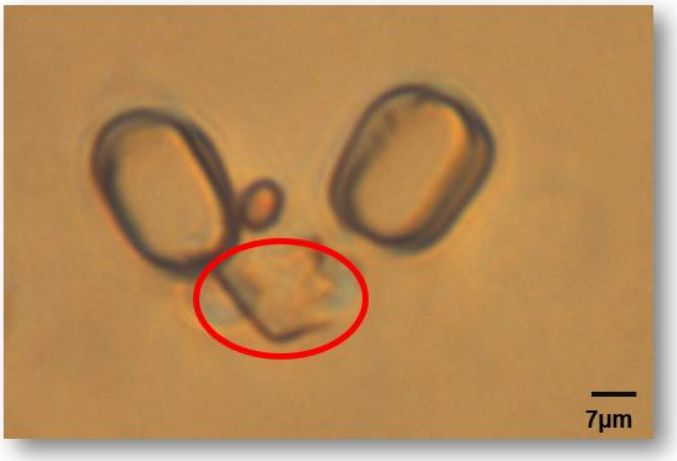

Figure 3.21 – Visualisation of a deformed trap in microfluidic chip. The image was acquired with a magnification of 400x in bright field.

Six different conformations of cell traps were used. As showed in figure 3.22, there are two regular shapes: the “U” (A, B and D) and “V” conformation (C, E and F). Each one has different openings and some of them have two (C and D) or three opened gaps (A and F) with 2µm size. These opened gaps allow the passage of the liquid flux through the traps.

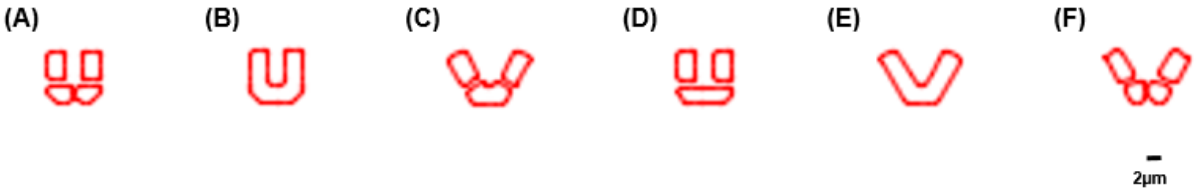

Figure 3.22 – Different structures of designed traps. The traps (A) to (F) were designed and tested on chip to perform the biological assay.

The passage of the liquid flux through the traps is an important factor which can increase the efficiency of cell trapping. Analysing the efficiency of different traps on capturing cells during the experiment, it was possible to observe that traps with gaps (Figure 3.23) are more efficient on catching the cells than the traps without opened gaps.

The displacement of cells from the traps are associated with minimal flow movements. Any perturbation triggered by several factors like temperature changes (due to continuous irradiation by microscope lamp) or mechanical movements, can cause changes in liquid flux because its density varies inside the microchip channels and due to the small dimensions of structures, these differences become relevant in the assay performance. These obstacles have hampered the continuous monitoring of trapped cell.

Figure 3.23 – Visualisation of cell trapping. A single-cell was stuck in trap with two opened gaps. The image was acquired with a magnification of 400x in bright field.

The process of RBCs trapping is not immediate because a large percentage of injected cells tends to circumvent the traps, as can be seen in sequence demonstrated in figure 3.24. Observing under the microscope, it can be seen that when cells were approaching the closed traps they passed by them instead of being trapped. The structures with opened gaps can trap a number of cells due to the passage of liquid flux between the small structures. Another aspect is the flexible characteristic of these cells which can be a problem if the cells pass by the small openings.

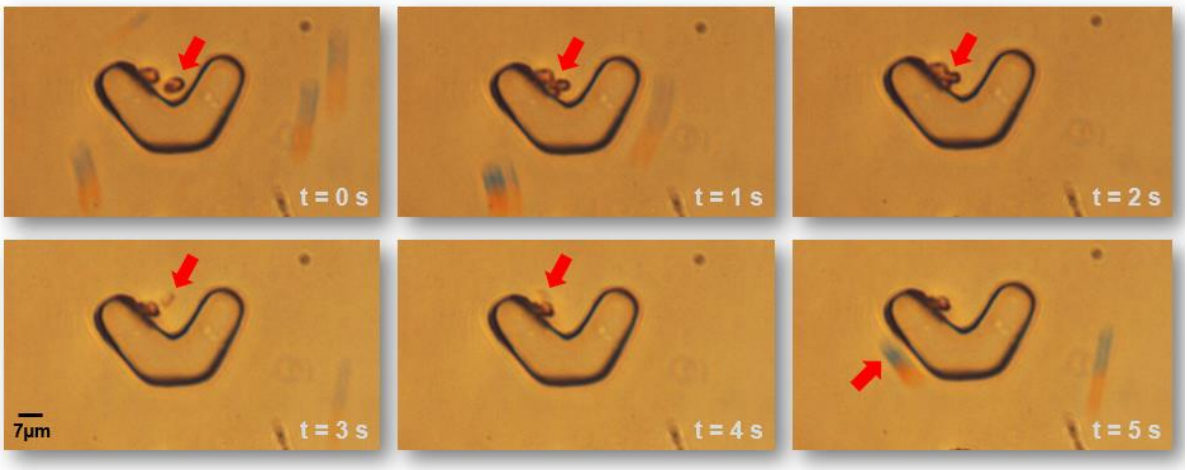

Figure 3.24 - Sequence of images taken during the cell trapping. It can be observed two cells (yellow and red) deviating from the direction of the same trap. Cells initially tend to align with the trap but they end up circumventing it and follow the direction of liquid flux with less resistance**.** The images were acquired with a magnification of 400x in bright field.

Between the changes in pressure and velocity of particles, one of the objectives of computational simulations performed by COMSOL software is to know the fluid behaviour throughout the chip, before the construction of the microfluidic platforms. This simulations also serve as guidelines to predict what will happen during the assay. In the simulations carried out

for erythrocyte chips, it was possible to observe the flux behaviour in different conformations of traps (Figure 3.25).

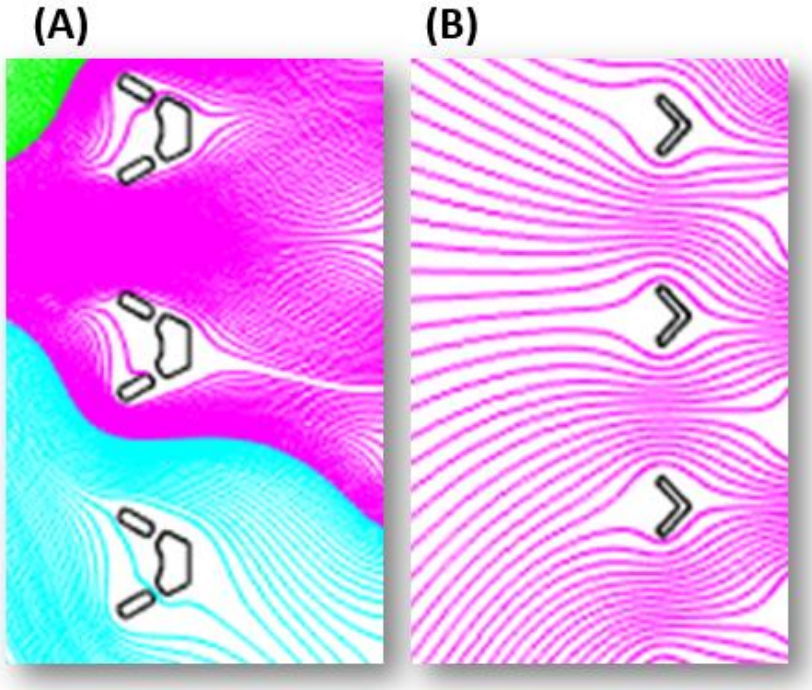

Figure 3.25 – Example of microfluidic simulation performed by COMSOL software. Streamlines representation of flux velocity applied to the device. In traps with opened gaps, the passage of fluid through the channels is observed (A) while in closed traps, the fluid tend to circumvent the trap.

In traps without opened gaps, the flux tend to circumvent the trap which difficult the capture of cells. For traps with two or more opened gaps, the passage of flux between them, facilitates the cell trapping, highlighting that this conformation is more efficient to catch and maintain these type of cells.

Additionally, it is also visible that some cells are stuck in the glass instead of being retained on traps (Figure 3.26).

Figure 3.26 – Visualisation of some problems during the experiment with erythrocyte cells incubated with QDs and H_2DCFDA. Initially, cells get stuck in traps (A) but they tend to escape from them due to the liquid flux (C). Figure (B) shows a trash stuck in glass which is fluorescent. The images were acquired with a magnification of 400x and under bright field (A) and (C) and under B-2A filter (B).

To overcome this situation, a pre-treatment and special cleaning protocol of chips were performed before starting the biological experiment. The chip is cleaned and treated with Ethanol. The surface of PDMS chips is naturally hydrophobic making it difficult to fill the PDMS channels with aqueous solution. A solvent like Ethanol gives PDMS walls hydrophilic properties. The following step is the treatment with PEG. The purpose of this treatment is to remove the charges from PDMS walls, preventing the cells being adsorbing indiscriminately to the channel surfaces during the experiment. Finally, the chip is washed with cell medium, in this case, 1X PBS, to eliminate residues of reagents previously used.

Another challenging issues is the presence of air bubbles during the microfluidic assay. When chip is wetted for the first time, is common to get some bubbles but they can also appear during the experiment which can be a problem and difficult the continuity of the experience. This can be due to the switch of the injected liquid, the porous characteristics of PDMS that makes it permeable to air, the leakages in the fittings of the setup and due to the existence of dissolved gas in the liquids used. It is complicated to remove bubbles from the channels but this can be solved by degassing of reagents and putting the chips in the exsiccator.

In general, the design and fabrication of structures in resolution limits was achieved and the chips obtained are efficient in capture cells even their small dimensions. However, the cell trapping and retention are dependent on liquid flux behaviour.

Conclusions and Future Perspectives

Within the aim of this work which is focused on the development of new tolls for studying erythrocytes, probes with COOH-QDs conjugated with specific antibodies were prepared. Two antibodies were used to detect specific proteins in erythrocytes: Glycophorin A, present on erythrocyte membrane and AMA1, expressed in infected erythrocytes with *Babesia ovis*. The final conjugates were incubated with non-infected and infected cells, respectively. Moreover, microfluidic platforms were designed and constructed to capture erythrocytes and to evaluate the oxidative stress produced by the interaction of QDs with these cells.

The data related with the electrophoretic mobility assays of QDs shows that it depends on the nature of their surface ligands (PDDA, PEG and COOH) and for these three types of QDs, that mobility is not affected by pH range between 5 and 8.

The evaluation of cytotoxic effect in RBCs allowed to conclude that QDs interaction with cells induces the production of ROS, proving that cells are suffering oxidative stress, which increase with the QDs concentration. It is also evident that COOH-QDs lead to a higher oxidative stress than PEG-QDs, meaning that the kind of coatings used for solubility and conjugation reduce the negative impact of QDs. Extending this type of study is important to investigate other surface ligands like dihydrolipoic acid or other with functional terminals such OH or NH_2. Another aspect that has been observed is the lack of specificity of the H_2DCFDA probe, which does not enable to know the type of reactive species is forming inside the cells. Thus, this assay is just a qualitative marker of cellular oxidative stress. In order to obtain a precise indicator of rates of reactive species (such H_2O_2) produced, 12-O-Tetradecanoylphorbol.13-acetate (TPA) and Amplex® UltraRed reagent (AuR) could be used to detect hydroxyl radicals (HO•) and peroxidases respectively. In that case, the concentration of fluorescent products can be determined fluorometrically.

In relation to the microfabrication, it would be of advantage of molding process to obtain appropriate standardised PDMS devices with same predefined dimensions, without casting errors in fabrication of traps. The manipulation of samples inside the microchip must be prudently performed to avoid the input of debris and impurities, filtering and controlling the velocity of samples insertion. To prevent the movement of cells away of the traps during the experiment, it is necessary to perform every experiment step very carefully, avoiding the irradiation of cells with microscope light for long periods of time and reducing any mechanical perturbation that could influence the stability of trapped cells.

In the characterization of bioconjugate products by agarose gel, it was demonstrated that bioconjugated QDs move slower than non-conjugated particles. This is a consequence of the higher size of complexes and the reduced negative surface charge. The SDS-PAGE using DTT as reducing reagent was suitable to clarify the binding properties of conjugates. The immunoblotting performed to evaluate the biological activity showed that antibodies present in QDs-Ab complexes were functional and recognize their specific antigen. However, alternative strategies using specific sites of Ab should also be carried out to achieve a higher conjugation

efficiency and a better stability of the QDs-Ab complexes. Even though these strategies imply the modification of antibodies, higher rates or complete conjugation may be reached, as well as an improved site specificity of the final complexes. It is possible to conjugate QDs with Ab by cross-linking reactions between amino-QDs and an aldehyde formed by oxidation of carbohydrate groups located on the Ab's Fc region (Xing et al., 2007). It is also reproducible the conjugation by reacting the NH_2 group on QDs surface with sulfo-SMCC through the sulphydryl groups present in Ab fragments derived from previously reduced IgG with DTT (Xing et al., 2007). This strategy can lead to bioconjugates with better biological activity, resulting in less interference in a posterior protein identification step. Moreover, the use of this techniques to characterize the final samples should be deeper studied in order to promote less aggregation and well dispersion of the bioconjugates in the wells, allowing a better mobility through the gels.

The bioconjugates tested with the biological samples demonstrated that the fluorescence emitted by the QDs is more intense than the fluorescence emitted by the standard dye (FITC) conjugated to secondary antibody. This highlights the higher capability of QDs to be more resistant to large periods of excitation at different wavelengths. Thus, when coupled with specific biomolecules, QDs could be useful in the development of an immunosensor for disease diagnosis. However, the direct immunofluorescence assay with QDs-Ab complexes did not show the recognition of AMA1 protein in infected erythrocytes with *B.ovis* neither the GPA protein. Further studies should be performed in order to optimize the concentration required of primary antibody that should be linked to the QDs. The stability of bioconjugated QDs must also be controlled to avoid the aggregates formation during the immunofluorescence assays.

Generally, the systems developed in this project proved that they are useful for the biological assays of single cells, even the small ones. However, several optimizations and alternative procedures should be addressed in order to achieve a higher efficiency.

Bibliography

Abcam Western Blotting - A Beginner's Guide. http://www.abcam.com/ps/pdf/protocols/WB-beginner.pdf

Agrawal A, Zhang C, Byassee T, Tripp RA, Nie S. 2006. Counting single native biomolecules and intact viruses with color-coded nanoparticles. *Anal Chem*;78:1061–70

Aktas M. Altay K. Dumanly N. 2005. Development of a polymerase chain reaction method for diagnosis of Babesia ovis infection in sheeps and goats. *Vet. Parasitol*, 133, pp. 277–281

Alivisatos AP, Gu W, Larabell C. 2005. Quantum dots as cellular probes. *Annu Rev Biomed Eng*;7:55–76

Alivisatos, P., 2004. The use of nanocrystals in biological detection. *Nat Biotechnol*, 22, (1), 47-52

Al-Omar MA, Beedham C, Alsarra IA. 2004. Pathological roles of reactive oxygen species and their defence mechanisms. *Saudi Pharm*;12:1–18.

Apel K, Hirt H. 2004. Reactive oxygen species: Metabolism, Oxidative Stress, and Signal Transduction. *Annual Review of Plant Biology*, 55:373–99.

Azzazy, H.M., Mansour, M.M., Kazmier, S.C., 2007. From diagnostics to therapy: prospects of quantum dots. *Clin. Biochem*. 40, 917–927

Bauer J. 1999. Advances in cell separation: recent developments in counter-flow centrifugal elutriation and continuous flow cell separation. *J. Chromatogr. B*. 722(1–2):55–69.

Baynes JW. 2005. Oxygen and life. In: Baynes JW, Domoniczak MH, editors. *Medical Biochemistry*. Philadelphia: Elsevier. p. 497–506

Bose, R.; Jorgensen, W. K.; Dalgliesh, R. J.; Friedhoff, K. T.; Devos, A. J., 1995. Current State and Future-Trends in the Diagnosis of Babesiosis. *Vet Parasitol*, 57, (1-3), 61-74.

Bolt, M. W.; Mahoney, P. A. 1997. High-Efficiency Blotting of Proteins of Diverse Sizes Following Sodium Dodecyl Sulfate–Polyacrylamide Gel Electrophoresis. *Anal Biochem***,** 247, 185-192

Branton, D., Cohen, C. M., & Tyler, J. 1981. Interaction of cytoskeletal proteins on the human erythrocyte membrane. *Cell*, *24*(1), 24-32.

Bretscher, M. S. 1975. C-terminal region of the major erythrocyte sialoglycoprotein is on the cytoplasmic side of the membrane. *Journal of molecular biology*, *98*(4), 831-833.

Bruchez MP. 2005. Turning all the lights on: quantum dots in cellular assays. *Curr Opin Chem* Biol;9:533–**7.**

Bunn HF. Pathophysiology of the anemias. In: Wilson JD, Braunwald E, Isselbacher KJ, editors. Harrison's Principle of Internal Medicine. New York: McGraw-Hill Inc; 1991. p. 1514–8

Carter , P. , Smith , L., and Ryan , M. 2004. Identification and validation of cell surface antigens for antibody targeting in oncology. *Endocr. Relat. Cancer* 11 , 659– 687 **.**

Chan WC, Maxwell DJ, Gao X, Bailey RE, Han M, Nie S. 2002. Luminescent quantum dots for multiplexed biological detection and imaging. *Curr Opin Biotechnol*;13:40–6

Chang, E.; Thekkek, N.; Yu, W. W.; Colvin, V. L.; Drezek, R., 2006. Evaluation of quantum dot cytotoxicity based on intracellular uptake. *Small,* 2, (12), 1412-1417

Chasis, J. A., & Mohandas, N. 1992. Red blood cell glycophorins. *Blood*,*80*(8), 1869-1879.

Chaudhuri, R. G.; Paria, S., 2012. Core/Shell Nanoparticles: Classes, Properties, Synthesis Mechanisms, Characterization, and Applications. *Chem Rev*, 112, (4), 2373-2433

Cheesman KH, Slater TF. An introduction to free radical biochemistry. In: Cheesman KH, Slater TF, editors. Free Radical in Medicine. New York: Chrchill Livingstone; 1993. p. 481–93

Çimen, M. B. 2008. Free radical metabolism in human erythrocytes. *Clinica Chimica Acta*, *390*(1), 1-11.

Clapp, A. R.; Goldman, E. R.; Mattoussi, H., 2006. Capping of CdSe-ZnS quantum dots with DHLA and subsequent conjugation with proteins. *Nat Protoc*, 1, (3), 1258-1266

Cooke, B. M., Mohandas, N., Cowman, A. F., & Coppel, R. L. 2005. Cellular adhesive phenomena in apicomplexan parasites of red blood cells. *Veterinary parasitology*, *132*(3), 273-295

Costa-Junior, L. M.; Rabelo, E. M. L.; Martins-Filho, O. A.; Ribeiro, M. F. B., 2006. Comparison of different direct diagnostic methods to identify Babesia bovis and Babesia bigemina in animals vaccinated with live attenuated parasites. *Vet Parasitol 2006*, 139, (1-3), 231-236

Dahan M, Levi S, Luccardini C, Rostaing P, Riveau P, Triller A. 2003. Diffusion dynamics of glycine receptors revealed by single-quantum dot tracking. *Science*;302:442–5.

Dahr, W. 1986. Immunochemistry of sialoglycoproteins in human red blood cell membranes. *Recent advances in blood group biochemistry*, 23-65.

Deans, J. A., Alderson, T., Thomas, A. W., Mitchell, G. H., Lennox, E. S., & Cohen, S. 1982. Rat monoclonal antibodies which inhibit the in vitro multiplication of Plasmodium knowlesi. *Clinical and experimental immunology*, *49*(2), 297.

Derfus, A. M.; Chan, W. C. W.; Bhatia, S. N., 2004. Probing the cytotoxicity of semiconductor quantum dots. *Nano Lett*, 4, (1), 11-18.

De Souza, W., 2006. Secretory organelles of pathogenic protozoa. *An Acad Bras Cienc*, 78, (2), 271-291**.**

Dittrich P.S, Tachikawa K. & Manz A. 2006. Micro total analysis systems. Latest advancements and trends. *Anal Chem,* pp. 3887–3907

Duan, H. W.; Nie, S. M., 2007. Cell-penetrating quantum dots based on multivalent and endosome-disrupting surface coatings. *J Am Chem Soc*, 129, (11), 3333-3338.

Dumaswala UJ, Zhuo L, Jacobsen DW, Jain SK, Sukalski KA. 1999. Protein and lipid oxidation of banked human erythrocytes: role of glutathione. Free Radic Biol Med;27:1041–9.

El-Ali J, P.K. Sorger P.K, & Jensen K.F. 2006. Cells on chips. *Nature*, 442, pp. 403–411

Elhadj, S., Rioux, R.M., Dickey, M.D., DeYoreo, J.J., Whitesides, G.M., 2010. Subnanometer Replica Molding of Molecular Steps on Ionic Crystals. *Nano Lett*. 10(10), 4140-4145.

Fairbanks, G., Steck, T. L., & Wallach, D. F. H. 1971. Electrophoretic analysis of the major polypeptides of the human erythrocyte membrane.*Biochemistry*, *10*(13), 2606-2617.

Fortina P, Kricka LJ, Surrey S, Grodzinski P. 2005. Nanobiotechnology: the promise and reality of new approaches to molecular recognition. *Trends Biotechnol*;23:168–73.

Franssila, S., 2010. Introduction to Microfabrication. John Wiley & Sons, Ltd, Chichester, UK. Garcia, D., Ghansah, I., LeBlanc, J., Butte, M.J., 2012. Counting cells with a low-cost integrated microfluidics-waveguide sensor. *Biomicrofluidics* 6(1), 014115.

Furthmayr, H., Tomita, M., & Marchesi, V. T. 1975. Fractionation of the major sialoglycopeptides of the human red blood cell membrane. *Biochemical and biophysical research communications*, *65*(1), 113-121.

Fukuda S, Schmid-Schonbein GW. 2002. Centrifugation attenuates the fluid shear response of circulating leukocytes. *J. Leukocyte Biol*. 72(1):133–139.

Gahmberg, C. G., Jokinen, M., & Andersson, L. C. 1978. Expression of the major sialoglycoprotein (glycophorin) on erythroid cells in human bone marrow.*Blood*, *52*(2), 379-387.

Gechev, T. S., Van Breusegem, F., Stone, J. M., Denev, I., & Laloi, C. 2006. Reactive oxygen species as signals that modulate plant stress responses and programmed cell death. *Bioessays*, *28*(11), 1091-1101.

Goff, W. L., & Yunker, C. E. 1988. Effects of pH, buffers and medium-storage on the growth of Babesia bovis in vitro. *International journal for parasitology*,*18*(6), 775-778.

Goldsby, RA.; Kindt, TJ.; Osborne, BA.; Kuby, J. *Immunology*. 5th ed. New York: W.H. Freeman; 2003. p. A-1-A-12.

Gohil, S.; Kats, L. M.; Sturm, A.; Cooke, B. M., 2010. Recent insights into alteration of red blood cells by Babesia bovis: moovin' forward. *Trends Parasitol*, 26, (12), 591-599.

Hardman R. 2006. A toxicologic review of quantum dots: toxicity depends on physicochemical and environmental factors. *Environ Health Perspect*;114:165–72

Healer, J., Crawford, S., Ralph, S., McFadden, G., & Cowman, A. F. 2002. Independent translocation of two micronemal proteins in developing Plasmodium falciparum merozoites. *Infect. Immun*. 70, 5751–5758

Hermanson, G. T. *Bioconjugate techniques*. San Diego. Academic Press.2008

Herold, K.E. and Rasooly, A. *Lab-on-a-Chip Technology (Vol.1): Fabrication and Microfluidics*. Maryland. Caister Academic Press. 2009

Hodder, A.N., Crewther, P.E., Matthew, M.L.S.M., Reid, G.E., Moritz, R.L., Simpson, R.J., and Anders, R.F. 1996. The disulphide bond structure of Plasmodium apical membrane antigen-1. *J Biol Chem* 271: 29446±29452.

Hoet P, Boczkowsky J. 2008. What's new in Nanotoxicology? Brief review of the 2007 literature. *Nanotoxicology*, 2: 171-182.

Homer, M. J.; Aguilar-Delfin, I.; Telford, S. R.; Krause, P. J.; Persing, D. H., 2000. Babesiosis. *Clin Microbiol Rev*, 13, (3), 451-469.

Horta, S., Barreto, M. C., Pepe, A., Campos, J., & Oliva, A. 2014. Highly sensitive method for diagnosis of subclinical *B. ovis* infection. *Ticks and tick-borne diseases*, *5*(6), 902-906.

Jackson, L. A., Waldron, S. J., Weier, H. M., Nicoll, C. L., & Cooke, B. M. 2001. Babesia bovis: culture of laboratory-adapted parasite lines and clinical isolates in a chemically defined medium. *Experimental parasitology*, *99*(3), 168-174.

Jain KK. 2003. Nanodiagnostics: application of nanotechnology in molecular diagnostics. *Expert Rev Mol Diagn*;3:153–61.

Jaiswal JK, Simon SM. 2004. Potentials and pitfalls of fluorescent quantum dots for biological imaging. *Trends Cell Biol*;14:497–504

Jin, S.; Hu, Y.; Gu, Z.; Liu, L.; Wu, H.-C., 2011. Application of Quantum Dots in Biological Imaging. *Journal of Nanomaterials*, 2011, 13.

Johnson RM, Goyette Jr G, Ravindranath Y, Ho YS. 2005. Hemoglobin autoxidation and regulation of endogenous H2O2 levels in erythrocytes. Free Radic Biol Med;39:1407–17.

Jorge, P; Martins, MA; Trindade, T; Santos, JL; Farahi, F. 2007. Optical fiber sensing using quantum dots. *Sensors*, 7, 3489–3534

Kain, K. C., Jassoum, S. B., Fong, I. W., & Hannach, B. 2001. Transfusion-transmitted babesiosis in Ontario: first reported case in Canada. *Canadian Medical Association Journal*, *164*(12), 1721-1723.

Kirchner, C.; Liedl, T.; Kudera, S.; Pellegrino, T.; Javier, A. M.; Gaub, H. E.; Stolzle, S.; Fertig, N.; Parak, W. J., 2005. Cytotoxicity of colloidal CdSe and CdSe/ZnS nanoparticles. *Nano Lett*, 5, (2), 331-338.

Kortan, A. R., Hull, R., Opila, R. L., Bawendi, M. G., Steigerwald, M. L., Carroll, P. J., & Brus, L. E. 1990. Nucleation and growth of cadmium selendie on zinc sulfide quantum crystallite seeds, and vice versa, in inverse micelle media. *Journal of the American Chemical Society*, *112*(4), 1327-1332.

Kuttel, C.; Nascimento, E.; Demierre, N.; Silva, T.; Braschler, T.; Renaud, P.; Oliva, A. G., 2007. Label-free detection of Babesia bovis infected red blood cells using impedance spectroscopy on a microfabricated flow cytometer. *Acta Trop*, 102, (1), 63-68

Lecault, V., White, A. K., Singhal, A. & Hansen, C. L. 2012. Microfluidic single cell analysis: from promise to practice. *Current Opinion in Biotechnology*. 16, 381–390

Lin Z, Su X, Mu Y, Jin Q. 2004. Methods for labeling quantum dots to biomolecules. *J Nanosci Nanotechnol*;4:641–5

Lundahl J, Hallden G, Hallgren M, Skold CM, Hed J. 1995. Altered expression of Cd11b/Cd18 and Cd62l on human mono-cytes after cell preparation procedures. *J. Immunol. Methods*. 180(1):93–100.

Lux, S. E., & Glader, B. E. 1981. Hematology of Infancy and Childhood.

Male K, Lachance B, Hrapovic S, Sunahara G, Luong J. 2008. Assessment of Cytotoxicity of Quantum Dots and Gold Nanoparticles Using Cell-Based Impedance Spectroscopy. *Analytical Chemistry*, 80: 5487– 5493**.**

Mattoussi, H.; Mauro, J. M.; Goldman, E. R.; Anderson, G. P.; Sundar, V. C.; Mikulec, F. V.; Bawendi, M. G., 2000. Self-assembly of CdSe-ZnS quantum dot bioconjugates using an engineered recombinant protein. *J Am Chem Soc*, 122, (49), 12142-12150

Maysinger D, Lovrić J, Eisenberg A, Savić R. 2007. Fate of micelles and quantum dots in cells. *European Journal of Pharmaceutics and Biopharmaceutics*, 65: 270–281.

Medintz, I. L.; Uyeda, H. T.; Goldman, E. R.; Mattoussi, H., 2005. Quantum dot bioconjugates for imaging, labelling and sensing. *Nature Materials*, 4, 435-446

Meira, M. 2015. *Microfluidics: A New Look At Cell Migration Analysis*. Msc Thesis. Faculdade de Ciências e Tecnologia da Universidade Nova de Lisboa

Mews, A., Eychmüller, A., Giersig, M., Schooss, D., & Weller, H. 1994. Preparation, characterization, and photophysics of the quantum dot quantum well system cadmium sulfide/mercury sulfide/cadmium sulfide. *The Journal of Physical Chemistry*, *98*(3), 934-941.

Michalet X, Pinaud FF, Bentolila LA, Tsay JM, Doose S, Li JJ, et al. 2005. Quantum dots for live cells, in vivo imaging, and diagnostics. *Science*;307:538–44

Mohanty, J. G., Nagababu, E., Friedman, J. S., & Rifkind, J. M. 2013. SOD2 deficiency in hematopoietic cells in mice results in reduced red blood cell deformability and increased heme degradation. *Experimental hematology*,*41*(3), 316-321.

Narum, D.L., and Thomas, A.W. 1994. Differential localization of full-length and processed forms of PF83/AMA-1 an apical membrane antigen of Plasmodium falciparum merozoites. Mol *Biochem Parasitol* 67: 59±68.

Nebija, D., Noe, C. R., Urban, E., & Lachmann, B. 2014. Quality Control and Stability Studies with the Monoclonal Antibody, Trastuzumab: Application of 1D- *vs.* 2D-Gel Electrophoresis. *International Journal of Molecular Sciences*,*15*(4), 6399–6411. http://doi.org/10.3390/ijms15046399

Ness JM, Akhtar RS, Latham CB, Roth KA. 2003. Combined tyramide signal amplification and quantum dots for sensitive and photostable immunofluorescence detection. *J Histochem Cytochem*;51:981–7

Ozkan M. 2004. Quantum dots and other nanoparticles: what can they offer to drug discovery? *Drug Discov Today*;9:1065–71

Parak W.J, Pellegrino T. and Plank C. 2005. Labelling of cells with quantum dots. *Nanotechnology*, 16 R9–25

Pellegrino T et al . 2004. Hydrophobic nanocrystals coated with an amphiphilic polymer shell: a general route to water soluble nanocrystals. *Nano Lett*. 4 703–7

Pereira, M.; Lai, E. P., 2008. Capillary electrophoresis for the characterization of quantum dots after non-selective or selective bioconjugation with antibodies for immunoassay. *Journal of Nanobiotechnology*, 6, 10

Qu, G., Wang, X., Wang, Z., Liu, S., & Jiang, G. 2013. Cytotoxicity of quantum dots and graphene oxide to erythroid cells and macrophages.*Nanoscale research letters*, *8*(1), 1-9.

Remarque, E.J. et al. 2008. Apical membrane antigen 1: a malaria vaccine candidate in review. *Trends Parasitol*. 24, 74–84

Rigler R, Vogel H. 2008. Single Molecules and Nanotechnology*. Springer Series in Biophysics 12*, pp:57,58, 61.

Roman G.T, Chen Y, Viberg P, Culbertson A.H, Culbertson C.T 2007 Single-cell manipulation and analysis using microfluidic devices. *Anal. Bioanal. Chem*. 387, 9–12

Rosenthal, S. J.; Chang, J. C.; Kovtun, O.; McBride, J. R.; Tomlinson, I. D., 2011. Biocompatible Quantum Dots for Biological Applications. *Chem Biol*, 18, (1), 10-24.

Rossetti R, Brus L. 1982. Electron–hole recombination emission as a probe of surface chemistry in aqueous CdS colloids. *J Phys Chem*;86:4470–2.

Salata O. 2004. Applications of nanoparticles in biology and medicine. *J Nanobiotech*;2:3

Santos, A. (2009). *Biotoxicity Assays of Quantum Dots in in vitro cultures of Medicago sativa amd Medicago truncatula.*. Msc Thesis. Faculdade de Ciências e Tecnologia da Universidade Nova de Lisboa

Schaefer, J. V., and Plückthun, A. 2012. Transfer of engineered biophysical properties between different antibody formats and expression systems. Protein Eng. Sel. Des. 25, 485-506.

Schauer, R. 1985. Sialic acids and their role as biological masks. *Trends in Biochemical Sciences*, *10*(9), 357-360.

Schmid, A., Kortmann, H., Dittrich, P.S. & Blank, L.M. 2010. Chemical and biological single cell analysis. *Current Opinion in Biotechnology*. 21, 12–20

Schnittger, L.; Yin, H.; Qi, B.; Gubbels, M. J.; Beyer, D.; Niemann, S.; Jongejan, F.; Ahmed, J. S., 2004. Simultaneous detection and differentiation of Theileria and Babesia parasites infecting small ruminants by reverse line blotting. *Parasitol Res*, 92, (3), 189-196

Schuster, F. L. 2002. Cultivation of Babesia and Babesia-like blood parasites: agents of an emerging zoonotic disease. *Clinical microbiology reviews*, *15*(3), 365-373

Sevinc F, Guler L, Sevinc M, Ekici OD, Isik N. 2013. Determination of immunoreactive proteins of Babesia ovis. *Vet Parasitol*.198(3-4):391-5**.**

Shao H, Chu L, Lu Z, Kang C. 2008. Primary antioxidant free radical scavenging and redox signalling pathways in higher plant cells. *International Journal of Biological Sciences*, 4: 8-14.

Shao, L. J.; Gao, Y. F.; Yan, F., 2011. Semiconductor Quantum Dots for Biomedicial Applications. *Sensors-Basel*, 11, (12), 11736-11751.

Shiohara A, Hoshino A, Hanaki K, Suzuki K, Yamamoto K. 2004. On the cyto-toxicity caused by Quantum Dots. *Microbiol. Immunol*., 48: 669- 675.

Silva, M. G., Henriques, G., Sanchez, C., Marques, P. X., Suarez, C. E., & Oliva, A. 2009. First survey for *Babesia bovis* and *Babesia bigemina* infection in cattle from Central and Southern regions of Portugal using serological and DNA detection methods. *Veterinary parasitology*, *166*(1), 66-72

Smith AM, Dave S, Nie S, True L, Gao X. 2006. Multicolor quantum dots for molecular diagnostics of cancer. *Expert Rev Mol Diagn*;6:231–44**.**

Smith, A. M.; Duan, H. W.; Mohs, A. M.; Nie, S. M., 2008. Bioconjugated quantum dots for in vivo molecular and cellular imaging. *Adv Drug Deliver Rev*, 60, (11), 1226-1240.

Spencer, A. M., Goethert, H. K., Telford III, S. R., & Holman, P. J. 2006. In vitro host erythrocyte specificity and differential morphology of Babesia divergens and a zoonotic Babesia sp. from eastern cottontail rabbits (Sylvilagus floridanus). *Journal of Parasitology*, *92*(2), 333-340.

Suarez, C. E.; Palmer, G. H.; Jasmer, D. P.; Hines, S. A.; Perryman, L. E.; Mcelwain, T. F., 1991. Characterization of the Gene Encoding a 60-Kilodalton Babesia-Bovis Merozoite Protein with Conserved and Surface Exposed Epitopes. *Mol Biochem Parasit*, 46, (1), 45-52

Sukhanova, A., Devy, J., Venteo, L., Kaplan, H., Artemyev, M., Oleinikov, V., ... & Nabiev, I. 2004. Biocompatible fluorescent nanocrystals for immunolabeling of membrane proteins and cells. *Analytical biochemistry*,*324*(1), 60-67.

Tabeling, P., 2006. Introduction to Microfluidics. Oxford University Press, Incorporated.

Talapin, D. V.; Lee, J. S.; Kovalenko, M. V.; Shevchenko, E. V., 2010. Prospects of Colloidal Nanocrystals for Electronic and Optoelectronic Applications. *Chem Rev*, 110, (1), 389-458.

Tayyab, S., & Qasim, M. A. 1988. Biochemistry and roles of glycophorin A.*Biochemical Education*, *16*(2), 63-66.

Telen MJ, Kaufman RE. The mature erythrocyte. In: Greer JP, Foerster J, editors. Wintrobe's Clinical Hematology. Philadelphia: Lippincott Williams & Wilkins; 1999. p. 217–47

Telford III, S. R., Gorenflot, A., Brasseur, P., & Spielman, A. 1993. Babesial infections in humans and wildlife. *Parasitic protozoa*, *5*, 1-47.

Thomas, A. W., Deans, J. A., Mitchell, G. H., Alderson, T., & Cohen, S. 1984. The Fab fragments of monoclonal IgG to a merozoite surface antigen inhibit Plasmodium knowlesi invasion of erythrocytes. *Mol. Biochem. Parasitol*. 13, 187–199

Tomita, M., & Marchesi, V. T. 1975. Amino-acid sequence and oligosaccharide attachment sites of human erythrocyte glycophorin.*Proceedings of the National Academy of Sciences*, *72*(8), 2964-2968.

Toner M, Irimia D. 2005. Blood-on-a-chip. *Annu Rev Biomed* Eng 7:77–103

Triglia T., Healer J., Caruana S.R., Hodder A.N., Anders R.F., Crabb B.S., Cowman A.F. 2000. Apical membrane antigen 1 plays a central role in erythrocyte invasion by Plasmodium species. *Mol. Microbiol*., 38, pp. 706–718

Tyler, J. S., Treeck, M. & Boothroyd, J. C. 2011. Focus on the ringleader: the role of AMA1 in apicomplexan invasion and replication. *Trends Parasitol* 27, 410–420

Uilenberg, G., 2006. Babesia - A historical overview. *Vet Parasitol*,138, (1-2), 3-10.

Vanderberg, J. P., Gupta, S. K., Schulman, S., Oppenheim, J. D., & Furthmayr, H. 1985. Role of the carbohydrate domains of glycophorins as erythrocyte receptors for invasion by Plasmodium falciparum merozoites.*Infection and immunity*, *47*(1), 201-210.

Vial, H. J.; Gorenflot, A., 2006. Chemotherapy against babesiosis. *Vet Parasitol*, 138, (1-2), 147-160.

Viitala, J., & Järnefelt, J. 1985. The red cell surface revisited. *Trends in Biochemical Sciences*, *10*(10), 392-395

Volpe EP. Blood and circulation. In: Dubuque WmC, editor. Biology and Human Concerns. Dubuque: Wm.C.Brown Publishers; 1993. p. 253–65

Walling, M. A.; Novak, J. A.; Shepard, J. R. E., 2009. Quantum Dots for Live Cell and In Vivo Imaging. *Int J Mol Sci*, 10, (2), 441-491

West JL, Halas NJ. 2003. Engineered nanomaterials for biophotonics applications: improving sensing, imaging, and therapeutics. *Annu Rev Biomed Eng*;5:285–92

Whitesides G.M. 2006. The origins and the future of microfluidics. *Nature*, 442, pp. 368–373

Wintrobe, M. M. 2009. *Wintrobe's clinical hematology* (Vol. 1). J. P. Greer (Ed.). Lippincott Williams & Wilkins.

Wyatt, C. R.; Goff, W.; Davis, W. C.,1991. A Flow Cytometric Method for Assessing Viability of Intraerythrocytic Hemoparasites*. J Immunol Methods*, 140, (1), 23-30

Xing, Y.; Chaudry, Q.; Shen, C.; Kong, K. Y.; Zhau, H. E.; WChung, L.; Petros, J. A.; O'Regan, R. M.; Yezhelyev, M. V.; Simons, J. W.; Wang, M. D.; Nie, S., 2007. Bioconjugated quantum dots for multiplexed and quantitative immunohistochemistry. *Nat Protoc*, 2, (5), 1152-1165**.**

Yezhelyev MV, Gao X, Xing Y, Al-Hajj A, Nie S, O'Regan RM. 2006. Emerging use of nanoparticles in diagnosis and treatment of breast cancer. *Lancet Oncol*;7:657–67

Yin H. & Marshall D. 2012. Microfluidics for single cell analysis. *Current Opinion in Biotechnology*, 23 (2012), pp. 110–119

Yokoyama, N.; Okamura, M.; Igarashi, I., 2006. Erythrocyte invasion by Babesia parasites: Current advances in the elucidation of the molecular interactions between the protozoan ligands and host receptors in the invasion stage. *Vet Parasitol*, 138, (1-2), 22-32

Yurchenco, P. D., & Furthmayr, H. 1980. Expression of red cell membrane proteins in erythroid precursor cells. *Journal of supramolecular structure*, *13*(2), 255-269.

Zare RN, Kim S. 2010. Microfluidic platforms for single-cell analysis. *Annu Rev Biomed Eng* 12:187–201